Geothermal Reservoir Evaluation Using Well Testing and Analytical Modelling - Case Example: Reykjanes Geothermal System, SW Iceland

Shakiru Idrissa Kajugus

Faculty of Earth Sciences
University of Iceland
2015

Geothermal Reservoir Evaluation Using Well Testing and Analytical Modelling - Case Example: Reykjanes Geothermal System, SW Iceland

Shakiru Idrissa Kajugus

60 ECTS thesis submitted in partial fulfilment of a
Magister Scientiarum degree in Geology

Advisors
Dr. Guðni Axelsson
Sæunn Halldórsdóttir

External Examiner
Dr. Egill Júlíusson

Faculty of Earth Sciences
School of Engineering and Natural Sciences
University of Iceland
Reykjavik, May 2015

Geothermal reservoir evaluation using well testing and analytical Modelling - Case example: Reykjanes geothermal system, SW Iceland
Geothermal reservoir evaluation using well testing and analytical Modelling
60 ECTS thesis submitted in partial fulfilment of a *Magister Scientiarum* degree in Geology

Faculty of Earth Sciences
School of Engineering and Natural Sciences
University of Iceland
Askja, Sturlugata 7
101, Reykjavik
Iceland

Telephone: 525 4000

Bibliographic information:
Kajugus, S.I., 2015, *Geothermal reservoir evaluation using well testing and analytical Modelling - Case example: Reykjanes geothermal system, SW Iceland*, Master's thesis, Faculty of Earth Sciences, University of Iceland, pp. 95.

Printing: Háskólaprent, Fálkagata 2, 107 Reykjavík
Reykjavik, Iceland, May 2015

Abstract

Geothermal development is a costly and risky process, which needs extensive studies to enable understanding and successful utilization of the resource. Well testing methods remain important evaluation tools for geothermal reservoirs at all stages of development. Well testing refers e.g. to injection, discharge, build-up, interference and tracer testing. Modelling of geothermal reservoirs is also a useful technique that helps in decision making. Lumped parameter modelling is e.g. a powerful, cost effective alternative to detailed numerical modelling.

The main goal of this study was to assess and discuss the role of well testing in evaluation of geothermal resources and for increasing the knowledge on geothermal systems. The work involves presentation of current techniques of well testing, and relevant analytical solutions, analysis and interpretation of temperature and pressure conditions as well as of injection, discharge and tracer test data. Finally, simulation of pressure behaviour due to production was also performed and predictions of reservoir response to future production. The Reykjanes geothermal system, SW Iceland, was selected as a case example for this study.

Evaluation of temperature and pressure conditions for wells RN-30 and RN-32 suggest that reservoir temperature and pressure are in the range of 280 – 290 °C and 30 – 100 bar, respectively. Wells RN-30 and RN-32 are characterized by relatively high transmissivity and storativity values which agree with the conceptual model of the Reykjanes system. The estimated negative skin factors of the wells indicate stimulated wells that are in a good connection with the surrounding reservoir. Simple analytical modelling for the representative wells RN-12 and RN-16 indicates that the current reinjection of 15% of the mass production needs to be increased to 50% so as to respond to the current pressure drawdown (around 41 bar), thus increasing the current reservoir pressure by over 6 bar in the next 10 years. Tracer breakthrough and mass recovery show that production wells RN-18, RN-21 and RN-24 are directly connected to injection well RN-33, and that a reinjection rate of 100 l/s into RN-33 can be maintained without serous cooling of these production wells. Drilling of reinjection wells in the region of RN-33 is recommended if they are drilled away from the Reykjanes production zone.

Útdráttur

Þróun jarðhitaverkefna er dýrt og áhættusamt ferli, sem þarfnast umfangsmikilla rannsókna til að auka skilning og gera nýtingu auðlindarinnar hagkvæma. Holuprófanir og túlkun þeirra eru mikilvæg verkfæri til að meta jarðhitakerfi á öllum stigum þróunar. Þar er t.d. átt við ádælingarpróf, blásturspróf, mælingar á þrýstingáhrifum milli holna og ferilprófanir. Líkanagerð af jarðhitasvæðum er einnig gagnlegt tækni sem hjálpar við ákvarðanatöku vegna reksturs jarðhitakerfa. Þjöppuð geymislíkön eru t.d. bæði öflug og ódýr í notkun, og geta oft komið í stað flókinna reiknilíkana.

Meginmarkmið þessarar rannsóknar var að meta og ræða hlutverk holuprófana við mat á jarðhitageymum og til að auka þekkingu á jarðhitakerfum. Verkefnið felst í kynningu á helstu prófunaraðferðum og viðeigandi greiningu viðkomandi gagna, túlkun á hitaástandi og þrýstingi í jarðhitakerfum auk túlkunar á ádælingarprófunum, blástursprófunum og ferilprófunum. Auk þess eru þrýstibreytingar vegna vinnslu hermdar og spár um viðbrögð jarðhitakerfa reiknaðar. Jarðhitakerfið á Reykjanesi er notað sem sýnidæmi fyrir þessar athuganir.

Mat á hitaástandi og þrýstingi fyrir holur RN-30 og RN-32 sýnir að hiti og þrýstingur sé á bilinu 280-290°C og 30-100 bar. Holur RN-30 og RN-32 einkennast af tiltölulega hárri vatnsleiðni og vatnsrýmd, sem er í samræmi við hugmyndalíkan jarðhitakerfisins. Áætluð skinn-gildi fyrir holurnar benda til þess að þær hafi örvast í borlok og að þær séu í góðu sambandi við jarðhitakerfið umhverfis. Einfaldir líkanreikningar fyrir holur RN-12 og RN-16 gefa til kynna að núverandi niðurdælingu uppá 15% af massaframleiðslunni úr kerfinu þurfi að auka í 50% til að sporna við áframhaldandi lækkun geymisþrýstings (nú um 41 bar), en þannig megi hækka þrýstinginn um rúmlega 6 bar á næstu 10 árum. Endurheimta ferilefnis sýnir að vinnsluholur RN-18, RN-21 og RN-24 eru í beinum tengslum við niðurdælingarholu RN-33 og að 100 l/s niðurdælingu í holu RN-33 sé hægt að halda án alvarlegrar kælingar þessara vinnsluholna. Mælt er með að niðurdælingarholur á svæðinu við holu RN-33 séu boraðar í áttina frá vinnslusvæðinu á Reykjanesi.

For my late wife, Latifa;

Who passed away one month before completion of this study.

Thanks for believing and sharing a life with me, and for making me a father of two wonderful kids (Idrissa & Idrak).

I love you every day. And now I will miss you every day.

Table of contents

List of figures ..... **ix**

List of tables ..... **xii**

Nomenclature ..... **xiv**

Acknowledgements ..... **xvii**

1 Introduction **1**
1.1 Geothermal systems 3
1.2 Geothermal wells 3

2 The Reykjanes geothermal system **5**
2.1 General information 5
2.2 Geological setting 5
2.3 Geophysical exploration 6
2.4 Conceptual model of Reykjanes geothermal system 8

3 Injection well testing **11**
3.1 Introduction 11
3.2 The pressure diffusion equation 11
3.3 Well test analysis and interpretation 18
3.3.1 Testing of well RN-30 18
3.3.2 Testing of well RN-32 22

4 Temperature and pressure conditions **25**
4.1 Introduction 25
4.2 Well RN-30 27
4.3 Well RN-32 28

5 Discharge tests **31**
5.1 Introduction 31
5.2 Methods 32
5.2.1 James lip-pressure method 32
5.2.2 Steam – water separator method 33
5.3 Data processing and interpretation 34
5.3.1 Discharge test for well RN-30 34
5.3.2 Discharge test for well RN-32 38

6 Simple analytical modelling – lumped parameter **43**
6.1 Theory 43
6.2 Modelling and reservoir response predictions 46
6.2.1 Well RN-12 47
6.2.2 Well RN-16 50

7 Tracer testing 55
7.1 Background 55
7.2 Tracer testing theory 56
7.3 Tracer test analysis and interpretation 57
7.3.1 Tracer recovery for wells RN-18, RN-21 and RN-24 58
7.3.2 Inverse modelling of tracer returns 59
7.3.3 Cooling predictions 60

8 Conclusions and recommendations 63

References 65

Appendix 69
A.3: Injection test 69
A.4: Well design 72
A.5: Discharge test 74

List of figures

Figure 2.1: Surface geological map of the Reykjanes high-temperature geothermal field (after Saemundsson 2000, Karlsdottir 1998 and Fridleifsson et al. 2000). 6

Figure 2.2: Resistivity map of Reykjanes geothermal field at 700 m b.s.l. of 3D model. (source; Karlsdóttir and Vilhjálmsson, 2014). 7

Figure 2.3: A geological map of Reykjanes with the main features of the conceptual model of the system superimposed. Blue rectangles represents boundaries with limited permeability and the main, hot up-flow zone is denoted by an orange ellipse. The yellow contours indicate the estimated shape of the pressure draw-down cone in the system based on reservoir pressure data, InSar images and gravity surveys. The arrows show inferred pathways of recharge into the reservoir Thorbjornsson et al. (2014). 9

Figure 3.1: Radial flow of a single phase fluid in a homogeneous medium (Hjartarsson, 1999). 12

Figure 3.2: Pressure change in the vicinity of the well as the results of the skin effect (Hjartarson, 1999). 16

Figure 3.3: Example of a type-curve match (Grant and Bixley, 2011). 17

Figure 3.4: location of well RN-30, well track marked with red line. 19

Figure 3.5: The pressure response of well RN-30 during the injection tests on 26th May 2011 (above) and 05th June 2011 (below). The response was measured at a depth of 1400m on both occasions. 20

Figure 3.6: location of well RN-32, well track marked with red line. 22

Figure 3.7: Pressure response of well RN-32 during the injection tests on 09th April 2013 (above) and 14th April 2013 (below), measured at 900 m depth. ... 23

Figure 4.1: Profiles for the injection, warm-up, discharge and estimated formation temperature (above) and reservoir pressure (below) for RN-30. 29

Figure 4.2: Profiles for the injection, warm-up, discharge and estimated formation temperature (above) and reservoir pressure (below) for RN-32. 30

Figure 5.1: Automatic and manual reading of the wellhead (a), critical (b) and differential pressures (c) for the discharge test of RN-30. Together with the opening of the well (valve opening). 35

Figure 5.2: Measured T and P at 2450 m during the step-rate discharge test together with the boiling point temperature for the measured pressure. 36

Figure 5.3: Estimation of productivity index, PI for RN-30. 38

Figure 5.4: Automatic and manual reading of the wellhead (a), critical (b) and differential pressures (c) for the discharge test of RN-32. 40

Figure 5.5: Measured temperature and pressure at 1025 m during the step-rate discharge test of well RN-32 together with the boiling point temperature for the measured pressure. 41

Figure 5.6: Estimation of productivity index, PI for RN-32 41

Figure 6.1: Example of lumped parameter models used to simulate pressure changes in geothermal system. One tank open model (left) and three tanks closed model (right) (Axelsson, 1989). 44

Figure 6.2: Flow configuration pattern of a three tank lumped parameter model assuming 2D-flow. 46

Figure 6.3: Mass production history of the Reykjanes high temperature geothermal system. 47

Figure 6.4: Observed and modelled pressure changes in well RN-12 using two-tank closed and open lumped parameter models. 49

Figure 6.5: Pressure prediction results for well RN-12 for the next 10 years for current mass production with 15%, 30% and 50% reinjection. 50

Figure 6.6: Observed and modelled pressure changes in well RN-16 using two-tank closed and open lumped parameter models. 51

Figure 6.7: Pressure prediction results for well RN-16 for the next 10 years assuming current mass production with 30% reinjection and 50% reinjection.....53

Figure 7.1: A map of the Reykjanes geothermal field showing the location of injection well RN-33 together with production wells RN-18, RN-21 and RN-24.....58

Figure 7.2: Measured (dots) and simulated (lines) 2-NS tracer recovery for wells RN-18, RN-21 and RN-24. 60

Figure 7.3: Cooling prediction for wells RN-18 calculated for reinjection into well RN-33, for a reinjection period of 20 years (240 months).....61

Figure 7.4: Cooling prediction for wells RN-21 calculated for reinjection into well RN-33, for a reinjection period of 20 years (240 months).....62

Figure 7.5: Cooling prediction for wells RN-24 calculated for reinjection into well RN-33, for a reinjection period of 20 years (240 months).....62

Figure A.3. 1: RN-30 Fit between model and measured data for step 1 using a logarithmic time scale (left) and log-log scale (right) for injection test on 26th May 2011. 70

Figure A.3. 2: RN-30 Fit between model and measured data for step 1 using a logarithmic time scale (left) and log-log scale (right) for injection test on 05th June 2011. 70

Figure A.3. 3: RN-32 Fit between model and measured data for step 2 using a logarithmic time scale (left) and log-log scale (right) for injection test on 09th April 2013. 71

Figure A.3. 4: RN-32 Fit between model and measured data for step 2 using a logarithmic time scale (left) and log-log scale (right) for injection test on 14th April 2013. 71

Figure A.4. 1: Casing program for RN-30 (source, ISOR). 72

Figure A.4. 2: Casing program for RN-32 (source, ISOR). 73

Figure A.5. 1: Deliverability curve of wells RN-30 and RN-32. 74

Figure A.5. 2: Plots of automatic and manual reading of the wellhead (a), critical (b) and differential pressures (c) for the discharge test of RN-32..... 75

List of tables

Table 3.1: Summarize information on the model selected for the injection test analysis for RN-30. 20

Table 3.2: Information on initial parameters used in the well test analysis for well RN-30 21

Table 3.3: Summary of parameters estimated on basis of nonlinear regression well-test analysis (WellTester) of two injection tests in well RN-30 in Reykjanes... 21

Table 3.4: Summarized information on the model selected for the injection test analysis for RN-32. 23

Table 3.5: Information on initial parameters used in the well test analysis for well RN-32 24

Table 3.6: Summary of parameters estimated on basis of nonlinear regression well-test analysis (WellTester) of two injection tests in well RN-32 in Reykjanes... 24

Table 5.1: Measured and calculated values for well RN-30 by the James lip-pressure method, with pipe diameter 16 cm and the separation pressure 1 bar-a.. 37

Table 5.2: Calculated values for well RN-30 by the James Lip Pressure Method, pipe diameter is 16 cm and the separation pressure is 15 bar-a. 37

Table 5.3: Productivity index, PI, of well RN-30. 37

Table 5.4: Measured and calculated values for well RN-32 by the James lip-pressure method, with a 16 cm diameter discharge lip pipe and separation pressure of 1 bar-a. 39

Table 5.5: Calculated values for well RN-32 by the James lip-pressure method, with lip pipe diameter of 16 cm and separation pressure of 15 bar-a. 39

Table 5.6: Productivity Index of RN-32, calculated from the manual data during the step rate flow testing and pressure at 1025 m. 41

Table 6.1: Lumped parameter model parameters for well RN-12. 48

Table 6.2: Estimated reservoir properties based on the parameters of the lumped parameter model for well RN-12. 48

Table 6.3: Lumped parameter model parameters for well RN-16. 51

Table 6.4: Estimated reservoir properties based on the parameters of the lumped parameter model for well RN-16. 52

Table 7.1: 2-NS tracer (injected into well RN-33) mass recovery and time of first tracer breakthrough. 59

Table 7.2: Model parameters estimated for the connections between injection well RN-33 and three production wells. 59

Table A.3. 1: Summary of injection tests pressure response for RN-30. 69

Table A.3. 2: Summary of injection tests pressure response for RN-32. 69

Nomenclature

A = Cross-section area of the lip used for lip-pressure measurements (cm^2);

A = Cross-section area of reinjection flow channel (m^2);

b = Flow channel width (m);

C = Wellbore storage coefficient (m^3/Pa);

C = Compressibility (Pa^{-1});

C = Tracer concentration *(kg/kg);*

D = Dispersion coefficient, *(m^2/s);*

g = Gravity *(m/s^2);*

H = Fluid enthalpy *(kJ/kg);*

H = Flow channel height (m);

h = Layer thickness *(m);*

II = Injectivity index *((L/s)/bar);*

k = Permeability *(m^2);*

L = Latent heat of fusion of water *(J/kg);*

m = mass *(kg);*

p = Pressure *(bar);*

P_0 = Initial pressure *(bar);*

P_c = Lip pressure *(bar-a);*

P_D = Dimensionless Pressure;

PI = Productivity index *((kg/s)/bar);*

q = Production or injection flow rate *(kg/s);*

Q = Production rate of well *(kg/s);*

R = Radius *(m);*

r = Radial distance *(m);*

r_D = Dimensionless radius *(m);*

r_w = Wellbore radius (m);

S = Steam saturation;

S = Storage coefficient (*m/Pa*);

S = Storativity *(kg/Pa.m^3)*

s = Skin factor;

T = Temperature (°*C*);

T = Transmissivity (*m^3/Pa s*);

t = Time (*s*);

t_D = Dimensionless time based on wellbore radius;

u = Velocity (*m/s*)

V = Volume *(m^3);*

W = Water level *(m);*

X = Steam mass fraction ratio;

x = distance along flow channel *(m);*

φ = Porosity *(%);*

β = heat capacity *(J/kg°C);*

σ = conductance of resistor (*kg/s Pa*);

α_L = Dispersivity of flow channel *(m);*

κ = storage coefficient (*kg/Pa*):

μ = Dynamic viscosity *(Pa s);*

ρ = Fluid density *(kg/m^3);*

Subscripts

s = Steam

t = Total

w = Water

Acknowledgements

I would like to express my sincere gratitude to The Government of Iceland through United Nations University Geothermal Training Programme (UNU-GTP) for awarding me a fellowship to study at the University of Iceland and my employer Tanzania Electric Supply Company ltd (TANESCO) for granting me study leave to pursue this MSc study.

Great thanks to my supervisors, Dr. Guðni Axelsson and Ms. Sæunn Halldórsdóttir, for their tireless supervision, instructions and guidance throughout my project.

My appreciation goes to the UNU-GTP Director, Mr. Lúdvík S. Georgsson, the Deputy Director, Mr. Ingimar G. Haraldsson, Environmental Sceintist/Editor, Ms. Málfrídur Ómarsdóttir, School Manager, Thórhildur Ísberg and Service Manager, Markús A.G. Wilde, for their incredible support during my study and stay in Iceland. And, to my fellow students, we had great moments that will be cherished forever.

I would like to thank and acknowledge HS-Orka for allowing use of their data from the Reykjanes geothermal system in this thesis.

Many thanks to my family and friends for their endless patience, strong encouragement and continuous support for the whole period of my study and stay in Iceland; I am blessed to have you in my life.

I am grateful to the almighty ALLAH for his protection and guidance during the entire time of my study and stay in Iceland.

1 Introduction

Geothermal energy is one of the renewable energy sources. It has e.g. played an important role in the lives of Icelanders since ancient times. Currently it accounts for over half (62%) of Iceland's primary energy needs, about 47% of the utilisation of geothermal resources is in space heating and 37% in generation of electricity (Björnsson et al., 2010). In the global perspective, currently 26 countries produce electricity from geothermal energy while over 90 countries have been identified to have geothermal energy potential (Bertani, 2015; Georgsson, 2013). In most of these countries many geothermal energy development activities have been ongoing with the purpose of exploiting the resource for economic growth of the country involved, for instance, the countries traversed by the East African Rift System.

Geothermal development is a costly and risky process, which needs extensive studies for better understanding of the resource and to enable sustainable utilization. With this in mind, many series of studies are performed, from the reconnaissance phase to detailed surface exploration, exploratory drilling of wells, resource assessment, field development, production as well as field monitoring and management, finally reaching shutdown and decommissioning (Steingrímsson, 2009). Drilling and plant construction are the most expensive phases for any geothermal development project. However, drilling remains by far the most risky phase due to the geothermal system complexity, with the little knowledge of the system available as it is located beneath the surface at great depth. Therefore, with the above in mind, it is of great importance to conduct extensive studies in drilled wells, once they're completed, to increase the knowledge of the geothermal systems.

Well testing is the first technique used in reservoir engineering to evaluate the conditions and properties of a well and its surroundings as well as geothermal reservoir at large (Axelsson, 2013). This involves injection tests, production/discharge tests, build-up tests, interference tests and tracer tests. Injection testing is applied early, or during drilling or just after a drilling project has been completed. It focusses on disturbing the pressure state of a reservoir by cold fluid injection into a well. Through such testing the parameters that control the reservoir behaviour, like porosity, storativity, transmissivity or permeability, wellbore storage, wellbore skin, fracture properties, initial pressure and reservoir boundaries are estimated. Discharge testing is performed after a well has been allowed to warm-up and recover its temperature. The main purpose of a discharge test is to test a well's production capacity and fluid chemistry. The testing is conducted by extracting fluid and observing the associated pressure change. Again, during this type of testing the temperature and pressure conditions of the wells are estimated and associated changes monitored as well. The information obtained through the tests helps in the decision making during project appraisal on whether a project should go to the next stage or not.

Reinjection into geothermal systems is regarded as an efficient reservoir management strategy for sustainable utilization. Tracer testing, which is also a kind of well test, yet not involving pressure change observations, has the purpose of studying the connectivity

of reinjection wells to production wells by tracing the flow within the reservoir and assessing the possible cooling of the production wells.

Modelling of geothermal reservoirs is a useful technique that can help in decision making during exploration and exploitation of the resources. It aims to understand the natural physical conditions in a geothermal system and estimating the properties of the system. Then the purpose of modelling is predicting the reservoir response to future production, estimate the production potential of the system as well as testing the outcomes of different management approaches (Axelsson, 2012). Different modelling approaches exist ranging from simple analytical to detailed numerical models. Lumped parameter modelling is one of the simple modelling methods which is a quite powerful, cost effective alternative to detailed numerical modelling (Axelsson, 1989).

The Reykjanes high–temperature geothermal system has been researched since 1956 when the first well was drilled. Currently thirty three geothermal wells have been drilled into the system, of which the last one was drilled in 2013. These includes production, monitoring and injection wells. Electricity generation started in 2006 with a power plant with a designed capacity of 100 MW_e, consisting of two 50 MW_e double-flash steam turbines with sea cooled condensers. The power plant utilizes steam from 14 production wells with average mass production from the reservoir at 518 kg/s in 2013. The original plans of HS-Orka, the power company utilizing the geothermal resource, assumed a power plant expansion up to 180 MW_e capacity. These have been postponed at present. The Reykjanes geothermal resource is the focus of this study.

The objectives of the study described in this thesis are the following:

a) To briefly introduce the variable types of geothermal systems, the different kinds of wells drilled to tap the resource and the role of reservoir engineering in geothermal development.

b) To present the current techniques of well testing, their role and relevant analytical solutions.

c) To evaluate the different types and stages of well testing used in reservoir engineering studies as well as their importance, scope and information needed for each well testing operation as well as expected outcome for each type of test and use for the further development of a given project and sustainable utilization.

d) To analyse and interpret the temperature and pressure conditions of selected, representative wells in the Reykjanes geothermal system, which help in understanding the overall reservoir conditions of the system.

e) To simulate (model) the pressure behaviour of the Reykjanes geothermal reservoir during production and use the model to predict the reservoir response to future production as well as recommend different approaches for sustainable utilization.

f) To analyse and interpret tracer test data from the Reykjanes geothermal system and predict the possible cooling of the production wells involved.

g) To infer the general conclusions regarding the utilization of the Reykjanes geothermal system, and other systems in general, that can be derived from the data analysis and modelling performed.

1.1 Geothermal systems

The term “geothermal system” comprises both the surface and subsurface hydrological pattern, heat source and surface activity associated with a geothermal resource. While geothermal field is considered to refer to the area of geothermal activity on surface, intended as a geographic description, it is regarded as a component of the geothermal system. The geothermal reservoir is the section in the geothermal system that can be economically exploited for energy utilization (Axelsson, 2012; Grant and Bixley, 2011).

Geothermal systems exist in different forms and are usually classified on the basis of reservoir temperature, enthalpy, physical state as well as geological setting and nature (Axelsson, 2012). Low temperature systems (<150°C), which are also referred to as low-enthalpy systems (<800 kJ/kg), are often associated with young tectonic fractures with the heat source being deep hot rock, Such systems involve deep circulation of groundwater from higher to lower elevation along fractures or other permeable structures. They also exist in sedimentary basins with permeability at great depth. These are liquid dominated systems.

High temperature systems (>200 °C) may also be described as high enthalpy systems (>800 kJ/kg). They are mostly characterised by active volcanism, the heat source being shallow magma, intrusions or dykes. These are convective systems with meteoric fluid (or sea, magmatic fluid) circulating through vertical fractures providing permeability down to the heat source, where the fluid mining heat. These may either have liquid or vapour dominated conditions or contain a mixture of liquid and vapour, i.e. be two phase. However, it should be noted that the conditions in a geothermal system may change depending on both time and position in a reservoir.

1.2 Geothermal wells

We cannot prove the potential of a geothermal resource unless a well has been drilled. The geothermal well is a crucial component in proving the resource as well as in understanding the characteristic of the reservoir of a particular system. Geothermal production wells are the wells drilled to tap into the geothermal reservoirs. Generally, geothermal wells are drilled in different design and style from slim to large diameter wells, shallow to deeper wells and vertical and directional wells.

There are number of different types of wells which can be utilized in various ways. Temperature gradient wells are designed as slim and shallow, typically less than 100 m in depth, drilled in the early stage of geothermal studies. Their main purpose is to determine temperature gradient near surface in shallow depth. Another type is the exploration wells which are drilled during the exploration phase, usually deeper than gradient wells to hit the geothermal reservoir with the purpose of exploring the condition of the geothermal system. Temperature, permeability and chemical conditions are the target information. In the later stages it may be turned into production wells. The

production wells have only the purposed of facilitating the geothermal energy extraction the reservoir. The Step-up wells are drilled to extend the confirmation of a particular geothermal reservoir while the make-up wells are used to make up for either the damaged (due to scaling or collapse) of the production wells or regular declining output of production wells with time. They are usually drilled inside the confirmed reservoir. Other types of wells are reinjection and monitoring wells. The Reinjection wells are used for injecting water back into the geothermal system which help in increasing production capacity, for environmental management and control pressure drops. The water injected may be separated fluid from high-temperature wells, return water from direct utilization applications or even surface- or ground-water. They are located inside or outside the production reservoir. The Monitoring wells are used for management purposes, i.e. for monitoring how the geothermal system how it reacts to with the production (Axelsson and Franzson, 2012).

After a well has been drilled the well logging begins, which can be viewed as the starting point of the geothermal reservoir engineering/physics research (Grant and Bixley, 2011; Stefansson and Steingrimsson, 1980). The primary purposes of the geothermal reservoir engineering/physics are to obtain information on nature, reservoir properties and physical conditions in a geothermal system, and to consequently then use them to predict the response of a reservoir to exploitation, estimating production potential and for management purposes, such as to maintain sustainable utilization Axelsson, 2012). This information is e.g. are obtained during well logging, the basic logs being temperature- and pressure-logs.

2 The Reykjanes geothermal system

2.1 General information

The Reykjanes high – temperature geothermal system is located on the Reykjanes Peninsula where the Mid-Atlantic Ridge connects with Iceland in the South – West (Figure 2.1). The geothermal exploration in the area started in 1956 when the first well was drilled. It is regarded as a unique among the high-temperature geothermal systems in Iceland since its thermal fluid is sea water in origin and not the meteoric water as in most other cases. The thermal activity in the Reykjanes geothermal field is concentrated in a small area, approximately 1 km^2, which makes it one of the smallest high – temperature fields in Iceland. The thermal activity in the field includes hot springs, hot ground, mud pots, steam vents and solfataras (Bjornsson et al., 1970; Gudmundsson et al., 1981; and Franzson et al., 2002).

Currently thirty three geothermal wells have been drilled in the field since 1956, of which the first well only reached was drilled in 1956 at 162 m depth. The first production well (RN-8) was drilled in 1969, to with 1754 m depth, and the latest production well, which is well RN-32, was drilled in 2013 to 1202 m depth. As of now 17 production wells are available in the area. Electricity generation started in 2006 with the operation of power plant with a design capacity of 100 MWe, consisting of two 50 MWe double-flash steam turbines with sea cooled condensers. The power plant utilizes steam from 14 production wells with the average mass production from the reservoir at 518 kg/s in 2013. Earlier plans assumed a power plant expansion to 180 MWe capacity. The additional 80 MWe were planned to be implemented in two phases, first through a 50 MWe steam turbine and then a 30 MWe binary plant to follow (Thorbjornsson et al., 2014). These plans have been delayed.

2.2 Geological setting

The geology of the area is well described in detail by Bjornsson (1970). The Reykjanes geothermal field is located in the active volcanic belt consisting of young basaltic lavas and hyaloclastite formations (Figure 2.1). The area is crossed by an intensely fractured NE-SW trending faults zone which is the continuation of the median central fault zone of the Mid-Atlantic Ridge. Resent volcanic activity in the area is characterized by lava producing fissure eruptions and central volcanoes, of which the fissure eruptions are younger than the central volcanoes. The fractures are considered small normal faults and tension cracks whereas the central part of the fault zone has subsided.

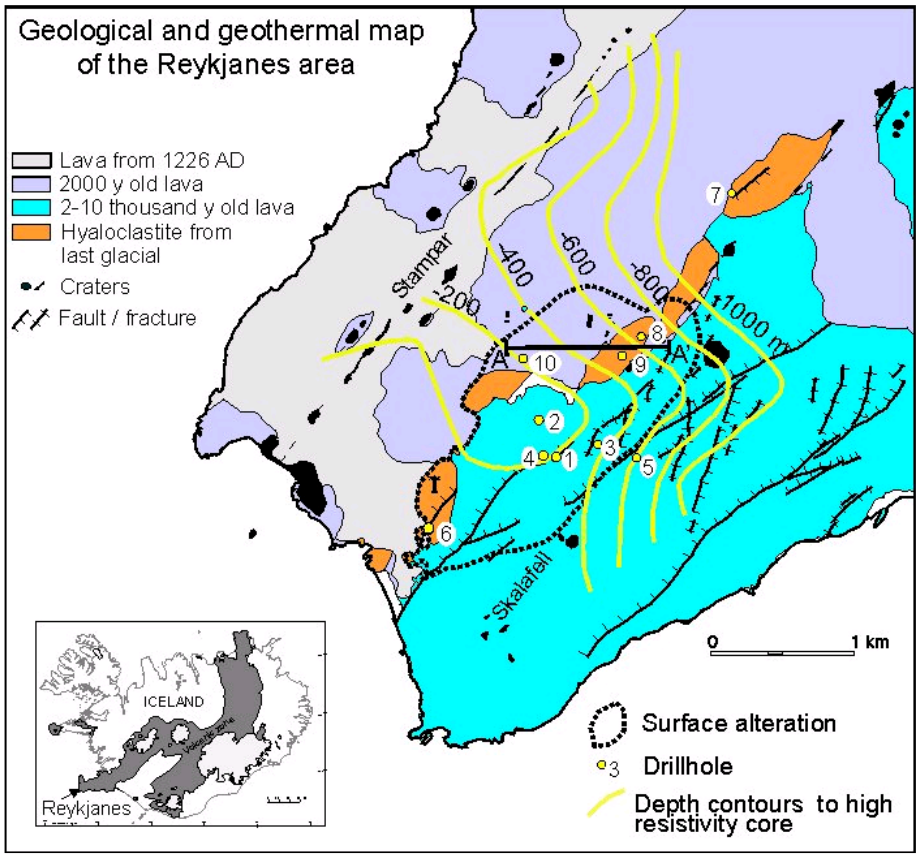

Figure 2.1: Surface geological map of the Reykjanes high-temperature geothermal field (after Saemundsson 2000, Karlsdottir 1998 and Fridleifsson et al. 2000).

2.3 Geophysical exploration

ÍSOR (Iceland GeoSurvey) has conducted geophysical exploration in Reykjanes Peninsula on behalf of HS Orka for many years, employing the TEM method, which is limited to shallow depth exploration, and the MT method for investigation of deeper structures. The 3D inversion of MT data in Reykjanes geothermal field was performed by Karlsdóttir et al. (2012) and the report published in 2012. From the 2012 report, additional MT sounding were recommended to cover big area, further to the northern part of the survey area.

The following are the main results of the 3D inversion of MT data presented in the report of Karlsdóttir and Vilhjálmsson (2014) which was carried out as extensive work from that published in 2012;

- A low resistivity cap involved of inter connected low resistivity anomalies inserted of one continuous layer covering the whole studied area. The forming of interconnected anomalies is the result of inversion. However, this is indeed that the low resistivity cap is continuous layer with variable thickness.

- The subsurface resistivity model in Reykjanes Peninsula reflects different hydrothermal alteration minerals which demonstrate a similar pattern as inother high-

temperature geothermal systems in Iceland, as well as in systems elsewhere where the host rock is basaltic, as described by Flóvenz et al. (2005).

- Thin low resistivity anomalies immediately below the surface are interpreted as outflow of geothermal fluid from the geothermal system infiltrating with saline groundwater.

- The low resistivity cap is underlain by higher resistivity (10–30 Ωm), the high resistivity core. The boundary between the two reflects the 230–240°C temperature boundary provided there is equilibrium between thermal alteration and temperature at present times. The high resistivity core reaches highest under Gunnuhver hot spring to 400–500 m b.s.l. Under the low resistivity cap the resistivity lies between 10–30 Ωm down to approximately 2500–3000 m depth. High resistivity bodies with resistivity > 70 Ωm are prominent below 3 km depth flanking a NE-SW zone of lower resistivity (< 50 Ωm) in the strike direction through the centre of the geothermal field. This low resistivity zone may reflect a fracture zone with higher permeability (Figure 2.2).

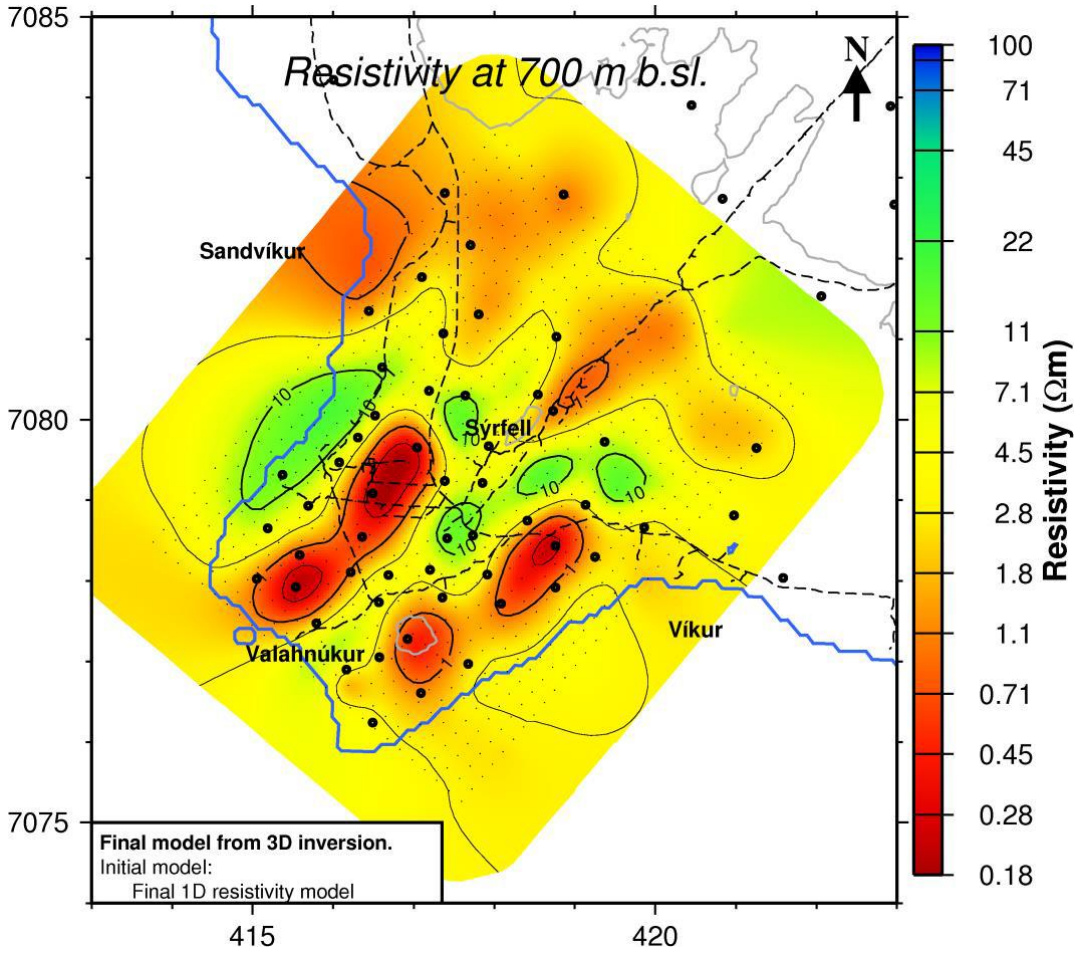

Figure 2.2: Resistivity map of Reykjanes geothermal field at 700 m b.s.l. of 3D model. (source; Karlsdóttir and Vilhjálmsson, 2014).

2.4 Conceptual model of Reykjanes geothermal system

The conceptual model of the Reykjanes geothermal system is presented in a report by Thorbjornsson et al. (2014). The heat source in Reykjanes system is associated with volcanic activity which has formed dyke intrusions. The reservoir recharge fluid is from seawater in composition and the average residence time of the water in the reservoir in the natural state is believed to be some hundreds of years based on the estimated natural steady state recharge. This recharge is estimated to be around 90 kg/s. Figure 2.3 shows a map of the Reykjanes geothermal system with the main features of the conceptual. It show the up–flow zone and limited permeability boundaries trending NE-SW, which both seem to be controlled by the structures in the area striking NE-SW. Feed zones in wells are apparently mainly associated with permeable formations and dykes. However those found near dykes are most likely associated to faults linked with the dykes. The reservoir temperature in the Reykjanes system is in range of 280 – 290°C, as shown in most wells.

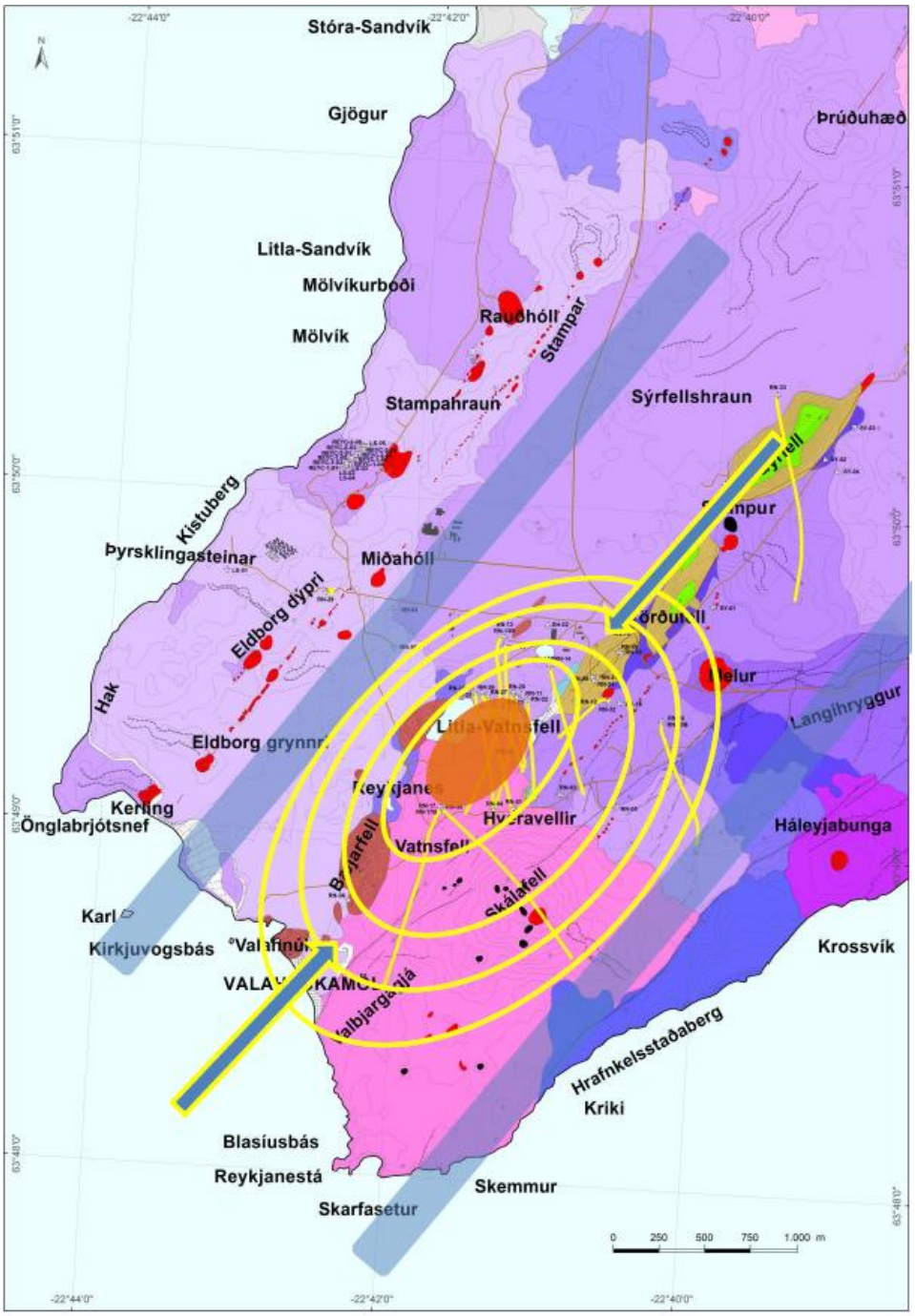

Figure 2.3: A geological map of Reykjanes with the main features of the conceptual model of the system superimposed. Blue rectangles represents boundaries with limited permeability and the main, hot up-flow zone is denoted by an orange ellipse. The yellow contours indicate the estimated shape of the pressure draw-down cone in the system based on reservoir pressure data, InSar images and gravity surveys. The arrows show inferred pathways of recharge into the reservoir Thorbjornsson et al. (2014).

3 Injection well testing

3.1 Introduction

The primary target of well testing is to assess the conditions of well and the properties of the reservoir intersected by the well, by subjecting it to injection or production. During injection fluid, which is usually colder than the reservoir, is injected into the well, causing the bottom hole pressure to increase, while during production the well is allowed to flow and the bottom hole pressure decreases as the mass flow increases. The focus during such testing is to monitor the pressure response, which is controlled by the properties of the reservoir. The parameters that control the reservoir response are storativity (partly controlled by porosity), transmissivity (or permeability), wellbore storage, wellbore skin, fracture properties, initial pressure and reservoir boundaries, all of which may be possible to infer when well testing has been conducted. To extract estimates of all these parameters models are needed to simulate the measured data, models which include the reservoir properties. The fundamental pressure diffusion equation is the basis of all models in well testing theory, as well as the basis of pressure transient analysis founded on the models.

In the following section the derivation of the pressure diffusion equation is reviewed and discussed in detail, as well as some basic solutions of the pressure diffusion equation. Moreover data collected during injection well-testing of wells RN-30 and RN-32 in Reykjanes are analysed and interpreted in section 3.3. These two wells are selected as examples and they are also different in term of location. Well RN 30 drilled at the boundary of the production zone while RN 32 drilled inside the production zone.

3.2 The pressure diffusion equation

The theory of pressure transient analysis has been developed in great detail in the groundwater literature, beginning with the work of Theis (1935). It was later adopted in the petroleum literature, consequently geothermal reservoir engineering inherited the theory. The technique is used to calculate the pressure (p) in the reservoir at a certain distance (r) after a given time (t) and from an injection (or production) well receiving (or producing) fluid at specific rate (Q), starting at time t = 0.

In deriving the pressure diffusion equation, we use the simplest model for a single phase fluid flow in porous medium, in a vertical well that full penetrates a reservoir which is homogenous, assuming that only horizontal flow occurs, a reservoir of uniform thickness and radially infinite, which is sealed above and below (Figure 3.1). No significant variation of reservoir permeability is allowed, and other physical properties are uniform in different directions (isotropic). Reservoir compressibility is assumed small. The parameters are, therefore, all constant. The fluid is assumed to occupy the entire volume. Isothermal conditions are also assumed and variation in dynamic viscosity therefore neglected. Finally pressure gradients are assumed to be small and gravity forces are

neglected (Bodvarsson and Witherspoon, 1989; Hjartarsson, 1999; Grant and Bixley, 2011).

The diffusion equation can be derived by taking into consideration three basic governing laws, namely the conservation of mass, conservation of momentum (Darcy's law) and the equation of state for the reservoir-fluid (fluid compressibility). This is done for a cylindrical shell extending vertically through the reservoir (see Figure 3.1).

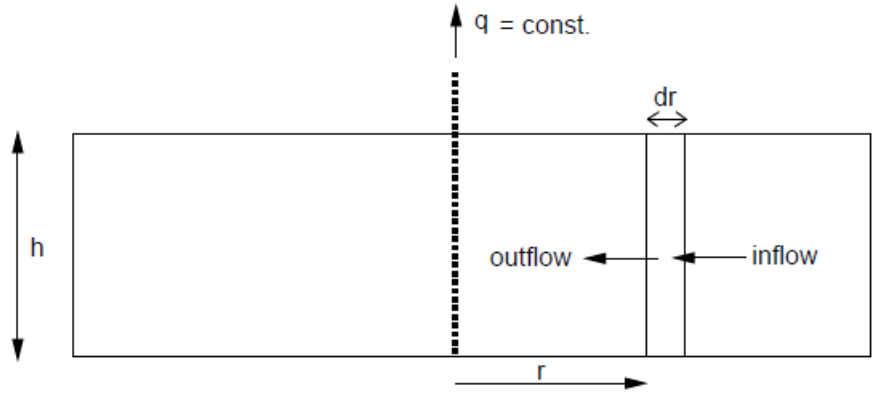

Figure 3.1: Radial flow of a single phase fluid in a homogeneous medium (Hjartarsson, 1999).

i) Law of conservation of mass (radial coordinates);

Mass rate in – Mass rate out = rate of change of mass in the cylindrical shell.

$$(2\pi rhu\rho)_{r+dr} - (2\pi rhu\rho)_r = \frac{\partial}{\partial t}(2\pi rdrh\varphi\rho) \tag{3.1}$$

Where ρ is density of fluid (kg/m^3), u is the velocity, h is reservoir thickness, porosity is denoted with φ, r denotes the distance from the centre of the well to the cylindrical shell and dr the thickness of the shell.

By dividing the equation by dr and taking the limit $dr \rightarrow 0$, the equation simplifies to

$$\frac{1}{r}\frac{\partial}{\partial r}(ru\rho) - \frac{\partial}{\partial t}(\varphi\rho) = 0 \tag{3.2}$$

ii) The law of conservation of momentum (Darcy's law) in radial form for horizontal flow;

$$u = \frac{k}{\mu}\frac{\partial P}{\partial r} \tag{3.3}$$

Where k is permeability, μ is the dynamic viscosity of the fluid and $\frac{\partial P}{\partial r}$ is the pressure gradient.

iii) The equation of state for fluid (fluid compressibility);

$$C = \frac{1}{\rho}\left(\frac{\partial \rho}{\partial P}\right)_T \tag{3.4}$$

$$\text{But,} \quad C_r = \frac{1}{1-\varphi}\frac{\partial \varphi}{\partial P} \quad \text{and} \quad C_t = \varphi C_w + (1-\varphi)C_r \tag{3.5}$$

Where C denotes isothermal compressibility, C_r, C_w and C_t are the rock, water and total compressibility, respectively.

Now, equations (3.2) and (3.3) can be combined resulting in;

$$\frac{1}{r}\frac{\partial}{\partial r}\left(r\rho\frac{k}{\mu}\frac{\partial P}{\partial r}\right) = \frac{\partial}{\partial t}(\varphi\rho) \tag{3.6}$$

This equation (3.6) is the fundamental differential equation for pressure changes in during radial single phase aquifer flow, at isothermal condition, or the so-called pressure diffusion equation. If we expand the right hand side of the equation, we get:

$$\frac{\partial}{\partial t}(\varphi\rho) = \rho\frac{\partial \varphi}{\partial t} + \varphi\frac{\partial \rho}{\partial t} \tag{3.7}$$

By using equations (3.4) and (3.5) we can also show that:

$$\varphi\frac{\partial \rho}{\partial t} = \varphi C_w \rho\frac{\partial P}{\partial t} \qquad \text{and} \qquad \rho\frac{\partial \varphi}{\partial t} = (1-\varphi)\rho C_r\frac{\partial P}{\partial t} \tag{3.8}$$

Now, equation (3.7) can be rewritten by inserting the equations under (3.8), thus we get:

$$\frac{\partial}{\partial t}(\varphi\rho) = \rho\frac{\partial P}{\partial t}[\varphi C_w + (1-\varphi)C_r] \tag{3.9}$$

By inserting equations (3.5) and (3.9) into the pressure diffusion equation (3.6) finally gives:

$$\frac{1}{r}\frac{\partial}{\partial r}\left(r\rho\frac{k}{\mu}\frac{\partial P}{\partial r}\right) = \rho\frac{\partial P}{\partial t}C_t \tag{3.10}$$

By introducing the parameters storativity, $S = C_t h$, and transimissivity, $T = \frac{kh}{\mu}$, into equation (3.10), gives:

$$\frac{1}{r}\frac{\partial}{\partial r}\left(r\frac{\partial P}{\partial r}\right) = \frac{S}{T}\frac{\partial P}{\partial t} \tag{3.11}$$

The pressure diffusion equation in radial form (3.11) is the basic equation for well testing theory. It is a second order partial differential equation, nonlinear with analytical solutions.

A number of different solutions to the pressure diffusion equation can be obtained depending on different boundary and initial conditions. These conditions are usually

based on assumptions established through knowledge gained on the reservoir system. Different reservoir system and conditions can have different well test analysis methods, which correspond to these conditions. For instance, Theis in 1935 (Earlougher, 1977; Honre, 1995) suggested an integral solution for the diffusion equation based on the following initial and boundary conditions for a well radius of infinitesimal radius, $r_w = 0$:

Initial condition:

Pressure is the same all through the reservoir equal to the initial pressure, P_0:

$$P(r,t) = P_0 \qquad \textit{for } t = 0, \textit{ all } r > 0 \tag{3.12}$$

Boundary conditions:

i. Outer boundary

Pressure is equal to the initial pressure at infinity;

$$P(r,t) = P_0 \qquad \textit{for } r \rightarrow \infty \textit{ and } t > 0 \tag{3.13}$$

ii. Inner boundary

Well flow at a constant rate q (m^3/s),

$$q = \frac{2\pi kh}{\mu}\left(r\frac{\partial P}{\partial r}\right) \qquad \textit{for } r \rightarrow 0 \textit{ and } t > 0 \tag{3.14}$$

The Theis solution to the radial diffusion equation (3.11) considering these conditions (initial and boundary) is given by the equation below:

$$\Delta P = P(r,t) - P_0 = \frac{q}{4\pi T} W\left(\frac{-Sr^2}{4Tt}\right) = \frac{q\mu}{4\pi kh} W\left(\frac{-\mu C_t r^2}{4kt}\right) \tag{3.15}$$

Where W(u) is known as the "well function" and $u = \frac{Sr^2}{4Tt}$:

$$W(u) = E_i(-u) = -\int_u^{\infty} \frac{e^{-x}}{x} dx \tag{3.16}$$

If $u < 0.01$ equation (3.16) can be approximated by $W(u) \approx -In(u) - \gamma \approx -In(u) - 0.5772$, with γ known as the Euler constant.

The equation (3.15) hold for , $t > 25\frac{Sr^2}{T}$

Therefore,

$$\Delta P = \frac{2.303q}{4\pi T}\left[log\left(\frac{Sr^2}{4Tt}\right) + \frac{\gamma}{2.303}\right] \tag{3.17}$$

Equation (3.17) is very frequently used in well testing theory. It describes the pressure response with time *t* and distance *r* for a constant flow rate *q* for the reservoir model in Figure 3.1. However, *the skin factor, s* has to be introduced in this relation as it is a fact that during the testing pressure transient data are commonly disturbed by local effects inside or near the well, which are wellbore storage and the skin effect.

Skin effect is introduced to quantify a difference in permeability next to a well compared with the permeability of the reservoir. This is often caused by drilling operations, being either damaged (positive skin factor) due to drilling cutting, cement or mud clogging the fractures or stimulated (negative skin factor) due to fracturing around the well (Figure 3.2). The skin factor, s, is dimensionless and defined by:

$$\Delta P_{skin} = \frac{q}{2\pi T} s \tag{3.18}$$

The skin factor can also be determined on basis of:

$$s = \left(\frac{k}{k_s} - 1\right) In\left(\frac{r_s}{r_w}\right) \text{ and } r_{weff} = r_w e^{-s} \tag{3.19}$$

Where, k_s is the reduced permeability, r_s the radius of the affected zone and r_{weff} is the effective radius of the well introduced to account for the effect, which is the same as either reducing or increasing the radius of a well.

Therefore, the Theis solution, for an active well with skin effect which apply only for drawdown inside the well is given by:

$$\Delta P = \frac{2.303q}{4\pi T}\left[log\left(\frac{Sr_w^2}{4Tt}\right) + \frac{\gamma - 2s}{2.303}\right] \tag{3.20}$$

The wellbore storage is the property that describes the capacity of wellbores to store fluid, as the well radius is in reality finite. This occurs due to variations in the liquid level in a well and fluid compressibility. The wellbore storage factor, *C*, is dimensionless and is defined by:

$$C = \frac{\Delta V}{\Delta P} \tag{3.21}$$

Where ΔV and ΔP are the change in volume and pressure inside the well, respectively.

Semi-logarithmic well test analysis

The Theis solution in equation (3.17) can be written as;

$$-\Delta P = \frac{2.303q}{4\pi T}\left[\log(t) + log\left(\frac{4T}{Sr^2}\right) - 0.2506\right] \tag{3.22}$$

By rearranging equation (3.22) in the form of $-\Delta P = A + m\ log(t)$ the pressure change can be plotted against *log(t)* giving a semi-logarithmic graph following a straight line with slope *m* and constant *A*. Then, the transmissivity, T can be evaluated from the slope by:

$$T = \frac{2.303q}{4\pi m} \tag{3.23}$$

The storativity, S, can be obtained, consequently, by rearranging equation (3.22):

$$S = 2.25T\left(\frac{t}{r^2}\right)10^{-\Delta P/m} \tag{3.24}$$

The presence of skin effect does not alter the evaluation of transmissivity in the semi logarithmic analysis but it does affect the storativity estimates, therefore in order to calculate the skin factor one must rearrange equation (3.20) to get (Grant and Bixley, 2011);

$$s = 1.151\left[\frac{\Delta P}{m} - log\left(\frac{4Tt}{Sr_w^2}\right) + 0.2506\right] \tag{3.25}$$

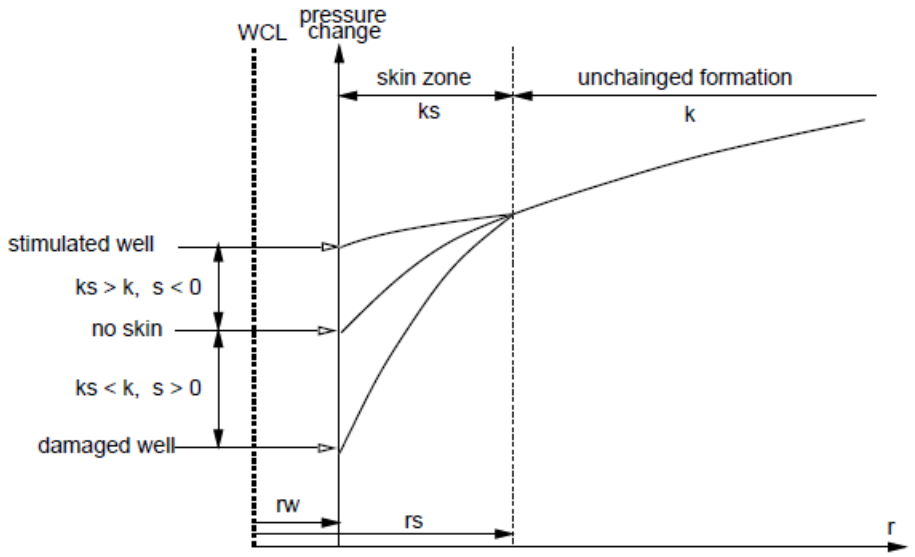

Figure 3.2: Pressure change in the vicinity of the well as the results of the skin effect (Hjartarson, 1999).

Dimensionless variables and type-curve matching

Another method of estimating reservoir properties from well-test data involves making use of dimensionless variables which simplify the reservoir models by representing the parameters in dimensionless form. Pressure change depends on the particular permeability, flow rate, viscosity, compressibility, porosity and radius of the well, all of which are assumed to be constant. The parameters are transformed by multiplying or dividing by these constants to obtain the dimensionless parameters. Thus the dimensionless pressure, time and radius (radial distance from well) are given by:

$$P_D = \frac{2\pi kh}{q\mu}\Delta P \quad - \quad \text{Dimensionless pressure change} \tag{3.26}$$

$$t_D = \frac{kt}{C_t \mu r_w^2} \quad - \quad \text{Dimensionless time} \tag{3.27}$$

$$r_D = {}^{r}/_{r_w} \quad - \quad \text{Dimensionless radius} \tag{3.28}$$

Thus equation (3.15) is transformed to an equation for the dimensionless pressure in an infinite humongous aquifer (Grant and Bixley, 2011):

$$P_D = P_D(t_D) = {}^{1}/_{2}\, W(4t_D) \tag{3.29}$$

This can also be further written as;

$$P_D = -1.151\, log(t_D) + 0.351 \tag{3.30}$$

A type-curve is consequently obtained by plotting the *log (P_D) vs. log (t_D)*. The actual measured pressure change data, ΔP, as a function of time, *t*, are also plotted on a transparent paper on the same log – log scale as the type-curve. The two graphs are superimposed together while sliding them to a point where a best match is obtained **(**see example in Figure 3.3). The curves will match only if the proper reservoir model has been selected. Then a convenient match point (M) is chosen and the values of $(\Delta P_M, P_{DM}, \Delta t_M, and\ t_{DM})$ are obtained from the curves. The matching values can now be used to calculate the transimisivity and storativity by inserting them into;

$$T = \frac{q}{2\pi}\left(\frac{P_D}{\Delta P}\right)_M \tag{3.31}$$

$$S = \frac{T}{r_w^2}\left(\frac{\Delta t}{t_D}\right)_M \tag{3.32}$$

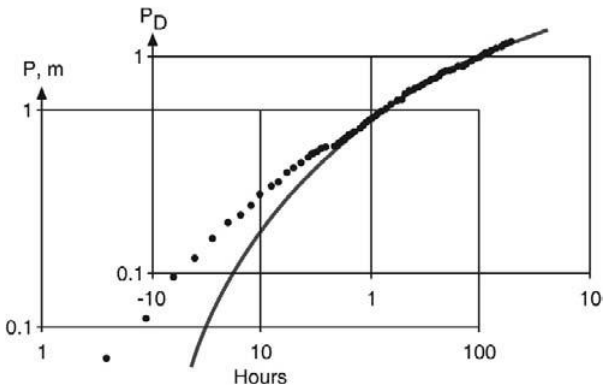

Figure 3.3: Example of a type-curve match (Grant and Bixley, 2011).

The type – curves matching was used extensively in the past in the ground water and petroleum industries and to some extent in the geothermal one, but with the advance of computers today, fitting are done with computer software with great variants for analysis the system.

3.3 Well test analysis and interpretation

Well testing is in most cases performed at drilling completion, this is a common practise in most geothermal fields in the world. Injection well testing was e.g. performed in wells RN-30 and RN-32 in Reykjanes, and the data collected in these tests are used here as examples. For each well, two injection tests were performed and the results have been analysed with the double purpose of estimating the reservoir and well properties for each well and to compare the results of the first and the second test of each well to see whether the wells were stimulated after the first test.

All the well test analysis and interpretation has been performed using the computer software *Well Tester (V1.0.0)* developed by Iceland GeoSurvey (ÍSOR). The software is designed to handle data manipulation and analysis of well test data (mainly multi-step injection tests) in Icelandic geothermal fields as well as other geothermal fields in the world. The process is user-friendly, divided into five (or in some cases six) simple steps that range from setting initial conditions to modelling and giving a final report (Júlíusson et al., 2008).

3.3.1 Testing of well RN-30

Well RN-30 is a directional well completed on 3rd of June 2011 with a final measured depth (MD) of 2869 m, and true vertical depth (TVD) of 2545 m (Figure 3.4). The first injection testing of the well was performed on 26th May 2011 (8 days before drilling completion) while the second test was done on 5th June 2011, two days after drilling completion. In each injection test only one step was conducted. A pressure (and temperature) logging tool was placed at a depth of 1400 m (TVD) inside the well. This measuring depth is often selected close to the pressure pivot point depth of a well (discussed in next chapter). Figure 3.5 shows the pressure response during the two injection tests while Table A. 3.1 in Appendix gives a summary of the pressure response for the two tests.

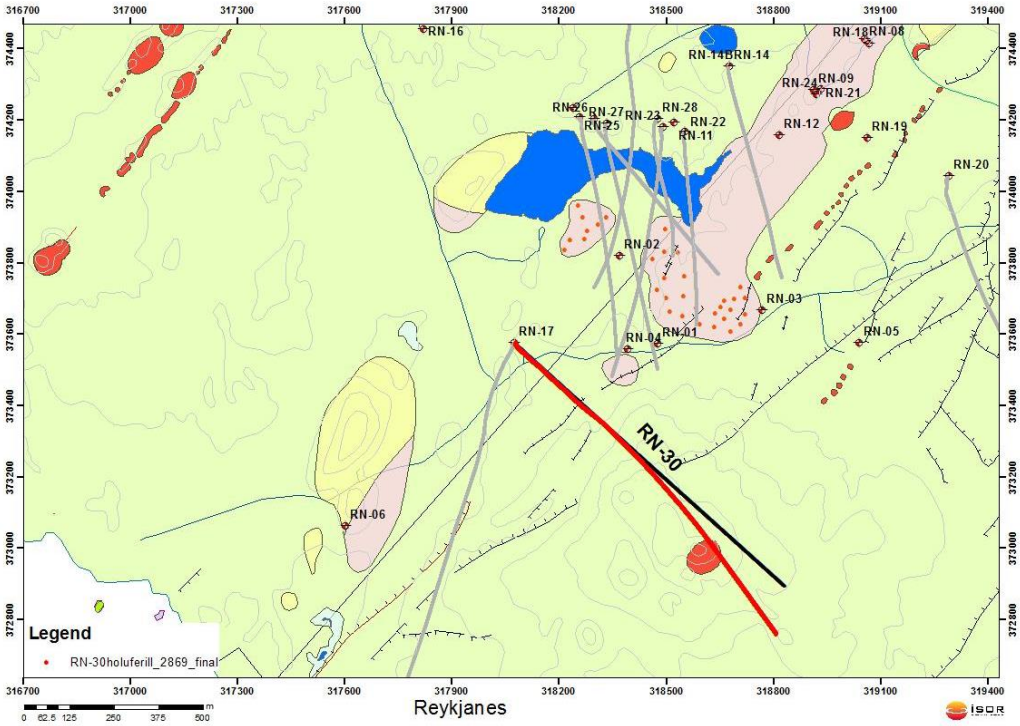

Figure 3.4: location of well RN-30, well track marked with red line.

During the well testing analysis, different models were tested by performing a nonlinear regression in order to find the best fitting model for the measured data. Table 3.1 and Table 3.2 gives a summary of the selected model and selected initial parameters for the injection tests, respectively. These initial parameters are assumed approximately by *WellTester* and it is not necessary for the initial parameters selected to be close to the best fitting parameters, for a meaningful output, however, good estimates help in deducing information from the well test, beyond the standard output.

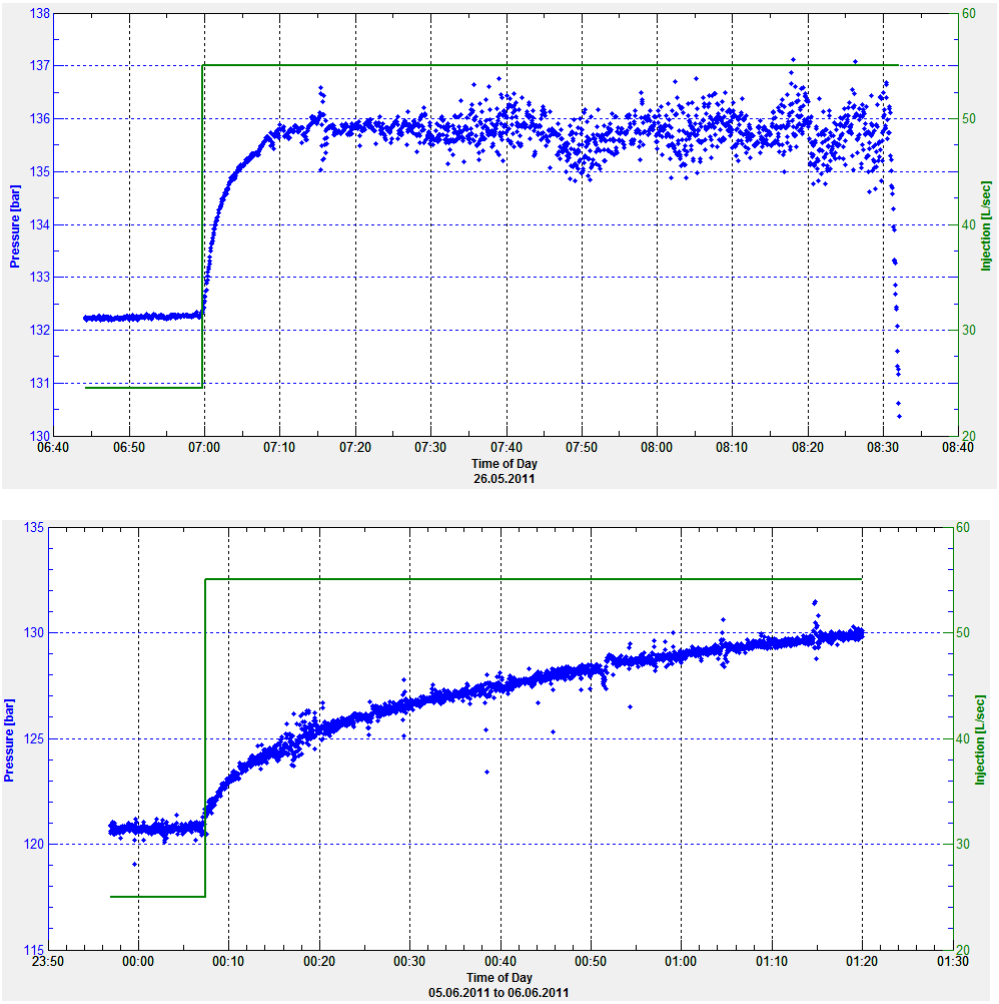

Figure 3.5: The pressure response of well RN-30 during the injection tests on 26th May 2011 (above) and 05th June 2011 (below). The response was measured at a depth of 1400m on both occasions.

Table 3.1: Summarize information on the model selected for the injection test analysis for RN-30.

Reservoir	Homogeneous
Boundary	Constant pressure
Well	Constant skin
Wellbore	Wellbore storage

Table 3.2: Information on initial parameters used in the well test analysis for well RN-30

Parameter for RN-30	**26/05/2011**	**05/06/2011**
Estimated reservoir temperature (T_{est}), °C	280	280
Estimated reservoir pressure (P_{est}), bar	135.7	127.3
Wellbore radius (r_w), m	0.16	0.16
Porosity (φ), %	0.1	0.1
Dynamic viscosity of reservoir fluid (μ), Pa.s	$9.58x10^{-5}$	$9.55x10^{-5}$
Compressibility of reservoir fluid (c_w), Pa^{-1}	$1.94x10^{-9}$	$1.9x10^{-9}$
Compressibility of rock matrix (c_r), Pa^{-1}	$2.44x10^{-11}$	$2.44x10^{-11}$
Total compressibility (c_t), Pa^{-1}	$2.15x10^{-10}$	$2.18x10^{-10}$

The results of the regression model analysis for well RN-30 are graphically presented in Figures A.3.1 and A.3.2 (in Appendix) for the injection tests of 26th May and 05th June, respectively. The resulting parameter estimates are summarized in Table 3.3.

The results obtained indicate that well RN-30 is more open to flow during the first injection test than the second one. This is clearly demonstrated by the injectivity index, *II*, as well as the effective permeability, k, as both are estimated to be smaller during the second injection test. This is different from what is normally expected, as one would expect fractures to be more open during the second test than the first, as the injection tests and deeper drilling may be expected to enhance the well. This reverse situation may be the result of the continuation of drilling work to greater depth, which may have caused some fractures to clog up by infiltration of drill cuttings, drilling mud or cement during continued drilling. Yet, the reservoir thickness and radius of investigation are estimated to be greater in the second injection test, as the well was much deeper (2869 m) than during the first test which was done at a depth of 2510 m. The transimissivity values are all of the order of 10^{-8} m^3/(Pa.s), which are comparable to values for geothermal wells in Iceland in general. The skin factor is estimated to be negative in both tests, which indicates that the well is well connected with the surround reservoir.

Table 3.3: Summary of parameters estimated on basis of nonlinear regression well-test analysis (WellTester) of two injection tests in well RN-30 in Reykjanes.

Parameter	**Step 1**	
	26th May 2011	**05th June 2011**
Transmissivity (T), *m^3/(Pa.s)*	$7.69x10^{-8}$	$1.0x10^{-8}$
Storativity (S), *$m^3/(m^2Pa)$*	$1.83x10^{-8}$	$4.14x10^{-8}$
Radius of investigation (r_e), *m*	98	126.5
Skin factor (s)	-0.7	-3.9
Wellbore storage (C), *m^3/Pa*	$1.22x10^{-5}$	$3.0x10^{-5}$
Injectivity index (II), *(L/s)/bar*	8.5	3.9
Reservoir thickness (h), *m*	85.2	190
Permeability (k), *m^2*	$8.64x10^{-14}$	$5.03x10^{-15}$

3.3.2 Testing of well RN-32

Well RN-32 is a directional well drilled to a depth of 1202 m (Figure 3.6). The drilling work was completed on 16th April 2013 as the operation encountered problems during drilling and no further attempts to drill deeper were made, but the original plan was to drill to 2500 m depth. Three injection tests were performed in this well; first on 3rd of April when the well was only 1117 m deep, then on 9th of April with an 1180 m deep well and the last was conducted on 14th of April, when the depth was 1202 m. The pressure logging-tool was placed at 900 m depth in the well for all three tests. In this report, only two injection tests (09th and 14th April 2011) are used for analysis and interpretation.

Figure 3.7 displays the pressure response during these injection tests (09th and 14th April 2011) and Table A.3.2 (in Appendix B) presents a summary of the pressure response during the tests. Table 3.4 and Table 3.5 provides a summary of the selected model and selected initial parameters for the *WellTester* analysis of the injection tests, respectively.

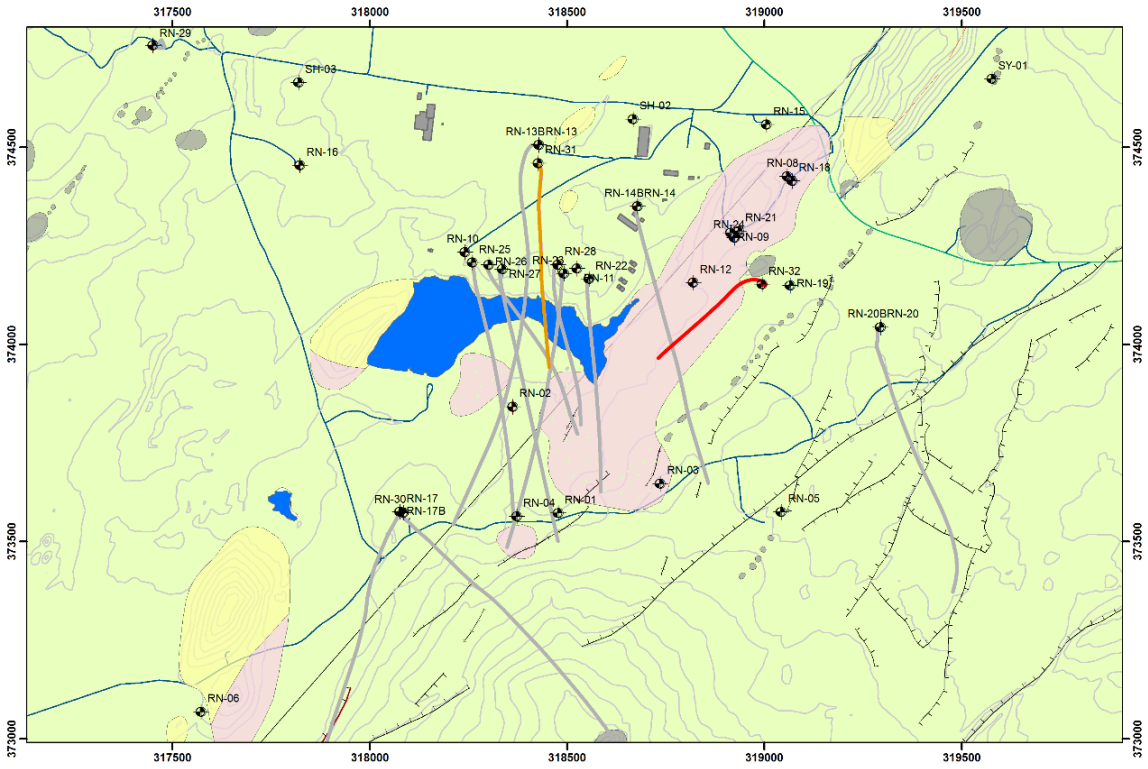

Figure 3.6: location of well RN-32, well track marked with red line.

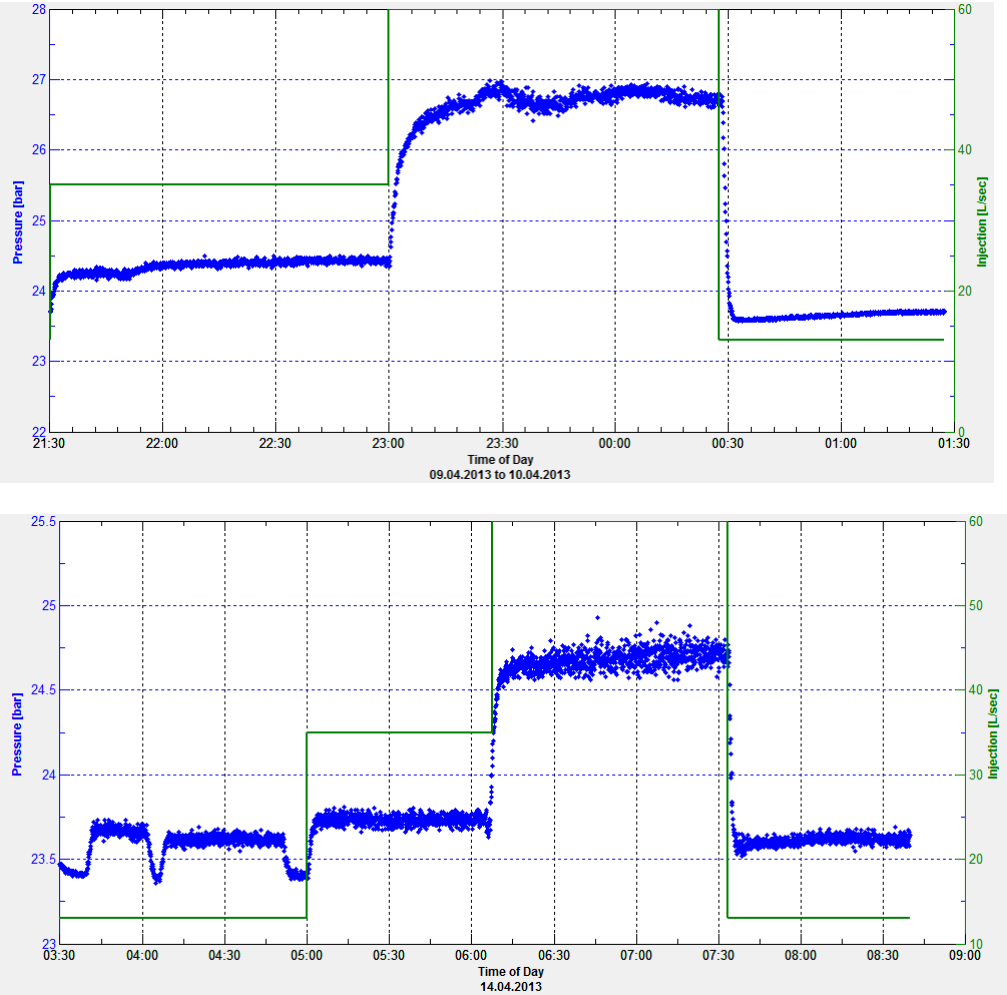

Figure 3.7: Pressure response of well RN-32 during the injection tests on 09th April 2013 (above) and 14th April 2013 (below), measured at 900 m depth.

Table 3.4: Summarized information on the model selected for the injection test analysis for RN-32.

Reservoir	Dual Porosity
Boundary	Constant pressure
Well	Constant skin
Wellbore	Wellbore storage

Table 3.5: Information on initial parameters used in the well test analysis for well RN-32

Parameter for RN-32	**09/04/2013**	**14/04/2013**
Estimated reservoir temperature (T_{est}), °C	280	280
Estimated reservoir pressure (P_{est}), bar	24.41	23.69
Wellbore radius (r_w), m	0.16	0.16
Porosity (φ), %	0.1	0.1
Dynamic viscosity of reservoir fluid (μ), Pa.s	$1.91x10^{-5}$	$1.91x10^{-5}$
Compressibility of reservoir fluid (c_w), Pa^{-1}	$4.46x10^{-7}$	$4.58x10^{-7}$
Compressibility of rock matrix (c_r), Pa^{-1}	$2.44x10^{-11}$	$2.44x10^{-11}$
Total compressibility (c_t), Pa^{-1}	$4.46x10^{-8}$	$4.58x10^{-8}$

The nonlinear regression well-test analysis was again performed with *WellTester* for the above stated best fit model, and both injection tests. The resulting parameter estimates are given in Table 8 while the fit of the model are graphically depicted in Figures A.3.3 (09^{th} April 2013) and A.3.4 (14^{th} April 2013) for the two injection tests. The second step of both injection tests yielded the best fits and have been used to estimate the parameters of the well and surrounding reservoir, summarized in Table 3.6.

Table 3.6: Summary of parameters estimated on basis of nonlinear regression well-test analysis (WellTester) of two injection tests in well RN-32 in Reykjanes.

Parameter	**Step 2**	
	09^{th} April 2013	**14^{th} April 2013**
Transmissivity (T), $m^3/(Pa.s)$	$7.35x10^{-8}$	$2.25x10^{-7}$
Storativity (S), $m^3/(m^2Pa)$	$4.91x10^{-6}$	$4.93x10^{-6}$
Radius of investigation (r_e), *m*	87.5	98.7
Skin factor (s)	-0.84	-0.06
Wellbore storage (C), m^3/Pa	$1.27x10^{-5}$	$2.1x10^{-5}$
Injectivity index (II), *(L/s)/bar*	10.96	26.3
Reservoir thickness (h), *m*	110.1	107.7
Permeability (k), m^2	$1.27x10^{-14}$	$4.0x10^{-14}$

The results of injectivity indexes suggesting that the well is enhance after the first injection test. The effective permeability and transimissivity both increase which also demonstrate that the well has been stimulated but it also became deeper. Again the storativity estimates are in order of 10-6 m3/(m2Pa) which suggests a two phase reservoir, which is agrees with the conceptual model of the Reykjanes system at this shallow depth. Radius of investigations and reservoir thicknesses are considered reasonable as well as being comparable in both tests.

4 Temperature and pressure conditions

4.1 Introduction

Temperature and pressure are the fundamental parameters in any geothermal investigation of which are obtained through well logging (Stefansson and Steingrimsson, 1980). During the drilling work, circulation fluids and cold water injection cools the surrounding rock. The drilled well usually takes some time to recover its initial temperature. This period of temperature recover is what's known as the warm-up period. How long depends on the local condition of the reservoir (whether the aquifer warm-up more rapid than the dry rock part of the reservoir) and the development of the project that follows, nevertheless, it usually takes up to few months (Stefansson and Steingrimsson, 1980; Axelsson and Steingrimsson, 2012). The temperature and pressure data obtained after well logging increase our understanding on the reservoir condition. Information like temperature condition of undisturbed system (formation temperature), reservoir pressure (initial pressure), location of feed zones/aquifers and flow patterns are determined.

Many of the logging technics applied in geothermal reservoirs were first developed in oil and groundwater fields and then found its use in geothermal industries. The logging is done by dipping down the logging tools to the bottom of the wells where data are recorded, and the tools are retrieved back to the surface. There are different well logging tools in use in geothermal industry, ranging from reasonably simple mechanical tools which can only measure temperature and pressure to high electronic tools which measure a variety of physical parameters. However, reliability, availability and accuracy are the most importance in selecting these tools. Measurements of temperature and pressure are done during drilling, in connection to various well testing, during warm-up period and as part of regular reservoir monitoring.

Condition inside the well during logging is not the same as in the surrounding formation or as undisturbed conditions in the reservoir before drilling. Different methods are used to estimate the temperature and pressure of the formation. For the formation temperature estimation, Horner – plot method (Dowdle and Cobb, 1975) and Albright method (Albright, 1976) are mostly used.

The Horner – plot method

This is an empirical technique developed to estimate the formation temperature for relatively long recovery period, usually ranging from weeks to months. The basic condition of the technique is the straight – line relationship between the maximum wellbore temperature and the natural logarithm of the relative time, τ , or *Horner time*, as described mathematically in equation 42.1 below.

$$\tau = \left(\frac{t_0 + \Delta t}{\Delta t}\right) \qquad \text{Horner time} \qquad (4.1)$$

Where;

Δt is the time passed since last circulation stopped.

t_0 is the circulating time.

By using the equation 4.1 above one can plot the maximum wellbore temperature as a function of $\ln(\tau)$ and then plot a straight line through the data by which the extrapolation to $\tau = 1$ we estimate the formation temperature (Helgason, 1993).

The Albright method

The method is used for direct determination of wellbore formation temperatures during economical acceptable interruption during drilling works; 12 to 24 hours depending on depth of the well and rock formation. The method is based on the assumption that for a random time interval, much shorter than the recovery time, the rate of temperature recovery is determined by the difference between the wellbore temperature and the formation temperature (Helgason, 1993).

$$e^{-c^i t} = \frac{T_\infty^i - T_t^i}{T_\infty^i - T_0^i} \qquad (4.2)$$

Where;

T_0^i = Estimated temperature at the circulation stop.

T_t^i = Temperature at time *t*.

T_∞^i = Estimated formation temperature for the time interval *i*.

c^i = Constant.

We can determine the formation temperature by assuming a liner relation between c^i and T_∞^i and plot c^i against T_∞^i then drawing a straight line through the data to intercept T_∞^i at $c^i = 0$ which gives the formation temperature (Helgason, 1993).

The BERGHITI programme (Helgason, 1993) from the ICEBOX software package is used to estimate the formation temperature for this study. The software offers both the Horner – plot and the Albright methods. In the respect of this study, the Horner – plot method has been used since temperature data for relatively long recovery period was available.

The reservoir pressure, also referred to as the initial pressure, is estimated from data obtained during the recovery period. It is determine with the help of another software called *Predyp* from ICEBOX by feeding the obtained formation temperature values and

known initial wellhead pressure or water level. The formation pressure is plotted together with the warm-up pressure profiles to determine their intersection. This intersection is known as *pivot point* which defines the reservoir pressure for the dominating single feed-zone, however, for two or more dominating feed-zones the pivot point represent the average pressure condition between feed zones.

In the following sections, the temperature and pressure conditions of wells RN-30 and RN-32 are analysed and interpreted with the purpose of understanding their formation temperature, initial pressure, locations of feed-zones and their flowing regimes.

4.2 Well RN-30

Twenty three logs of temperature and pressure were available from well RN-30, of which eleven out of them were done during drilling operation, four during injection, six during warm-up period and two during discharge test. In Figure 4.1 are shown the profiles of these temperature (above) and pressure (below) logs. Profiles from 14/04 to 08/05/2011 were logged during drilling operation, injection profiles logged in 26/05 and 04/06 2011, warm-up profile are between 05/06/2011 to 08/03/2012 and the discharge profiles logged on 21/06/2012. The profiles are plotted against the true vertical depth of the well and are plotted along with their boiling point depth curve. The injection temperature profiles have been used to determine the feed-zone locations inside the well. A total of five feed-zones are observed from these profiles. First feed-zone located at 390 m, second at a depth of 768 m and the third at 907 m depth. Another feed-zone was located at around 1770 m and the last one at 2260 m depth. The first three feed-zones were cemented and cased off and the last two are in the production part of the well (see the Figure A.4.1 in appendix).

The temperature warm-up profiles have been used to explain the flow pattern and for estimation of the formation temperature. At the top of the well, 0 – 180 m, the profiles show indication of cold inflow lowering the temperature (10 – 20 °C), then follows a conductive pattern in an interval between 180 – 500 m. The boiling point depth curve is shifted at a depth around 270 m were the boiling starts at that depth, this may be as the results of the hot inflow at the 390 m. At a depth between 500 and 2000 m the convective profiles are encountered which can reflect the fluid circulation in this section of the well. In the bottom section of the well, the conduction profiles appear again.

The data points to be used in the BERGHITI programme were selected from the temperature logs at the depth of the feed-zones, their estimated formation temperature were determined and then plotted in the same graph (Figure 4.1). The formation temperature of the well was estimated from these points and a line drawn connecting these points. The formation temperature appear to follow the boiling point depth curve with the maximum temperature range in the production part 300 – 355 °C.

The pressure profiles reveal a pivot point at approximately 1520 m depth with 98 bar pressure, which is above the two main feed zones at 1770 and 2260 m depth. Since the feed zones detected above are behind casing. This suggest possible feed zones between the casing depth and the pivot point not detected in temperature logs. The boiling point pressure curve is also shifted to 270 m which show same trend as the formation pressure in the bottom section of the well.

4.3 Well RN-32

Figure 4.2 show the temperature (above) and pressure (below) profiles plotted from the data logged during injection, warm-up and discharge testing of the well RN-32. Profiles from 11/02 to 03/04/2013 were logged during drilling operation, injection profiles logged in 09/04 and 14/04 2013, the discharge profiles logged on 08/04/2014, the rest are the warm-up profiles**.** The Figure A.4.2 in Appendix describes the casing types and depths for this well.

From the injection and warm-up temperature profiles, two feed-zone are observed one at around 883 m and another at 1040 m depth. The warm-up temperature profiles show an isothermal pattern from about 100 m to the bottom of the well with quite constant temperature change with depth. The boiling seems to start inside the well at a depth around 550 m. The formation temperature obtained from the warm-up profiles seems to trend same way as the warm-up profiles and the maximum temperature at the production zone of the well is around 250 °C.

The pressure profiles plotted together with the reservoir pressure indicates that the pivot point is close to 880 m and pressure is 27 bar at that point. The boiling pressure point depth curve is again shifted at 550 m depth which suggest that the boiling is inside the well and start at that depth. Also, the pressure warm-up profiles indicate that pressure builds up at the wellhead which can suggest that water is boiling inside the well, which then results in steam accumulation in the upper part of the well.

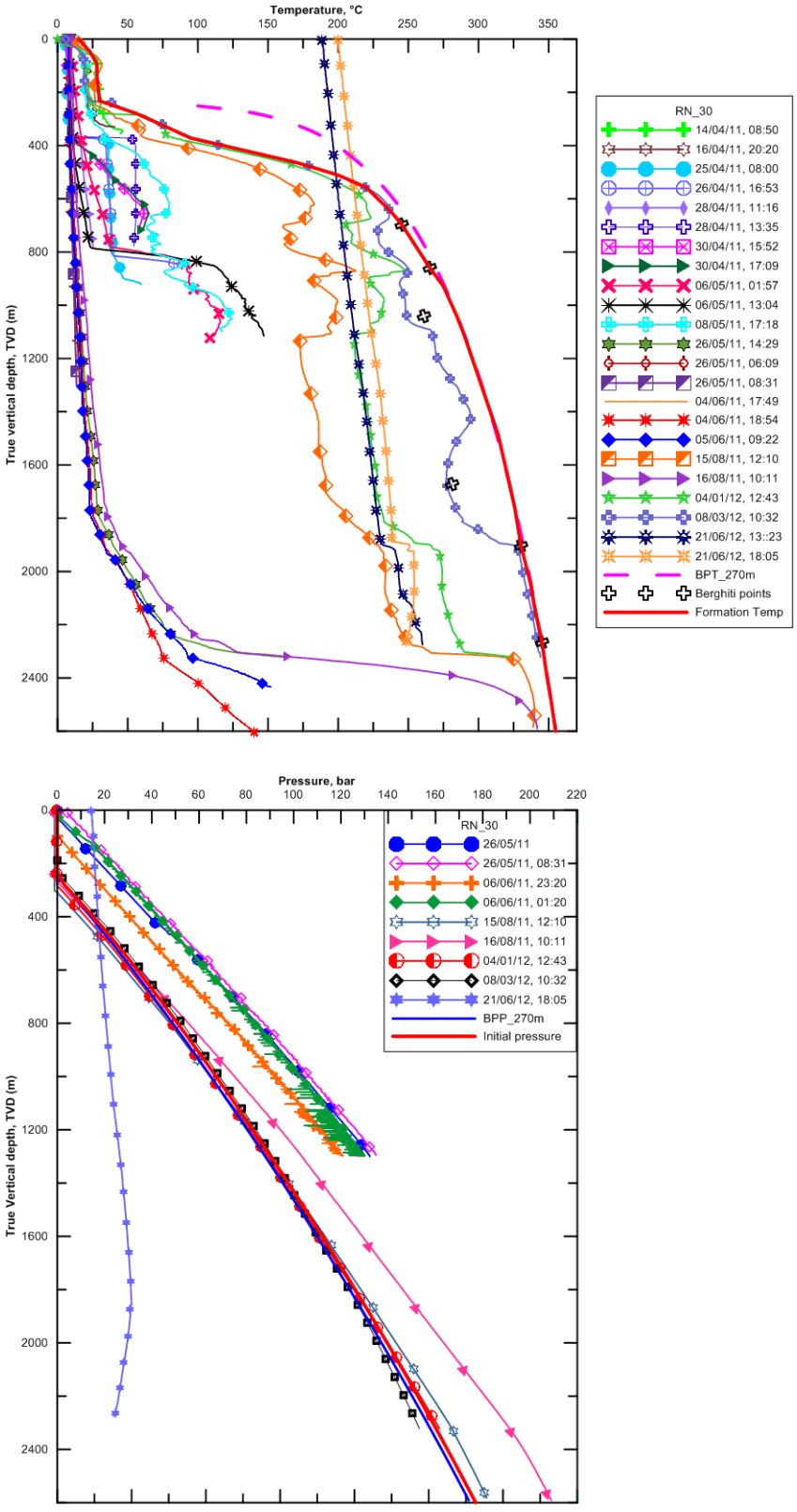

Figure 4.1: Profiles for the injection, warm-up, discharge and estimated formation temperature (above) and reservoir pressure (below) for RN-30.

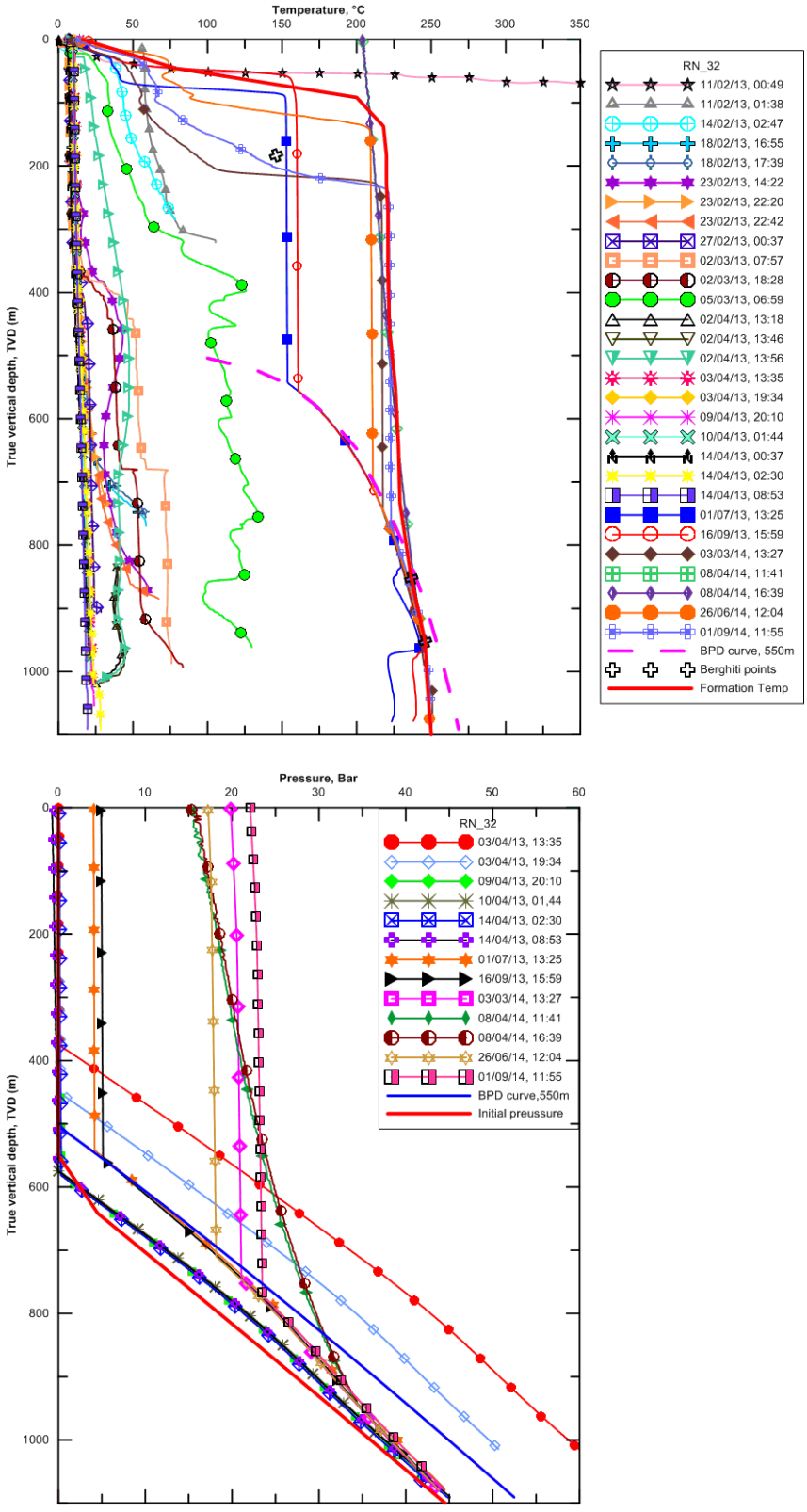

Figure 4.2: Profiles for the injection, warm-up, discharge and estimated formation temperature (above) and reservoir pressure (below) for RN-32.

5 Discharge tests

5.1 Introduction

Upon completion of a geothermal well, the well is given a certain period to warm up and recover its temperature. As temperature of the fluid increases during the warm up period, the wellhead pressure builds up. In most cases, wells only need a pressure built at the wellhead to start their own flow (self-sustained flow) to the surface. Unfortunately this is not the case for every well, some are difficult to start. The non-self-sustained flow occurs in wells due to under pressured or where there is cold section in the upper section of the wellbore (Grant and Bixley, 2011). Again in higher elevation areas the self-sustained flow of the wells can be difficulty especially for liquid dominated systems as the liquid level appears to be deep inside the well. To start flowing for these type of wells, the boiling fluid need to replace the cold column in the well. Different methods can be applied to stimulate geothermal wells and start them up. Pressurizing the well, gas lift, stream injection and work-over are some of the methods used to stimulate wells in order to initiate flow and are discussed in detail by Grant and Bixley (2011).

After the well has been started, a discharge test is carried out with the main purposes of obtaining information on the well's productivity and fluid chemistry. The wellhead pressures as function of time, gas and fluid chemistry are measured. Downhole measurements are also done where temperature and pressure logging tools are lowered down to the bottom of the well and retrieved back to the surface. Equipment selection in team of size and type is based on availability, accuracy and expected production rate, pressure and fluid type (also information from logging prior to the production test which can be obtained from nearby wells). A short time vertical discharge together with the James lip-pressure method can be used to determine the suitable equipment for long time testing as well as to estimate the production rate. The liquid flow is measured in a V-notch weir while the vapour is allowed to escape into the atmosphere. Enthalpy and chemistry of the fluid can also be estimated during short time discharge by observing the discharge plume. The discharge can also help to clear debris from the well (Grant and Bixley, 2011).

Number of standard techniques can be used to determine the flowing characteristics and production capacity of the well during discharge testing. James lip-pressure method and steam-water separator method are among them and are discussed in detail in the following sections.

5.2 Methods

5.2.1 James lip-pressure method

This method is based on an empirical formula developed by James (1966). The method is economical and more useful for the highly productive two – phase geothermal wells, but not efficient as the steam – water separator method (Grant and Bixley, 2011). The method involves first the discharge of the steam – water mixture from the tested well through the sized pipe into the silencer (or the separator of steam and water phase) at atmospheric pressure. The lip pressure is measured at the end of the discharge pipe when enters the silencer and water separated from the silencer is measurement in a V-notch weir. The steam is allowed to escape into the atmosphere.

The James formula relates the enthalpy, mass flow, area of the discharge pipe and the lip pressure. It is represented as follows;

$$\frac{GxH^{1.102}}{P^{0.96}} = 184 \tag{5.1}$$

with $$G = W/A \tag{5.2}$$

Where; G is the mass flow per unit area (kg/s.cm^2), W is the total mass flow (kg/s), H is the enthalpy (kJ/kg), P is the lip-pressure in bar – absolute and A is the cross-sectional area of the pipe in cm^2.

When the two – phase fluid is discharged at atmospheric pressure, the enthalpies of steam (H_s) and water (H_w) together with total enthalpy (H) are used in calculations. If the water flow, W_w separated is known then the total mass flow, W is given by;

$$W = W_w \frac{H_s - H_w}{H_s - H_t} \pi r^2 \tag{5.3}$$

Combining the equations (1.1) – (1.3), we get;

$$\frac{W_w}{AP^{0.96}} = \frac{184}{H^{1.102}} \frac{H_s - H}{H_s - H_w} \tag{5.4}$$

By measuring the lip pressure, water flow, cross – sectional area of the pipe then the total enthalpy can be obtained numerically. The enthalpies of steam and water can be obtained with the help of steam – table from their corresponding temperatures (and pressures). The steam mass fraction, X is given by the relationship below;

$$X = \frac{H - H_w}{H_s - H_w} \tag{5.5}$$

5.2.2 Steam – water separator method

The steam-water separator method is an empirical approach developed first in late 1950's and is the method resulted from steam-water separator uses in geothermal fields. The steam-water separators have been designed since then and progressed with some modifications (Lazanlde-Crabtree, 1984). They are often characterised by their orientations as either horizontal or vertical. After tests in many part of the world the vertical cyclone separator is the best for geothermal application (Banma, 1961 and Lazanlde-Crabtree, 1984). The horizontal separator is the new Icelandic design (since 1990) and mostly used in Iceland.

The method uses an efficient separator to separate the liquid phase from the steam (plus non-condensable gas) and permit the measurement of individual phase by conventional methods. If a properly designed separator is used, the separation efficiency can be up to 99.9%. According to Grant and Bixley (2011), the overall accuracy will normally not exceed ±2% of the separated steam and water flows, however the improvement of the overall results can always be attained for some wells, such as wells the feed zones of which temperature is known. By using the differential pressures across standard orifice, the separated water phase is measured. During measurement caution should be taken in order to prevent the water boiling across the orifice by cooling the water before measurement.

The general formula for the total mass flow, W (kg/s) by using the differential pressure, ΔP (mbar) through an orifice is given in equation (5.6) where C is the orifice constant, ε is the expansibility factor for the compressible gases, V_{fluid} is the specific volume of the fluid through the orifice and β is diameter ratio of the measuring orifice and stream pipe (d/D).

$$W = C\ x\ \varepsilon\ x\ \sqrt{\frac{\Delta P}{V_{fluid}}} \tag{5.6}$$

and $$\varepsilon = 1 - (0.41 + 0.35\beta^4)\frac{\Delta P}{1.3xP} \tag{5.7}$$

The steam expansibility factor becomes significant if the differential pressure is large and is greater than 0.3 bar (or line pressure is less than 3 bar). For water flow, the expansibility factor is 1 (Grant and Bixley, 2011).

Mass flow of water at atmospheric pressure into the v-notch can be estimated from the measured water height with the equation (5.8) below. Also equation (5.9) can be used for steam mass flow estimation.

$$Q_s = 2.733\sqrt{\Delta P} \tag{5.8}$$

$$Q_w = 0.0146W_{height}^{2.47} \tag{5.9}$$

Where W_{height} is the water height in the V-notch weir.

5.3 Data processing and interpretation

5.3.1 Discharge test for well RN-30

The discharge (step–rate) test was carried out on 21st June 2012 after the well had been successfully started on 29th May 2012. The well discharged without problems but prior to the 29th discharge, some attempts were made to initiate discharge in the well after self-sustained discharge failed. In March 2012 the well was stimulated by pressurizing the well (pumping air in the well) but self-sustained discharge only lasted for a few days. In April 2012, scaling problems caused the well to be closed after discharging for one day. The third attempt started on 12th May and then discharge was successfully initiated on 29th May (Gylfadóttir and Hardardóttir, 2013).

The well was discharged through a lip-pressure pipe which was 16 cm in diameter, into a steam separator (silencer) and the test was carried out in four steps. During the first step, the valve opening was 5 cm and the average wellhead pressure was 11.2 bar while the critical pressure was 0.8 bar and the differential pressure measured about 113 mbar. For the second step the valve opening was changed to 3.5 cm and the average wellhead pressure increased to 13.5 bar, critical pressure to 0.4 bar and differential pressure was changed to about 107 mbar. In the third step the opening was increased to 8 cm and the well head pressure decreased to 10.1 bar, critical pressure to 1.1 bar and differential pressure to about 91 mbar. For the fourth step, which was the last step, the opening was reduced again to 3.5 cm during the wellhead pressure was approximately 14.1 bar, the critical pressure about 0.5 bar and the differential pressure about 97 mbar. In Figures 5.1 **(a-c)** are shown the automatic and manual reading of the wellhead, critical and differential pressures respectively, plotted together with the valve opening (in percentages).

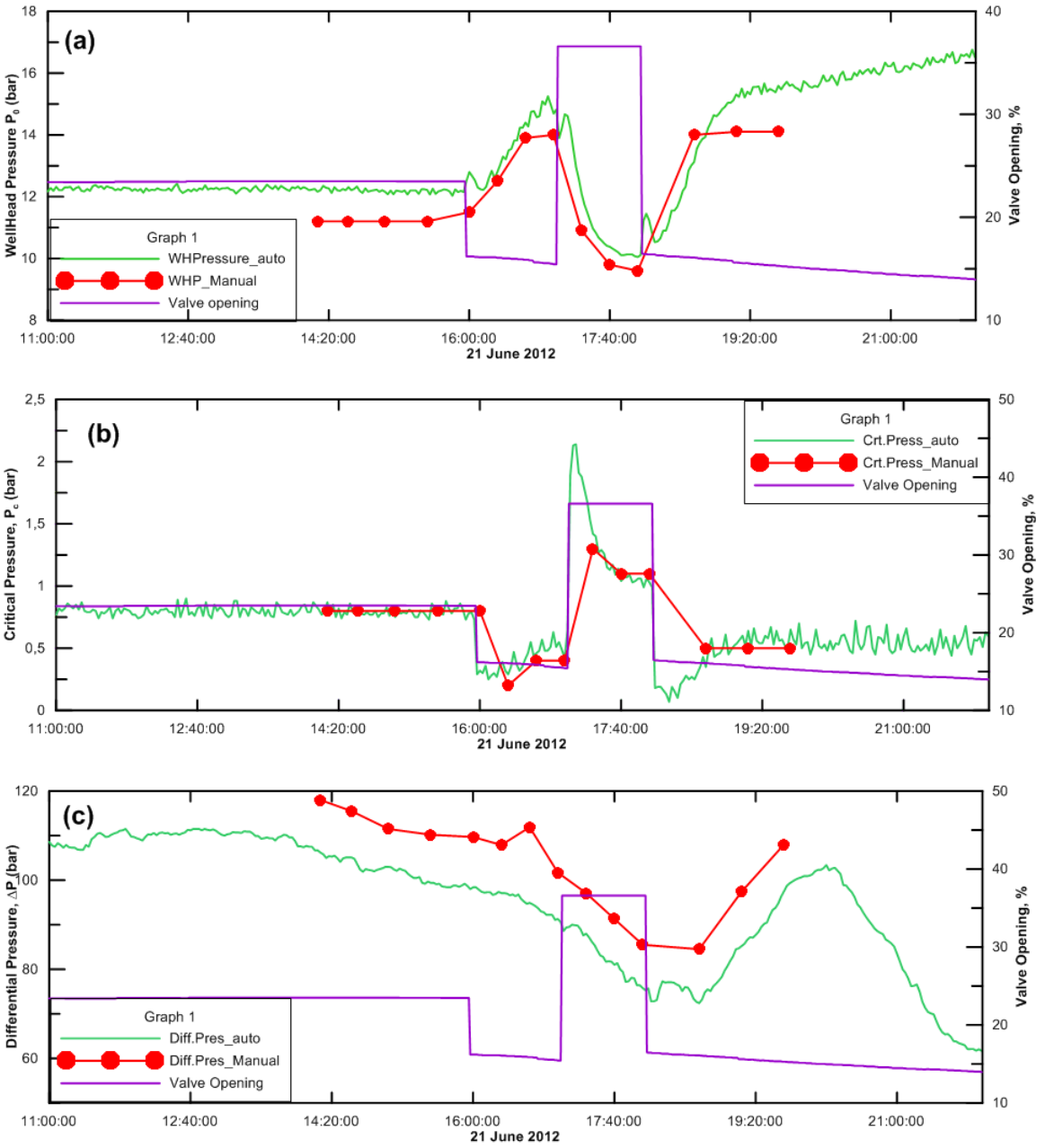

Figure 5.1: Automatic and manual reading of the wellhead (a), critical (b) and differential pressures (c) for the discharge test of RN-30. Together with the opening of the well (valve opening).

The water height and the water flow are measured in the V-notch weir while the temperature and pressure are measured by the K10 logging tool. For well RN-30 the K10 was situated at 2450 m depth in the well during the test. In Figure 5.2 the temperature and pressure measurements are plotted together with the boiling point temperature for the measured pressure. During the test, the V-notch weir clogged with silica precipitation which made difficult in measuring water height in v-notch.

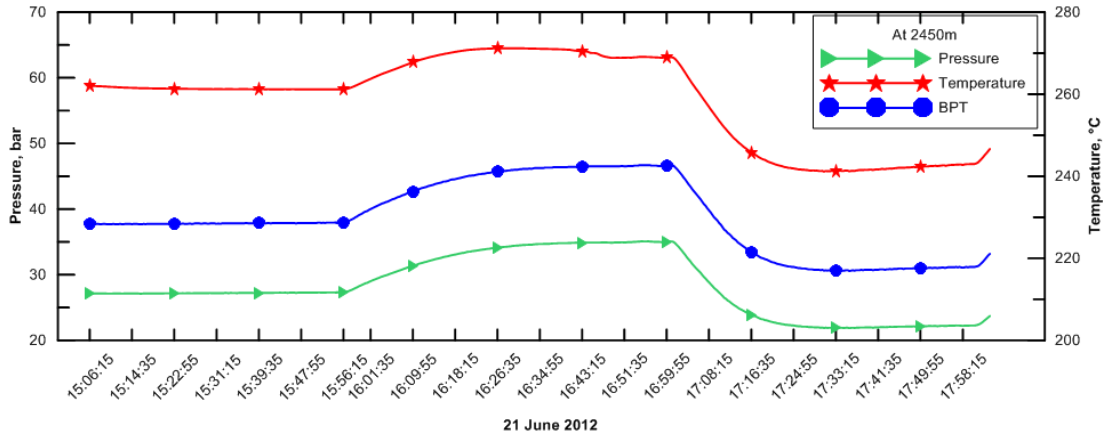

Figure 5.2: Measured T and P at 2450 m during the step-rate discharge test together with the boiling point temperature for the measured pressure.

After the information about wellhead, critical, differential pressures, water height and water flow in V-notch weir are obtained, the flow characteristics of the well are analysed and the production capacity of the well is estimated. The James lip-pressure method, as described in the section 5.2.1 above, is applied for this case. With the help of the LIP program from the ICEBOX software package, the enthalpies and flow rates are calculated (Arason et al., 2004). Tables 5.1 and 5.2 below show the average measured parameters and the calculated values. For values in Table 5.1 the separation pressure was taken to be 1 bar-a while in table Table 5.2 the separation pressure was 15 bar-a. It should be noted that, the separation pressure for the Reykjanes power plant is 19 bar-a, however, the maximum discharge pressure for this well is below 19 bar. Therefore, for the sake of electric power estimation, 15 bar-a separation pressure was used. This was taken as average discharge pressure during the test. As stated before, the V-notch weir clogged when the water discharged into it and therefore measurements for the height of the water was difficult. Instead the water flow was measure directly and the height of the water was calculated with equation (5.9) above to get the correct input for the LIP program.

In Table 5.3 are displayed the productivity indexes (PI) of the well, calculated for each step of the test, which were calculated by ratio of the change in flow rate to the change in pressure measured at 2450 m depth in the well. Figure 5.3 illustrates how the productivity index can be estimated from the slope of the line connecting the data points of total mass flow vs. measured pressure at 2450 m.

Table 5.1: Measured and calculated values for well RN-30 by the James lip-pressure method, with pipe diameter 16 cm and the separation pressure 1 bar-a.

Step	Time	Valve (cm)	Q_w (kg/s)	P_c (bar)	W_{height} (cm)	H (kJ/kg)	Q_t (kg/s)	Q_w (kg/s)	Q_s (kg/s)	X
1st	14:12 – 16:00	5	1.09	0.8	5.73	2464.2	12.0	1.1	10.9	0.9
2nd	16:20 – 17:00	3.5	1.08	0.4	5.71	2415	9.7	1.1	8.6	0.9
3rd	17:20 – 18:00	8	1.01	1.1	5.56	2503.1	13.7	1.1	12.6	0.9
4th	18:40 – 19:40	3.5	0.97	0.5	5.47	2452.1	10.4	1.0	9.4	0.9

Table 5.2: Calculated values for well RN-30 by the James Lip Pressure Method, pipe diameter is 16 cm and the separation pressure is 15 bar-a.

Step	Q_w (kg/s)	Q_s (kg/s)	X
1st	2.0	10.0	0.8
2nd	1.9	7.8	0.8
3rd	2.0	11.7	0.9
4th	1.8	8.6	0.8

Table 5.3: Productivity index, PI, of well RN-30.

Step	Q_t (kg/s)	P (bar)	ΔQ (kg/s)	ΔP (bar)	PI [(kg/s)/bar]
1st	12	27.25			
2nd	9.66	34.62	-2.34	7.37	0.32
3rd	13.66	22.13	4	-12.49	0.32
4th	10.44		-3.22		

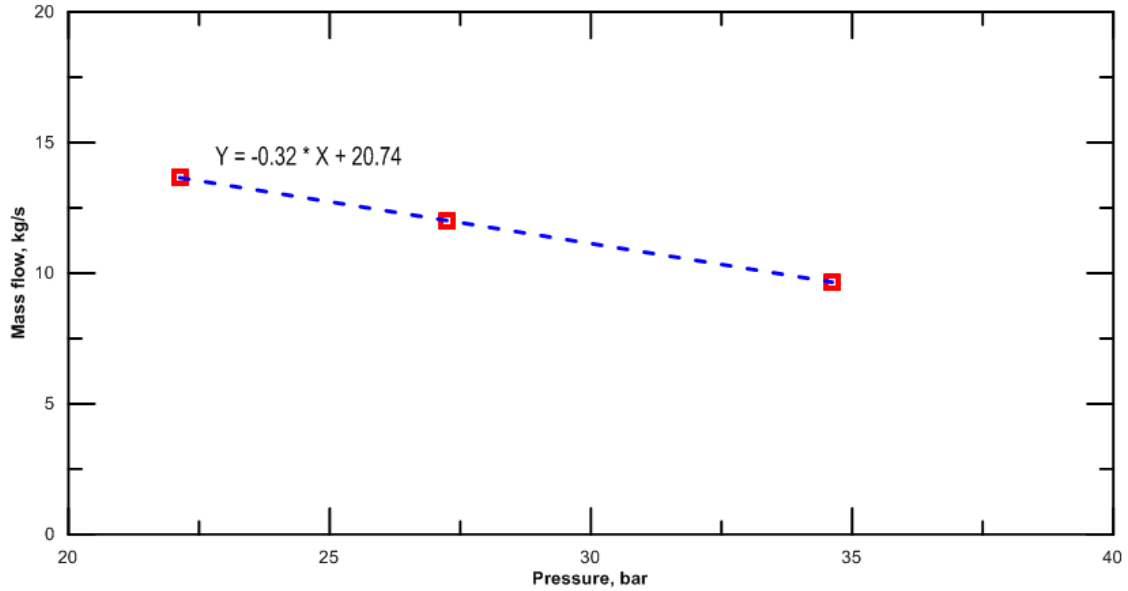

Figure 5.3: Estimation of productivity index, PI for RN-30.

The deliverability characteristics of well RN-30 indicates that the well can provide a steam flow of range 7.8 to 11.7 kg/s at a separation pressure of 15 bar. Grant et al., (1982) put an assumption that averagely 2 kg/s of steam flow is needed for a geothermal power plant to convert into 1 MW_e. However, the Reykjanes geothermal power plant need 1.68 kg/s steam flow for 1 MW_e (Gylfadóttir and Hardardóttir, 2013). Therefore, a range of 4.6 – 7.0 MW_e can be produced from this well. The deliverability curve is attached in the Appendix A, Figure A.5.1. The productivity index is estimated to be 0.32 (kg/s)/bar which is very low and it indicates that the well may be poor producer.

5.3.2 Discharge test for well RN-32

In well RN-32, a self-sustained discharge was possible and it was allowed to discharge into a separator since 20th March 2014. The discharge (step–rate) test was then carried out on 8th April 2014 and on 09th April 2014 when few additional measurements were carried out and in total, 6 steps were performed (Gylfadóttir et al., 2014). Measurements on 08th April were done by first opening the valve to 4 cm then decreasing it to 3.2 cm in the second step, then decreasing it further to 2.2 cm and lastly increasing the valve opening to 5.4 cm in the fourth step. In the following day further measurements were performed in two steps by increasing the opening to 10 cm and 13 cm respectively. Figures 5.4 (a) to (c) depicts the automatic and manual reading of the wellhead, critical and differential pressures done on 08th April 2014 (in Appendix, Figures A. 5.2(a) – (c) are the plots for the 09th April measurements). In Figure 5.5 are shown the temperature and pressure measurements plotted together with the boiling point temperature for the measured pressure. Tables 5.4 and 5.5 present a summary of the average measured parameters and the calculated ones at 1 bar and 15 bar-a separation pressure respectively. One should note that the maximum discharge pressure for this well is below the separation pressure use in the Reykjanes power plant for electric power, which is 19 bar-a. Therefore the electric power was estimated using 15 bar-a separation pressure which was an average discharge pressure during the test. Values for enthalpies and flow rates were calculated with the LIP programme.

Table 5.4: Measured and calculated values for well RN-32 by the James lip-pressure method, with a 16 cm diameter discharge lip pipe and separation pressure of 1 bar-a.

Step	Time	Valve (cm)	P_0 (bar)	Pc (bar)	Wheight (cm)	H (kJ/kg)	Qt (kg/s)	Qw (kg/s)	Qs (kg/s)	X
1st	11:48 – 12:53	4	15.5	0.73	19.1	1039	29.9	21.7	8.2	0.3
2nd	13:25 – 14:14	3.2	15.3	0.53	18.167	1043	26.5	19.2	7.3	0.3
3rd	14:26 – 15:03	2.2	14.9	0.13	16	1056	19.5	14.0	5.5	0.3
4th	15:12 – 16:35	5.4	15.5	1.2	20.97	1038	37.7	27.4	10.3	0.3
5th	16:05 – 16:40	10	15.6	2.3	23.5	1101	52.0	36.3	15.7	0.3
6th	16:50 – 17:10	13	15.5	2.7	24	1128	55.8	38.2	17.5	0.3

Table 5.5: Calculated values for well RN-32 by the James lip-pressure method, with lip pipe diameter of 16 cm and separation pressure of 15 bar-a.

Step	Q_w (kg/s)	Q_s (kg/s)	X
1st	26.9	3.0	0.1
2nd	23.8	2.7	0.1
3rd	17.4	2.1	0.1
4th	34.0	3.7	0.1
5th	45.1	6.9	0.1
6th	47.7	8.1	0.1

Table 5.6 below shows the production indices, PI, which was calculated from the ratio of the change in total flow rate to the change of the pressure measured at 1025 m inside the well. In the Figure 5.7 is another way of determining the production indices as the slope from the plotting of total mass flow vs. measure pressure at 1025 m during the test. Also the flow is taken as zero at 1025 m before the discharge and the formation pressure at that depth is used. The estimated determined by the slope gives PI = 6.57 (kg/s)/bar which differ with the average calculated PI.

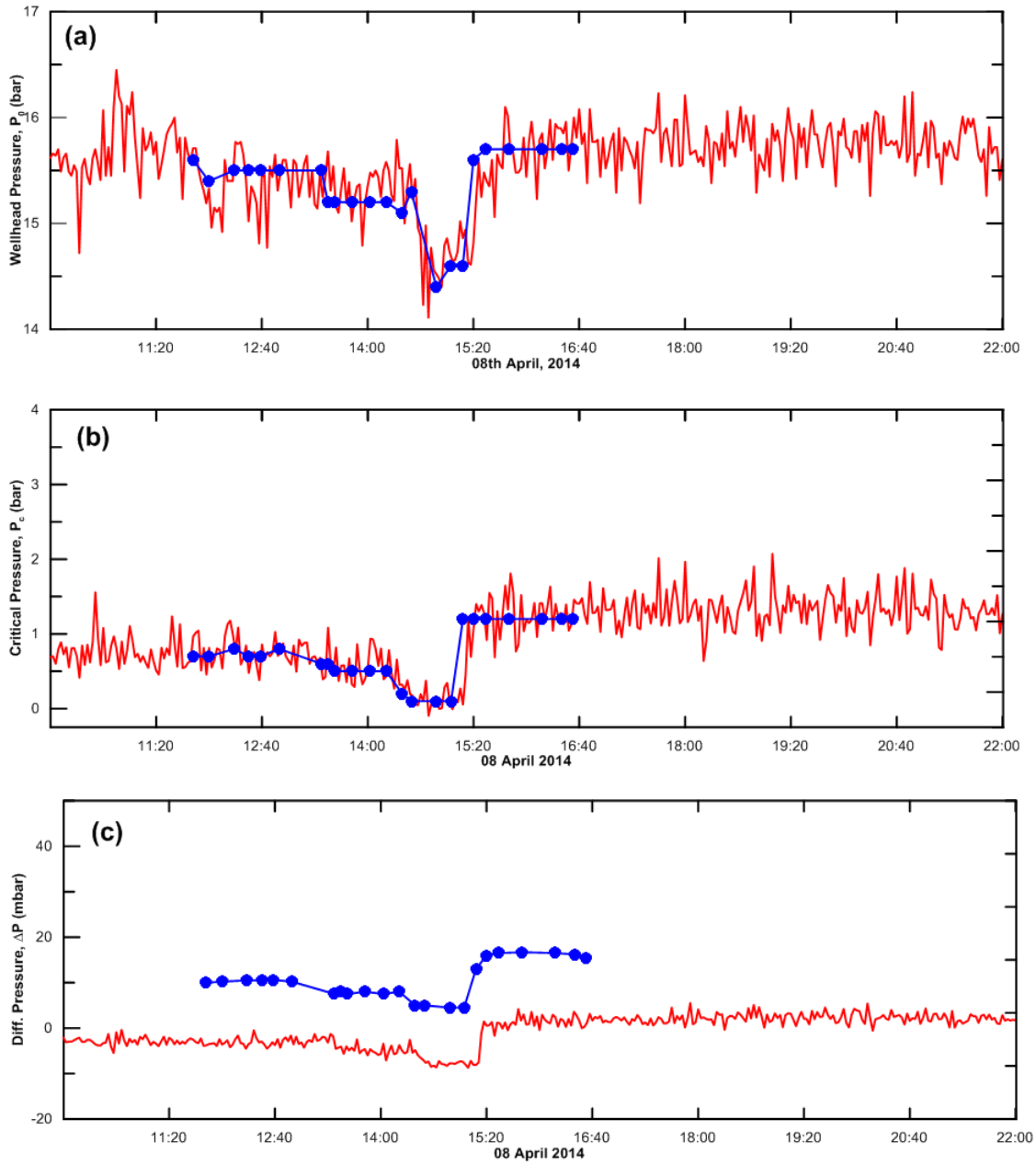

Figure 5.4: Automatic and manual reading of the wellhead (a), critical (b) and differential pressures (c) for the discharge test of RN-32.

The analysis of the measurements form the discharge test of well RN-32 on 08th and 09th April 2014 give an estimates of steam flow in range 2.1 – 8.1 kg/s at the separation pressure of 15 bar-a which is equivalent to a maximum of electric power of 1.3 – 4.8 MW_e if the 1.68 kg/s of steam flow convert 1 MW_e. The well has a production index of, PI, of 6.57 (kg/s)/bar which. Comparison of injectivity indices (*II* (10.96 and 26.3 (l/s)/bar) obtained in injection test and the productivity index PI, (6.57 (kg/s)/bar) give the relationship of PI= II/4 which indicates that it can be a good producer. The relation is not much far from that in the study of Rutagarama, (2012) about the comparison of PI and II for the wells in Reykjanes geothermal field.

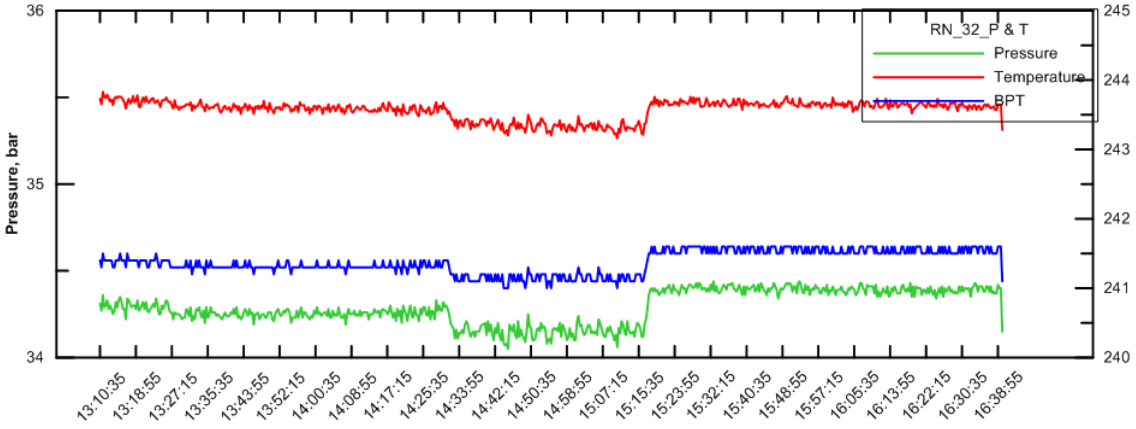

Figure 5.5: Measured temperature and pressure at 1025 m during the step-rate discharge test of well RN-32 together with the boiling point temperature for the measured pressure.

Table 5.6: Productivity Index of RN-32, calculated from the manual data during the step rate flow testing and pressure at 1025 m.

Step	Q_t (kg/s)	P (bar)	ΔQ (kg/s)	ΔP (bar)	PI [(kg/s)/bar]
1st	29.92	34.3			
2nd	26.5	34.25	-3.42	-0.05	68.4
3rd	19.51	34.17	-6.99	-0.08	87.38
4th	37.69	34.38	18.18	0.21	86.57

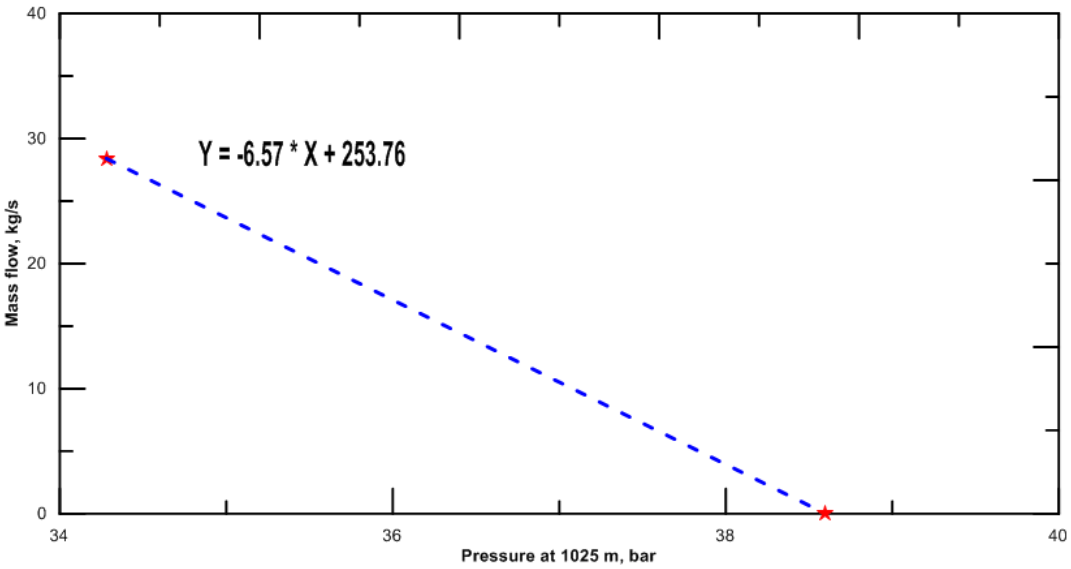

Figure 5.6: Estimation of productivity index, PI for RN-32

6 Simple analytical modelling – lumped parameter

Modelling of geothermal reservoir is a useful technique that can help with decision making during exploration and exploitation of the resources. It aims to help define the natural, physical conditions and estimate properties of the geothermal system in question. It is also an important tool for predicting reservoir response to future production, to estimate the production potential of the system as well as to test the outcome of different management approaches (Axelsson, 2012). Different modelling approaches exist ranging from simple analytical to detailed numerical modelling. Lumped parameter modelling is one of the simple modelling method, which is powerful and, cost effective alternative to detailed numerical modelling (Axelsson, 1989).

Lumped parameter modelling of reservoir pressure changes involves modelling the hydrological properties of a reservoir, or parts of a reservoir, by lumping them together in one or two parameters for the reservoir, or each sub-part. The lumped models can consequently be used to predict the responses of a reservoir to different future production schemes and to help in understanding the properties of the reservoir being simulated. It has been successfully used for many decades to simulate data from many geothermal systems in the world includes Iceland, China, Central America, Turkey, Philippines and Eastern Europe. (Axelsson, 1989; Axelsson and Arason, 1992; Axelsson et al., 2005).

6.1 Theory

The theoretical description of lumped parameter modelling is based on that presented by Axelsson (1989). Figure 6.1 shows sketched examples of lumped parameter networks, which consist of tanks/capacitors (storage coefficients) and conductors/resisters. A capacitor has the mass storage coefficient κ when responding to a load of mass m by a pressure increase P, which is given by $P = m/\kappa$. The mass flow over a conductor is given as $q = \sigma \Delta P$ when it is transferred through the mass conductor σ at differential pressure ΔP. The pressure inside the tanks simulates the pressure in different parts of the reservoir and the water extraction from the tanks simulates the production from the reservoir.

A lumped model is either open or closed. The open models are connected by a resistor to an infinity large imaginary reservoir which maintains a constant pressure throughout. The closed models are isolated from any external reservoirs. Real reservoirs may be presented by a few tank open and closed lumped parameter models (Axelsson, 1989; Axelsson and Arason, 1992).

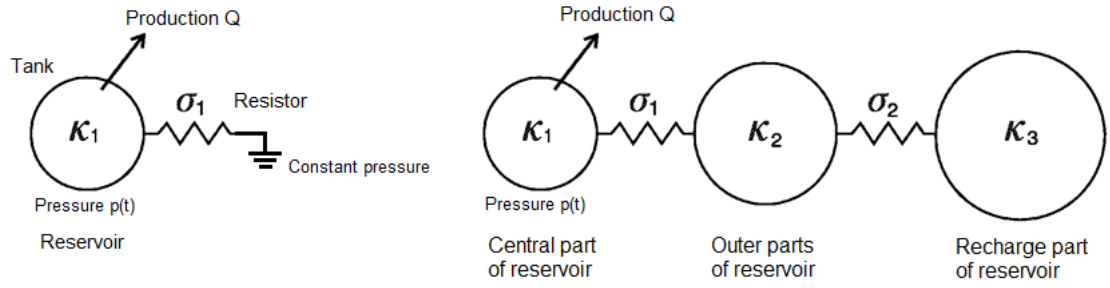

Figure 6.1: Example of lumped parameter models used to simulate pressure changes in geothermal system. One tank open model (left) and three tanks closed model (right) (Axelsson, 1989).

The two equations below are the basic equations that describe the behaviour of lumped parameter models used to simulate mass flow and pressure changes in geothermal reservoirs;

$$q_{ik} = \sigma_{ik}(P_k - P_i) \qquad \text{Mass flow equation} \qquad (6.1)$$

$$\frac{\kappa_i dP_i}{dt} = \sum_{k=1}^{N} q_{ik} - \sigma_i P_i + Q_i \qquad \text{Conservation of mass} \qquad (6.2)$$

Here P_k is the pressure in capacitor number k, q_{ik} is the mass flow from capacitor number k to capacitor number k and Q_i is an external source mass flow into capacitor number i.

In an open one tank model the pressure response, ΔP, to a constant production, Q, starting at time $t=0$, is given by;

$$\Delta P(t) = -\left(Q/\sigma_1\right)\left[1 - e^{-\sigma_1 t/\kappa_1}\right] \qquad (6.3)$$

The general equation for the pressure response of a multiple tank open lumped model with N tanks is;

$$\Delta P(t) = -\sum_{j=1}^{N} Q\frac{A_j}{L_j}\left[1 - e^{-L_j t}\right] \qquad (6.4)$$

Similarly the pressure response of an N tank closed model is given by;

$$\Delta P(t) = -\sum_{j=1}^{N} Q\frac{A_j}{L_j}\left[1 - e^{-L_j t}\right] + QBt \qquad (6.5)$$

The coefficients A_j, L_j and B are functions of the storage coefficients of the tanks (κ_j) and the conductance coefficients of the resistors (σ_j) of the model.

PyLumpfit is a powerful computer program developed to perform the lumped parameter modelling. The software solves the simulation problem as an inverse problem and automatically fits the analytical response functions of lumped models to the measured

data by a nonlinear iterative least-squares technique for estimating the model parameters (Axelsson, 1989). The procedure is easy to follow and usually takes a very short time. The pressure data required are either from a single well monitored during short-term testing or for the whole reservoir during long–term monitoring. The program accepts pressure or water level data from either observation well or production wells. During modelling we aim at getting the best fitting parameters and the simplest way is to start with the simple one-tank model, first a closed one and then an open one. Consequently a two-tank closed or open model is applied and from that one can proceed to three-tank models, if the data allows. However, the goal is to end up with two models, an open and a closed model that fits best the data (Axelsson et al., 2005).

The best fit models obtained by the *PyLumpfit* program involve parameters that can be used to estimate the geothermal reservoir properties of a particular system by assuming a 2D flow pattern (Figure 6.2). Storage coefficients based on two storage mechanisms are generally applicable for liquid – dominated reservoirs, one for a confined reservoir and the other for an unconfined (free–surface) reservoir:

$$\kappa_i = V_i . s \qquad \text{Confined reservoir} \tag{6.6}$$

$$\kappa_i = {A_i . \emptyset}/{g} \qquad \text{Unconfined Reservoir} \tag{6.7}$$

Here, κ_i, V_i and A_i are the storage coefficient, volume and area of tank number *i*, respectively, where $s, \emptyset$ and g are storativity, porosity and specific gravity.

For a high temperature two phase reservoir the storativity is given as (Axelsson, 2012);

$$s = \rho_t \frac{\langle \rho\beta \rangle T}{L^2} \left(\frac{\rho_w - \rho_s}{\rho_w \rho_s} \right)^2 \tag{6.8}$$

$$\frac{1}{\rho_t} = \frac{X}{\rho_s} + \frac{(1 - X)}{\rho_w} \tag{6.9}$$

where $\langle \rho\beta \rangle$ denotes the volumetric heat capacity of the wet rock (J/m^3°C), T the reservoir temperature (°C), ρ_t, ρ_w and ρ_s the density of the two-phase mixture, density of water and density of steam (kg/m^3), respectively. L is the latent heat of vaporization of water at reservoir temperature (J/kg) and X is the steam mass fraction. In a high – temperature, two – phase reservoir storativity may change with time e.g. when a steam – zone expands. The lumped parameter modelling applied here assumes a constant storativity, an average for the simulation period.

The radius, *R*, and the half radii, *r*, of a tank are given by (see Figure 6.2);

$$R = \sqrt{{V}/{\pi H}} \tag{6.10}$$

$$r_1 = {R_1}/{2}\ ;\ r_2 = R_1 + \frac{R_2 - R_1}{2} \tag{6.11}$$

and the conductance σ_i, of tank i for 2D flow is defined by;

$$\sigma_i = \frac{2\pi Hk}{\ln\left({}^{r_{i+i}}/_{r_i}\right) v} \tag{6.12}$$

Here k is the reservoir permeability and ν is the kinematic fluid viscosity.

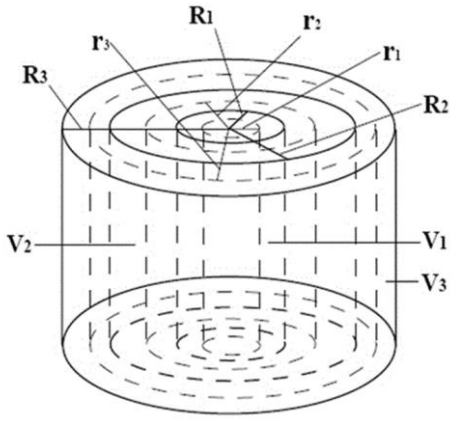

Figure 6.2: Flow configuration pattern of a three tank lumped parameter model assuming 2D-flow.

6.2 Modelling and reservoir response predictions

The mass production from the Reykjanes high temperature geothermal reservoir has been monitored since 1970 after the first production well was drilled. The average net mass production before electricity generation began in 2006 was around 41 kg/s, while in 2013 the generation was based on a net mass production of 436 kg/s after 15% reinjection of around 82 kg/s (Figure 6.3). The reinjection in Reykjanes started in 2009. Information obtained from different wells drilled in the field indicates that the reservoir temperature is in the range of 280 – 290 °C.

The Reykjanes reservoir is a two phase reservoir and some assumptions have been made for the parameter calculation based on the lumped modelling results. The average steam mass fraction, *X*, was assumed to be 0.1, average reservoir porosity $\emptyset$ = 0.1 and the reservoir temperature was taken as 280 °C. The reservoir thickness was estimated to be 1500 m.

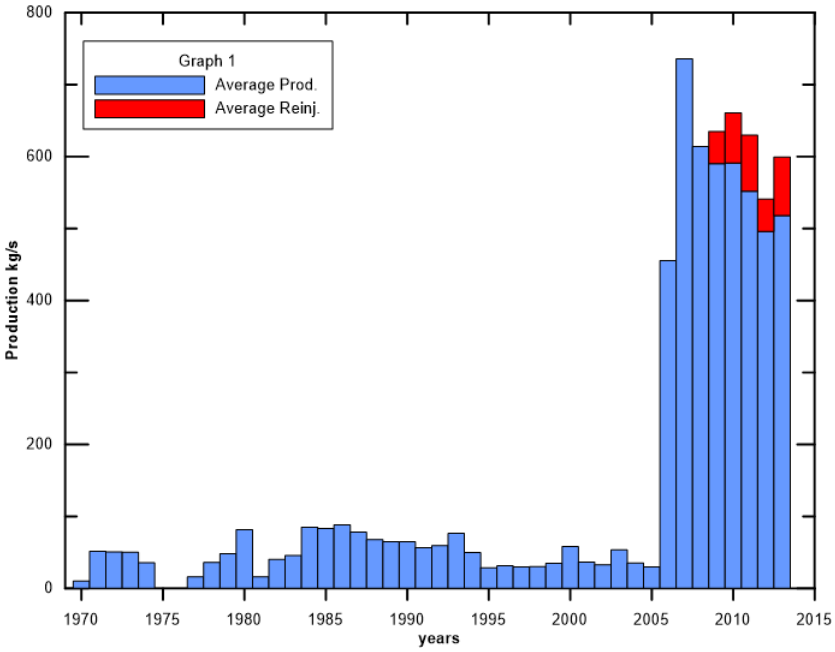

Figure 6.3: Mass production history of the Reykjanes high temperature geothermal system.

6.2.1 Well RN-12

RN-12 is a production well located in the centre of the Reykjanes production field, near well RN-09 (Figure 2.1). The well was drilled to a final depth of 2506 m in 2002. Change in the reservoir pressure has been monitored in the well since 2003 to date. Due to the electricity generation from 2006 the pressure in the well at 1500 m depth has dropped from around 122 bar in 2006 to 82 bar in 2014.

During the lumped parameter modelling different models were tested and the two–tank closed and open models fitted the measured data well, as depicted in the Figure 6.4 below. Table 6.1 lists the parameters for the two models and Table 6.2 presents the estimated reservoir properties based on the model parameters.

Table 6.1: Lumped parameter model parameters for well RN-12.

Parameters	2-tanks closed model	2-tanks opened model
A_1	1.83×10^{-9}	2.23×10^{-9}
L_1	4.51×10^{-8}	7.19×10^{-8}
A_2	-	3.27×10^{10}
L_2	-	2.97×10^{-9}
B	1.95×10^{-10}	-
κ_1 (kg/m^{3}Pa)	5.038×10^{4}	3.99×10^{4}
κ_2 (kg/m^{3}Pa)	4.738×10^{5}	3.0×10^{5}
σ_1 (kg/sPa)	2.054×10^{-3}	2.52×10^{-3}
σ_2 (kg/sPa)	-	1.01×10^{-3}
Coefficient of determination	99.83%	99.96%
Root mean square	0.61	0.28
Standard deviation	0.72	0.36

The results in table 6.2 are calculated assuming both a two-phase and a free-surface storativity (see equations 6.7 and 6.8). The calculated results suggest that assuming a 5.52×10^{-5} *kg/(Pa m^3)* storativity, the volume ranges from 5.4 km^3 of the two–tank open model to 8.6 km^3 for the two-tank closed model. While, if the reservoir is considered as unconfined (free-surface) the range is 44 – 70 km^3. However, the two – phase reservoir results in this case appear to make more sense than the unconfined. The reservoir permeability is in the range of 0.02 – 0.05 Darcy, which agrees with other estimates for wells drilled within the area.

Table 6.2: Estimated reservoir properties based on the parameters of the lumped parameter model for well RN-12.

Model	**Properties**	**Tanks**	
		1st tank	**2nd tank**
2-Tanks Closed	Reservoir volume for two-phase storativity (km^3)	0.9	8.6
	Area (km^2)	0.6	5.7
	Reservoir volume for free surface storativity (km^3)	7.4	70
	Permeability, k (D)	0.04	-
2-Tanks Opened	Reservoir volume for two-phase storativity (km^3)	0.7	5.4
	Area (km^2)	0.5	3.6
	Reservoir volume for free surface storativity (km^3)	5.9	44
	Permeability, k (Darcy)	0.05	0.02

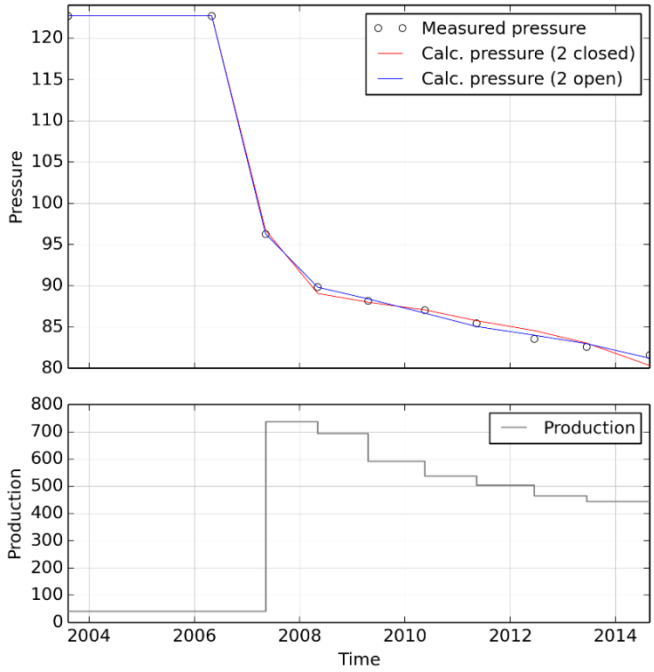

Figure 6.4: Observed and modelled pressure changes in well RN-12 using two-tank closed and open lumped parameter models.

After having modelled a particular geothermal system and estimated its properties, the next step is to use the model to predict the reservoir response to future production, assuming different scenarios. Based on the lumped parameter models presented above, three different scenarios for future prediction for the next 10 years have been considered. The first prediction is for what would be the pressure response if the current net mass production is maintained (with around 15% reinjection). The second scenario assumes 30% reinjection and the third one is based on 50% reinjection, which is considered the maximum reinjection target to achieve for Reykjanes.

Figure 6.5 below shows the prediction results for the current mass extraction with 15% reinjection (left) and with 30% (right). For 15% reinjection the predictions indicate that the pressure draw down in the next 10 years will be in the range of 9 – 24 bar. If reinjection of 30% is attained, and the mass extraction remains the same, the pressure draw down is predicted to be in the range of 2 – 17 bar. For 50 % reinjection, the predictions indicate that the pressure may increase by 10 bar if the prediction by the two-tank open model is considered.

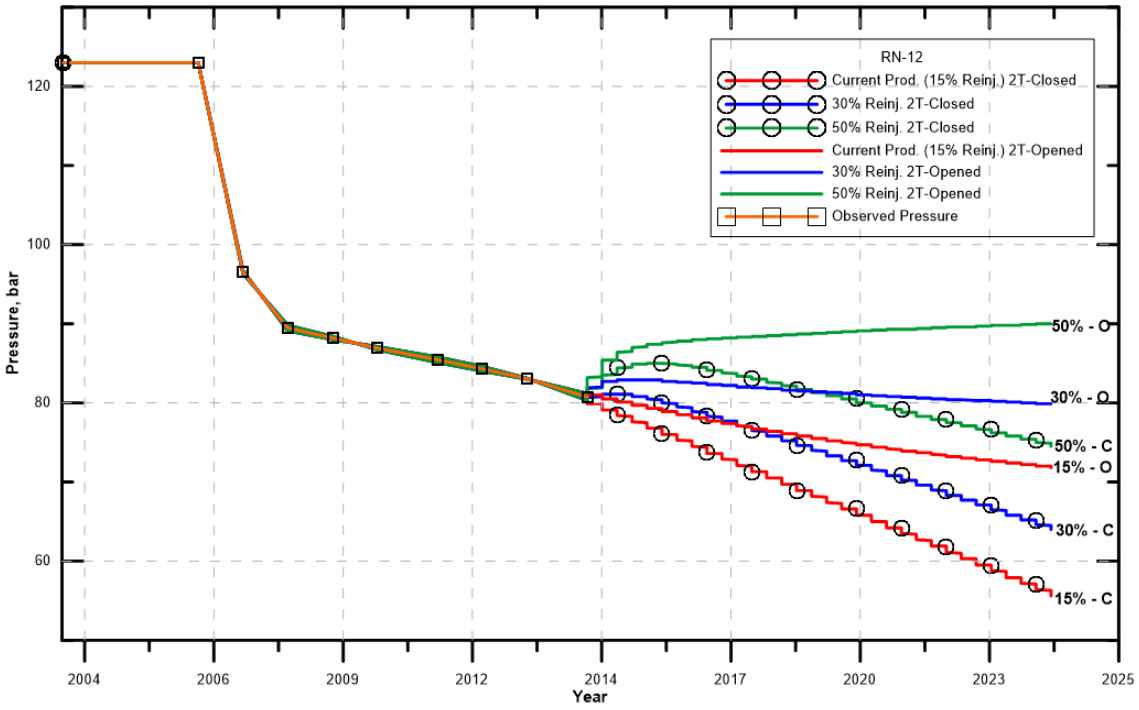

Figure 6.5: Pressure prediction results for well RN-12 for the next 10 years for current mass production with 15%, 30% and 50% reinjection.

6.2.2 Well RN-16

Well RN-16 is a well in the Reykajnes geothermal field drilled in 2004, located on the west peripheral of the main production area. It turned out to be poorly productive and is used as an observation well. The formation pressure of the well has been monitored since 2004 and the pressure down of over 22 bars has been observed since electricity generation began and up to 2014.

Two lumped parameter models provided an adequate fit for well RN-16, a two-tank closed model and a two-tank open model, after testing different models. Figure 6.6 shows the models results and Table 6.3 lists the parameters of the two models while Table 6.4 summarise calculated results of the models.

The results indicate that the estimated reservoir volume for the two – phase storativity is 10 to 17 km^3. However, if the reservoir is unconfined (free – surface storativity) then the estimated volume is 83 – 140 km^3, which is considered unrealistically large. The estimated reservoir permeability is 0.03 – 0.05 Darcy. The estimated values are slightly larger than those estimated for well RN-12; they are most likely influenced by the position of the well on the peripheral of the production reservoir.

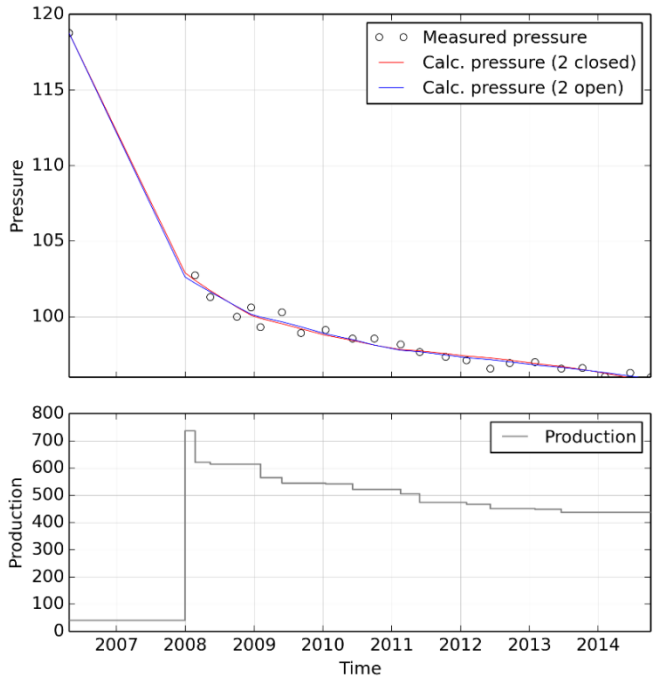

Figure 6.6: Observed and modelled pressure changes in well RN-16 using two-tank closed and open lumped parameter models.

Table 6.3: Lumped parameter model parameters for well RN-16.

Parameters	**2-tanks closed model**	**2-tanks opened model**
A_1	5.70×10^{-10}	5.71×10^{-10}
L_1	2.20×10^{-8}	3.23×10^{-8}
A_2	-	1.77×10^{10}
L_2	-	2.94×10^{-9}
B	9.26×10^{-11}	-
κ_1 (kg/m^{3}Pa)	1.54×10^{5}	1.36×10^{5}
κ_2 (kg/m^{3}Pa)	9.48×10^{5}	5.64×10^{5}
σ_1 (kg/sPa)	2.91×10^{-3}	3.46×10^{-3}
σ_2 (kg/sPa)	-	2.11×10^{-3}
Coefficient of determination	99.29%	99.36%
Root mean square	0.38	0.36
Standard deviation	0.41	0.40

Table 6.4: Estimated reservoir properties based on the parameters of the lumped parameter model for well RN-16.

Model	Properties	Tanks	
		1st tank	**2nd tank**
2-tanks closed	Reservoir volume for two-phase storativity (km^3)	2.8	17.2
	Area (km^2)	1.9	11.5
	Reservoir volume for free surface storativity (km^3)	22.7	139.5
	Permeability, k (D)	0.05	-
2-tanks opened	Reservoir volume for two-phase storativity (km^3)	2.5	10.2
	Area (km^2)	1.6	6.8
	Reservoir volume for free surface storativity (km^3)	20	83
	Permeability, k (D)	0.05	0.03

Pressure predictions for well RN-16 for the next 10 years have been calculated based on the above models. Current net mass production (with 15% reinjection), 30% reinjection and 50% reinjection have been considered as prediction scenarios (Figure 6.7). Using current net mass production (15% reinjection), the additional pressure draw down is predicted to reach 5-11 bar in the next 10 years. While a pressure draw down of 1 – 7 bar is predicted when 30% reinjection is achieved and a pressure increase by 6 bar in the next 10 years if the reinjection is 50%.

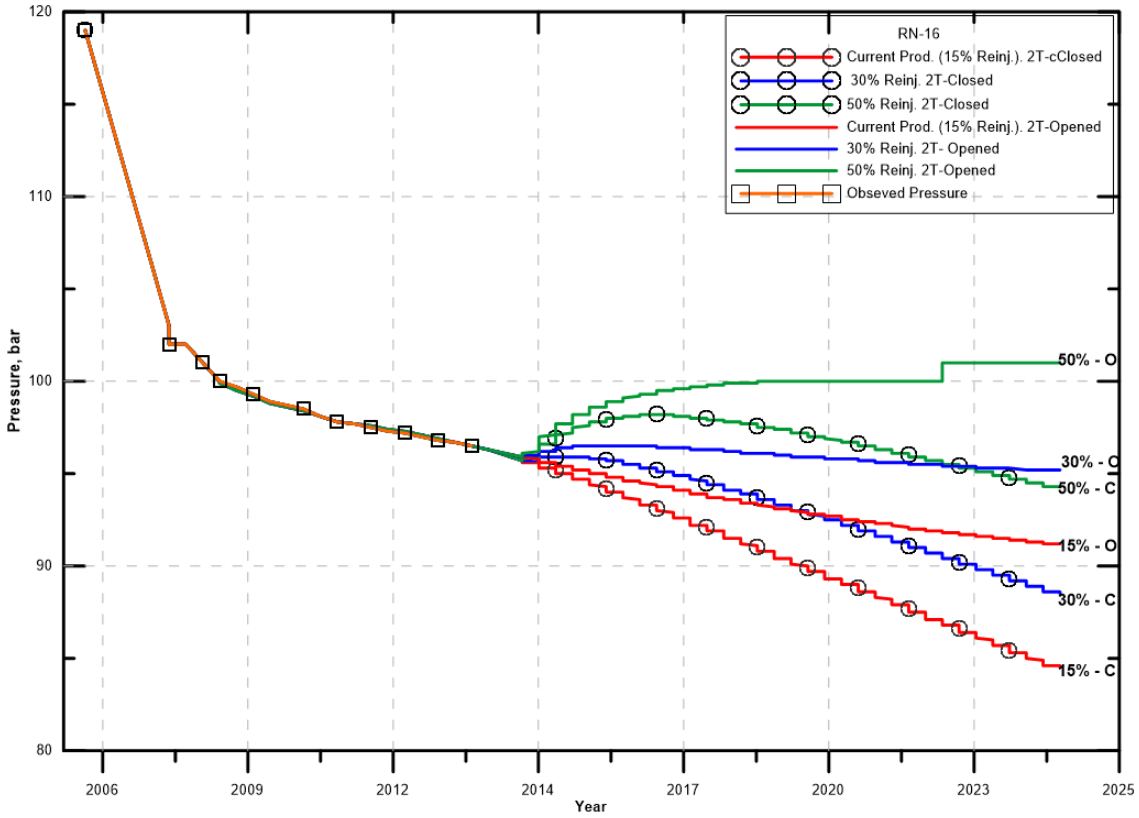

Figure 6.7: Pressure prediction results for well RN-16 for the next 10 years assuming current mass production with 30% reinjection and 50% reinjection.

7 Tracer testing

7.1 Background

Tracer testing is another type of well testing even though it doesn't involve the observation of pressure changes, rather it is a specific type of testing done during reinjection research and monitoring. Reinjection in geothermal fields is regarded as a reservoir management strategy aimed at sustainable and environmentally friendly geothermal utilization. Reinjection is referred to as the process of returning produced water back into the geothermal system after energy extraction. This helps keeping the utilization environmentally friendly, while providing extra recharge into the system, and to counteract pressure drawdown. While reinjection is very important in the management of geothermal resources, it still has some obstacles which can cause cooling of production wells, scaling and corrosion during operation as well as clogging of aquifers.

Tracer testing is a process of injecting a chemical tracer into a hydrological system and monitoring its recovery, through time at various observation points. Recovery time for a tracer depends on a number of factors which control fluid movement, including hydrogeological conditions and separation distance of wells. However, recovery often takes a few weeks to a few years. In geothermal research, the tracer testing technique serves the purpose of examining the connectivity of reinjection wells to production wells by tracing the flow within the reservoir and consequently assessing the possible cooling of production wells due to long term reinjection.

Axelsson et al. (2005) mention that the possible cooling of production wells is the main reinjection disadvantage, which has discouraged its application in some geothermal operations. In most cases this has happened as a result of small separating distance between reinjection and production wells or when direct flow-paths otherwise exist between the wells (open fractures).

Tracer testing techniques have a broad application in various disciplines of science; they have e.g. been used in hydrogeology for more than a century to characterize flow-paths and to estimate groundwater velocities. History reveals that quantitative tracer tests using chloride, fluorescein and bacteria were first used in Europe in the late 1800s (Divine and McDonnell, 2005). In geothermal research many types of tracer chemicals are used and their selection has to meet certain criteria, which include; the tracer should not be present in the reservoir (or at a concentration much lower than the expected tracer concentration), it should not react or absorb to reservoir rocks, it should be thermally stable at reservoir condition, and it should be easy to analysis, relatively inexpensive, and environmental friendly. Moreover, different tracers are selected according to phase-conditions of the geothermal system, either liquid, steam or two-phase dominated. For instance, halides (iodide (I) or bromide (Br)), radioactive tracers e.g. isotopes iodide (^{125}I) and (^{131}I), fluorescent dyes e.g. fluorescein and rhodamine, aromatic acids such benzoic acid, and naphthalene are applied in liquid dominated reservoirs (Axelsson, 2013).

Axelsson (2013) also lists other tracers commonly used for steam systems, such as fluorinated hydrocarbons, e.g. R-134a and R-23, and sulphur hexafluoride (SF_6). For two–phase systems use tracers like tritium (^3H) and alcohols, like methanol and n-propanol, are often used.

When the suitable tracer has been selected based on the criteria mentioned above, then a fixed amount of the tracer is injected into an injection well, usually approximately instantaneously, and the recovery in production wells turning is monitored. The sampling frequency is usually higher in the beginning and becomes lower as time passes.

7.2 Tracer testing theory

Tracer test results are evaluated by make a systematic record of the tracer concentration measured in each production well and the respective travel time. A fixed amount of tracer is injected at time zero and then the cumulative mass recovered, $m_i(t)$, as a function of time, *t*, in production well number *i* is calculated on basis of the following equation:

$$m_i(t) = \int_0^t c_i(s) Q_i(s) ds \tag{7.1}$$

Here c_i is the tracer concentration in kg/kg, or kg/l, Q_i the rate of production of the well (kg/s) and s is the integration variable.

Analysis of tracer recovery data from many injection experiments in various geothermal systems in Iceland described by Axelsson et al., (1995) has shown that a simple one–dimensional flow channel tracer transport model is quite powerful in modelling tracer recovery data. The model assumes flow between injection and production wells through approximately one–dimensional channels. The tracer transport in such channels is approximately governed by the equation below.

$$D\frac{\partial^2 C}{\partial x^2} = u\frac{\partial C}{\partial x} + \frac{\partial C}{\partial t} \tag{7.2}$$

The dispersion coefficient, D (m^2/s), is given by $D = \alpha_L u$, the tracer concentration is denoted by *C*, x is the distance along the flow channel (m), u is the average fluid velocity in the channel (m/s), expressed as $u = q/\rho A\emptyset$. The parameter $\alpha_L$is the longitudinal dispersivity of the channel (m), q is injection flow rate along the channel (kg/s), ρ is the density of water (kg/m^3), A the cross-sectional area of the flow channel and $\emptyset$ is flow channel porosity.

If instantaneous injection of mass *M* (kg) of tracer at time *t = 0* is assumed, the solution to equation (7.2) is given by;

$$c(t) = \frac{uM}{Q}\frac{1}{2\sqrt{\pi D t}} e^{\frac{1(x-ut)^2}{4Dt}} \tag{7.3}$$

Here $c(t)$ is the tracer concentration in the production well fluid.

Axelsson et al. (2005) discuss the one–dimensional flow channel tracer transport model in detail. They also present the analytical solution for the cooling of the production well fluid during long-term reinjection, which is expressed as;

$$T(t) = T_0 - \frac{q}{Q}(T_0 - T_i)\left[1 - erf\left\{\frac{kxh}{c_w q\sqrt{\kappa(t - x/\beta)}}\right\}\right] \quad (7.4)$$

$$\kappa = \frac{k}{\rho_r c_r} \quad (7.5)$$

$$\beta = \frac{q c_w}{\langle \rho c \rangle_f hb} \quad (7.6)$$

$$\langle \rho c \rangle_f = \rho_w c_w \emptyset + \rho_r c_r (1 - \emptyset) \quad (7.7)$$

Here $T(t)$, T_0 and T_i are production fluid, initial reservoir and injection temperature (°C), respectively, q and Q are the injection and production rates, respectively, in kg/s. The symbol erf stands for the error–function, k the thermal conductivity of the reservoir rock (W/m °C) and κ the thermal diffusivity of the rock (m^2/s). And ρ and c are the density (kg/m^3) and heat capacity (J/kg °C) of water (*w*) and rock (*r*) respectively. Also *h* and *b* are the vertical (or long) and horizontal (or short) sides of the flow channel, respectively.

The *TR family of programmes* in the ICEBOX software package (Arason et al., 2004), which includes software like TRMASS, TRINV and TRCOOL, were used in the tracer test analysis and interpretation of this project, as discussed in the next sections of this chapter.

7.3 Tracer test analysis and interpretation

Two tracer tests were conducted in the Reykjanes geothermal field during 2013 – 14 with the aim of improving the understanding of hydrological conditions and pathways within the reservoir system. The first test was done through injection well RN-20, starting in August 2013, and the second through the new injection well RN-33, starting in January 2014. In this report, data from the second tracer test through well RN-33 are used for analysis, interpretation and cooling prediction. Figure 7.1 presents a simplified map of the Reykjanes geothermal field showing the location of well RN-33 together with wells RN-18, RN-21 and RN-24, which are the wells showing the greatest tracer recovery.

On the 10th of January 2014, 150 kg of 2-napthalene sulfonate (2-NS) tracer was injected into injection well RN-33. The injection rate into the well was approximately 55 kg/s of cold water. The tracer recovery was monitored in several production wells, with the most significant recovery through wells RN-18, RN-21 and RN-24 since its initial breakthrough, lasting up to February 2015. These three production wells are located within the main production zone. Distances from the main feed zones in well RN-33 to production wells RN-18, RN-21 and RN-24 are approximately 1150 m, 1310 m and 1370 m, respectively.

The following sub-sections describe the analysis and interpretation of the tracer test data. First the tracer recovery through wells RN-18, RN-21 and RN-24 is presented, with the software TRMASS used to calculate the observed tracer recovery through each of the wells. Consequently utilization of the TRINV software is used for tracer data simulation. Finally the program TRCOOL was applied to calculate and predict the cooling of production fluid from the three wells due to injection of colder water into well RN-33.

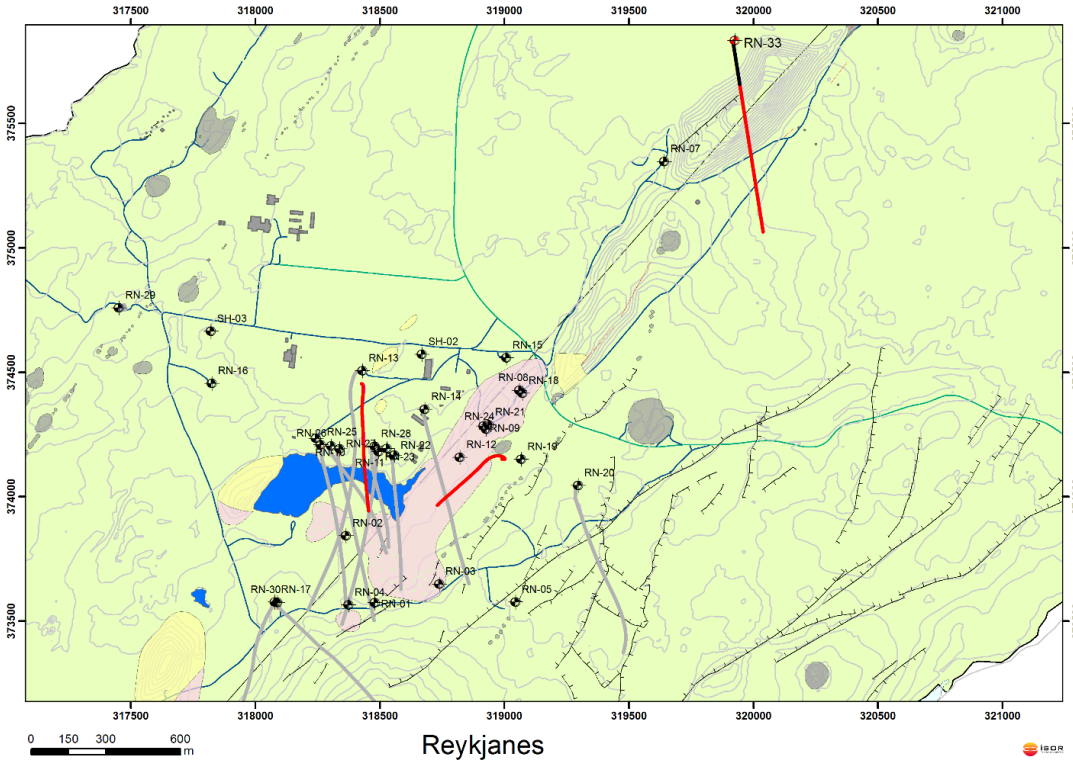

Figure 7.1: A map of the Reykjanes geothermal field showing the location of injection well RN-33 together with production wells RN-18, RN-21 and RN-24.

7.3.1 Tracer recovery for wells RN-18, RN-21 and RN-24

After more than 13 months continuous monitoring of the recovery of the 2-NS tracer injected into well RN-33, the results from the three wells (RN-18, RN-21 and RN-24) selected as the observation wells for analysing the tracer recovery were evaluated using TRMASS, which is based on equation 7.1. Table 7.1 summarize the recovery results of the wells as well as their estimated first breakthrough.

The results in the table show that the production wells (RN-18, RN-21 and RN-24) are directly connected to injection well RN-33, probably along a NE-SW trending fracture zone. The difference in their mass recovery appears to depend on the distance between the production wells and the injection well, the shorter the distance the earlier breakthrough and greater recovery. However, well RN-21 may be somehow indirectly connected with the injection well if compared with the other two wells (RN-21 and RN-

24). In total, about 13.7 kg (9.1%) have been recovered from the three wells (RN-18, RN-21 and RN-24) so far.

Table 7.1: 2-NS tracer (injected into well RN-33) mass recovery and time of first tracer breakthrough.

Well	Recovery mass (kg)	Recovery mass (%)	Time of first break through (days)	Peak concentration (kg/m^3)
RN-18	6.6	4.4	64	1.4×10^{-5}
RN-21	2.7	1.8	77	6.2×10^{-6}
RN24	4.4	3.0	91	6.1×10^{-6}

7.3.2 Inverse modelling of tracer returns

The method presented by Axelsson et al. (2005), and reviewed in section 7.2, was used to interpret the 2-NS tracer recovery from production wells RN-18, RN-21 and RN-24. A simple one–dimensional flow channel tracer transport model, which involves the connection of representative feed-zones between injection wells and production wells, was used in this respect. Parameters involved in the model simulation include: length of flow channel (x), flow velocity (u), dispersivity (α_L), flow cross-sectional area ($A\phi$) and mass recovery.

Figure 7.2 shows the results of the simulation of the tracer data for wells RN-18, RN-21 and RN-24, all of which demonstrate quite a good fit between measured and simulated data. Some data scattering may be due to sampling and/or measurement inaccuracy. Table 7.2 summarizes the parameters of the models.

Table 7.2: Model parameters estimated for the connections between injection well RN-33 and three production wells.

Well	Flow channel length, x (m)	Flow velocity, u (m/s)	Area*porosity, $A\phi$ (m^2)	Dispersivity, α_L (m)	Mass recovery (%)
RN-18	1150	5.3×10^{-5}	84	185	6.1
RN-21	1310	4.9×10^{-5}	49	260	3.2
RN-24	1370	5.0×10^{-5}	76	210	5.2

The model results show that about 14.5% of the 2-NS tracer injected is estimated as being transported along the flow channels to the three wells. From the flow velocity results it appears that well RN-21, which is close to well RN-24, has comparable flow speed as that estimated for well RN-24, but to have only about half the mass recovery mass of RN-24. Again the dispersivities of these two well are general similar with very small discrepant. This may give the indication that well RN-21 maybe somewhat more indirectly connected to injection well RN-33. Well RN-18 appears to be most directly connected to injection well RN-33, as is clearly supported by the model results.

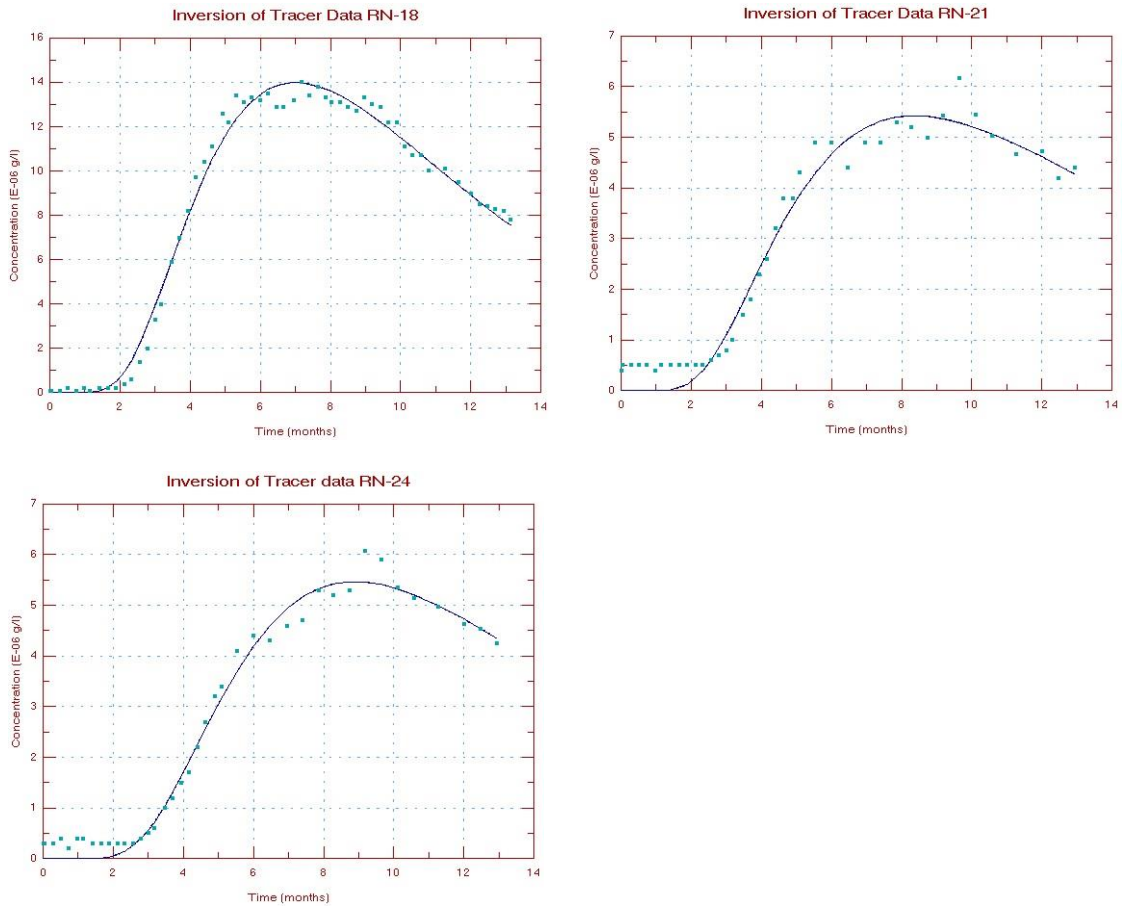

Figure 7.2: Measured (dots) and simulated (lines) 2-NS tracer recovery for wells RN-18, RN-21 and RN-24.

7.3.3 Cooling predictions

The model parameters estimated by the inverse modelling of the data from wells RN-18, RN-21 and RN-24 are used to calculate cooling predictions for the wells during long-term reinjection, as described in section 7.2 above. Two reinjection scenarios for a period of 20 years long-term reinjection have been considered. The first scenario assumes 100 l/s of cold fluid is continuously injected into well RN-33 and the second assumes 150 l/s cold fluid reinjection. The reservoir models used are basically the same as assumed in the tracer inverse modelling. The width and height of the fracture zone is obtained from the cross–sectional area of the flow path, with the height taken as 100 times the width, because geological conditions clearly indicate that the flow channels are most likely near-vertical fracture zones. The flow of water through a flow channel is determined from the percentage of mass recovery estimated by the inverse modelling (Table 7.2). The flow channel porosity is assumed 10% while an initial reservoir temperature of 280°C is assumed. The TRCOOL software, which is based on Equation (7.4), is employed as described by Axelsson et al. (2005).

The prediction results are graphically presented in Figures 7.3 – 7.5 below. The results indicate that a reinjection rate of 100 l/s into well RN-33 can be maintained with minor cooling danger during long-term reinjection. Temperature changes are 3°C, 1°C and 1°C for wells RN-18, RN-21 and RN-24 respectively in the next 20 years of reinjection into RN-33. The scenario for a 150 l/s reinjection rate is probably not feasible without causing serious cooling of many production wells. The predictions for all three production wells (RN-18, RN-21 and RN-24) show serious effect of cooling in the long run, and especially well RN-18 shows a drastic cooling of about 18°C. However, well RN-21 is least affected for both of the two scenarios, as it may not be as directly connected to the reinjection well.

Reinjection in the Reykjanes geothermal field is still essential and needs to increase to around 50% of the production mass in order to counteract the pressure draw-down in the field, as discussed in the previous chapter. This brings the attention to the drilling of more reinjection wells so as to reach the intended reinjection target. However, drilling of reinjection wells in the region of well RN-33 is not recommended, if necessary further reinjection wells should be drilled in the opposite direction from the production zones (away from the production zone). Moreover, a greater distribution of reinjection wells around the field is more feasible than localized reinjection, and may minimize the cooling danger for production wells during long term reinjection.

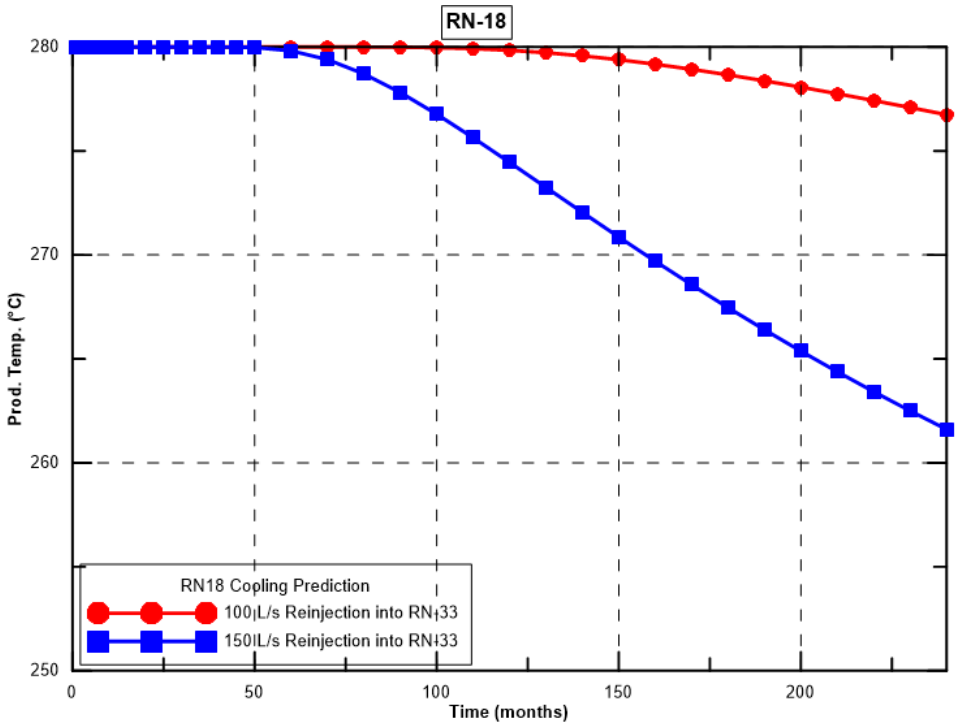

Figure 7.3: Cooling prediction for wells RN-18 calculated for reinjection into well RN-33, for a reinjection period of 20 years (240 months).

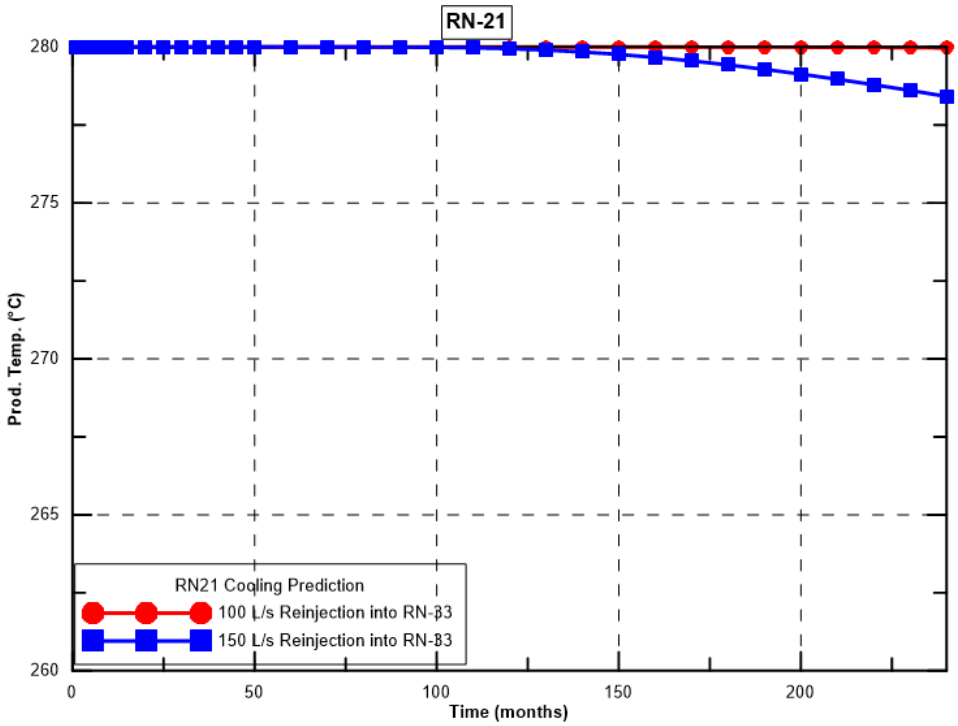

Figure 7.4: Cooling prediction for wells RN-21 calculated for reinjection into well RN-33, for a reinjection period of 20 years (240 months).

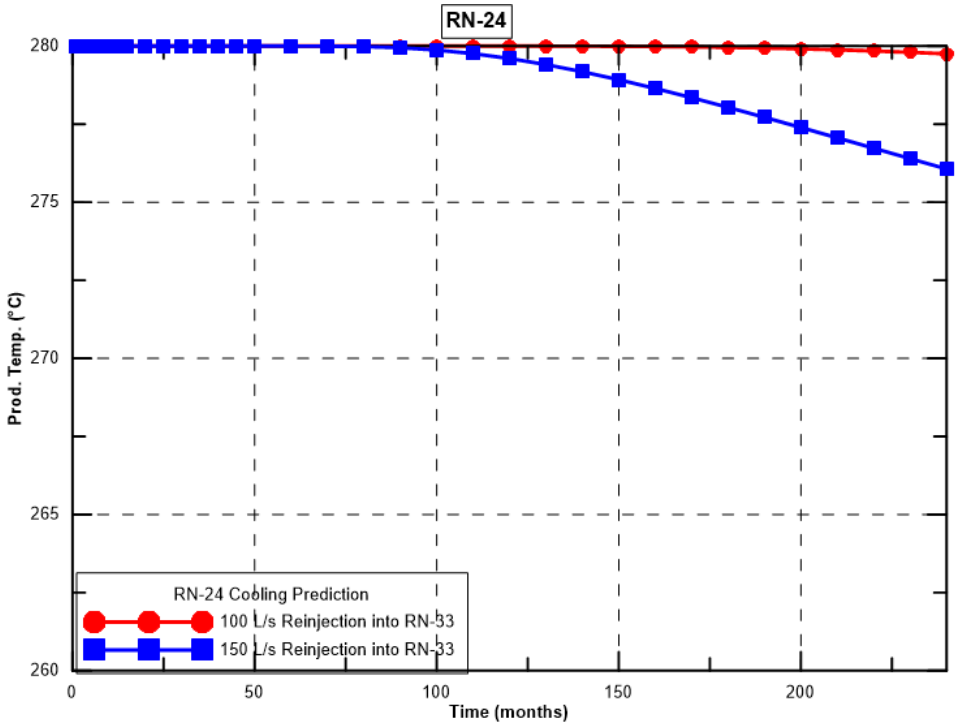

Figure 7.5: Cooling prediction for wells RN-24 calculated for reinjection into well RN-33, for a reinjection period of 20 years (240 months).

8 Conclusions and recommendations

The main goal of this study was to assess and discuss the role of well testing in evaluating the potential of geothermal resources and how the methods can offer valuable information in increasing the knowledge of a particular geothermal system. Different types and stages of well testing have been clarified, putting emphasis on the theories, information required, applications and importance. Well testing methods remain important evaluations tools for geothermal reservoirs from the exploration to the exploitation phase. The Reykjanes Geothermal system, SW Iceland is selected as a case example for this study.

Injection well testing performed in early stage of the reservoir evaluation, stimulates the well while provide information on the nature and behaviour of the reservoir. Discharge well testing, performed after a warm-up period that can lasts from a few days up to some months, is useful in estimating the productivity and fluid chemistry of the well before its utilization for energy production. Tracer testing in geothermal reservoirs is applied during geothermal utilization to assess the possible cooling effects on production wells as reservoir reinjection commences.

Temperature and pressure well logging is a continuous process that should be done regularly to infer well condition with regard to the reservoir. As production and monitoring data become available, through geothermal utilization period, modelling of the reservoir becomes possible. Simple analytical modelling is essential in predicting the reservoir future response to production.

Based on the results, after applying the methods described on data from the Reykjanes geothermal system, the following conclusions can be drawn.

- Well RN-30 has five main feed-zones of which only two feed-zones (at 1770 m and 2260 m) are located in production part of the well. For well RN-32, only two feed-zones are observed (at 883 m and 1040 m depth).
- Analysis of temperature and pressure log profiles from wells RN-30 and RN-32 suggests cold inflow at shallow depth. Boiling point depth curves are shifted down in the wells (RN-30 at 270 m and RN-32 at 550 m). The reservoir temperature is in the range of 280-290 °C.
- Comparing injectivity indices, *II* (8.5 and 3.9 (l/s)/bar) and effective permeability, *k* (86.4 and 5.03 mD) estimated from the two injection tests conducted in well RN-30, suggests that the well was more open during the first test. This suggest the well fractures may be clogged from the ongoing drilling operation as the first test was done as drilling was going on, while the second was performed after the drilling completion. From the discharge testing of RN-30, productivity index, *PI*, of 0.32 (kg/s)/bar is derived. This value is quite low compared to the injectivity index, *II*, which may imply that the well is a poor production well.

- Comparing injectivity indices, *II* (10.96 and 26.3 (l/s)/bar) and effective permeability, *k* (12.7 and 40 mD) estimated from the two injection tests conducted in well RN-32, suggests that the well is stimulated after the first injection test. The estimated production index, *PI*, (6.57 (kg/s)/bar) and II for well RN-32 has a relationship of PI= II/4 which indicates that it can be a good producer. The relationship is comparable to many geothermal wells drilled in the Reykjanes geothermal field.
- The wells (RN-30 and RN-32) are characterized by good transmissivity and storativity values. Their negative skin factors indicate that they are stimulated and in good connection with the surrounding reservoir.
- Simple analytical modelling performed for the two representative wells in the Reykjanes geothermal system (RN-12 and RN-16) propose that the current reinjection of 15% of the mass production needs to be increased to 50% so that the mass production capacity will increase and respond to the current pressure drawdown (around 41 bar) by increasing the current pressure over 6 bars in production zone for the next 10 years.
- Tracer breakthrough and recovered mass show that the production wells (RN-18, RN-21 and RN-24) are directly connected to the injection well RN-33. Cooling predictions calculated based on a simulation model for tracer recovery indicated that long-term reinjection rate of 100 l/s into RN-33 is likely to be applied without serous cooling of the production wells. However, 50 % of total mass production (260 l/s) reinjection should be reached and therefore more reinjection wells are needed in the field. Distribution of these wells around the field is more feasible so as to minimize the cooling danger.
- Drilling of reinjection wells in the region of well RN-33 is not recommended, however, if necessary then such wells should be drilled in the opposite direction from the production field (away from the production field).
- It is recommended to carry out discharge testing simulation of the production wells (RN-30 and RN-32) using software like *HOLA* or *WellSim* in order to determine fluid properties, relative flow rates and enthalpy at each feed zone. Also to predict deliverability curves for the wells after simulating series of discharge tests.

References

Albright, J.N., 1976: A new and more accurate method for the direct measurement of Earth temperature gradients in deep boreholes. *Proceedings, Second United Nations Symposium on the development and use of geothermal resources*, San Francisco, 20-29 May 1975, vol. 2, sec. IV, pp.847-851.

Arason, Th., Björnsson, G., Axelsson, G., Bjarnason, J.Ö., and Helgason, P., 2004: *The geothermal reservoir engineering software package Icebox, user´s manual*. Orkustofnun, Reykjavík, 80 pp.

Axelsson, G., 2012: The physics of Geothermal Energy. In: Saying A, (Ed.) *Comprehensive Renewable Energy*, Vol 7, pp. 3-50. Oxford: Elsevier.

Axelsson, G., 2013: Geothermal well logging. *Proceedings of the "Short Course V on Conceptual Modelling of Geothermal Systems", UNU-GTP and LaGeo*, Santa Tecla, El Salvador, 30 pp.

Axelsson, G. and Franzson, H., 2012: Geothermal drilling targets and well siting. *Proceedings of the "Short Course on Geothermal Development and Geothermal Wells", organized by UNU-GTP and LaGeo*, Santa Tecla, El Salvador, 16 pp.

Axelsson, G., and Steingrímsson, B., 2012: Logging, testing and monitoring geothermal wells. *Proceedings of the "Short Course on Geothermal Development and Geothermal Wells", UNU-GTP and LaGeo*, Santa Tecla, El Salvador, 20 pp.

Axelsson, G., Björnsson, G., and Quijano, J., 2005: Reliability of lumped parameter modelling of pressure changes in geothermal reservoirs. *Proceedings of the World Geothermal Congress 2005, Antalya, Turkey*, 8 pp.

Axelsson, G., Björnsson, G., and Montalvo, F., 2005: Quantitative interpretation of tracer test data. *Proceedings of World Geothermal Conference 2005, Antalya, Turkey, 12 pp.*

Axelsson, G., and Arason, Th., 1992: *LUMPFIT, automated simulation of pressure changes in hydrological reservoirs. Version 3.1, user´s guide.* Orkustofnun, Reykjavík, 32 pp.

Axelsson, G., 1989: Simulation of pressure response data from a geothermal reservoir by lumped parameter models. *Proceedings of the 14th Workshop on Geothermal Reservoir Engineering, Stanford University, California*, 257-263.

Bangma, P., 1961: The development and performance of a steam – water separator for use on geothermal bores. *Proc. UN conference on New Sources of Energy. V3.*

Bertani, R., 2015: Geothermal Power Generation in the World 2010-2014 Update Report. *Proceedings World Geothermal Congress, Melbourne, Australia.*

Björnsson, S., Arnórsson, S. and Tómasson, J., 1970: Exploration of the Reykjanes thermal brine area. *Geothermics* 56, 2380-2391.

Björnsson, S., Gudmundsdottir, I.D., Ketilsson, J., 2010: *Geothermal development and research in Iceland*. Orkustofnun, Reykjavik, pp.39.

Bodvarsson, G.S. and Witherspoon, P.A., 1989: Geothermal Reservoir Engineering. Part I. *Geothermal Science and Technology* 2:1-68.

Dowdle, W.L., and Cobb, W.M., 1975: Static formation temperature from well logs – an empirical method. *J. Petrol. Tech.*, 27, 1326-1330.

Divine, C.E. and McDonnell, J.J., 2005: The future of applied tracers in hydrogeology. *Hydrology Journal, 13, 117-138.*

Earloughr, R.C., 1977: *Advances in well test analysis*. Soc. Petr. Eng., Monograph 5, pp. 264

Flóvenz, Ó.G., Spangenberg, E., Kulenkampff, J., Árnason, K., Karlsdóttir, R. and Huenges, E., 2005: The role of electrical interface conduction in geothermal exploration. *Proceedings World Geothermal Congress 2005*, Antalya, Turkey, CD, 9 pp.

Franzson, H., Thordason, S., Bjornsson, G., Gudlaugsson, S.T., Richter, B., Fridleifsson, G.O. and Thorhallsson, S., 2002. Reykjanes high-temperature field, SW-Iceland. Geology and hydrothermal alteration of well RN-10. *Proceedings, 27th Workshop on Geothermal Reservoir Engineering*. Stanford University. 233–240.

Georgsson, L.S., 2013: Geothermal Energy in the world from energy perspective. *Presented at Short Course VIII on Exploration for Geothermal Resources.* Naivasha, Kenya.

Grant, M.A., Donaldson, I.G., and Bixley, P.F., 1982: Geothermal Reservoir Engineering. Academic Press, NY, pp.369.

Grant, M.A., and Bixley, P.F., 2011: *Geothermal reservoir engineering* (2nd Ed.). Academic Press, NY, 349 pp.

Gudmundsson, S.J., Hauksson, T., and Tomasson, J., 1981: The Reykjanes Geothermal field in Iceland: Exploration and well discharge characteristics. *Proceedings 7th Workshop Geothermal Reservoir Engineering,* Stanford, pp. 61-69.

Gylfadóttir, S. S., and Harðardóttir, V., 2013: *Discharge Testing of Well RN – 30*. Iceland GeoSurvey, ÍSOR-2013/007, 29 pp.

Gylfadóttir, S. S., Óskarsson, F., and Halldórsdóttir, S., 2014: *Production Testing of Well RN-32 in April 2014*. Iceland GeoSurvey, ÍSOR-2014/022, 29 pp.

Helgason, P., 1993: Step by step guide to BERGHITI. User's guide. In. Arason, Th., Björnsson, G., Axelsson, G., Bjarnason, J.Ö., and Helgason, P., 2004: *The geothermal reservoir engineering software package Icebox, user´s manual*. Orkustofnun, Reykjavík, 80 pp.

Hjartarson, A., 1999: *Analysis of reservoir data collected during reinjection into the Laugaland*

Geothermal system in Eyjafjördur, N-Iceland. University of Iceland and Orkustofnun, MSc. thesis, Reykjavík, 107 pp.

Horne, R.N., 1995: Modern well test analysis, a computer aided approach. (2nd Ed.). Petroway Inc., USA, pp.257

James, C.R., 1966: Measurement of steam – water mixtures discharging at the speed of sound to the atmosphere. *New Zealand Engineering 21 (10).*

Júlíusson, E., Grétarsson, G.J., and Jónsson, P., 2008: *Well Tester 1.0b, user´s guide*. ÍSOR – Iceland GeoSurvey, Reykjavík, report ÍSOR-2008/063, 27 pp.

Karlsdóttir, R., and Vilhjálmsson, A. M., 2014: *Reykjanes Geothermal Area, Southwest Iceland. Extension of 3D Inversion of MT Data*. Iceland GeoSurvey, ÍSOR-2014/016, 134 pp.

Karlsdóttir R., Árnason, K. and Vilhjálmsson, A. M., 2012: *Reykjanes Geothermal Area, Southwest Iceland. 3D Inversion of MT Data.* Iceland GeoSurvey, ÍSOR-2012/059.

Lazalde-Crabtree, H., 1984: Design approach of steam – water separators and steam dryers for geothermal applications. *Geothermal Resource Council Bulletin September 1984.*

Rutagarama, U., 2012: *The role of well testing in geothermal resource assessment*, Master's thesis, Faculty of Earth Sciences, University of Iceland, pp. 86.

Stefánsson, V., and Steingrímsson, B., 1980: *Geothermal Logging I – An introduction to techniques and interpretation*. National Energy Authority of Iceland (Orkustofnun), report OS-89917/JHD-09, Reykjavík, Iceland, 117 pp.

Theis, C.V., 1935: The relation between the lowering of the piezometric surface and the rate and duration of discharge of a well using ground-water storage. *Transactions, American Geophysical Union, 16, 519-524*

Thorbjornsson, D., Nielsson, S., Einarsson, G.M., Franzson, H., Karlsdottir, R., Halldorsdottir, S., Fridriksson, Th., and Oskarsson, F., 2014: *Reykjanes Conceptual model; Update to March 2014.* ÍSOR – Iceland GeoSurvey, Reykjavík, report ÍSOR-2014/049, 60 pp.

Appendix

A.3: Injection test

Table A.3. 1: Summary of injection tests pressure response for RN-30.

	Time period	Period Length, hr	Injection, L/s	Pressure at the end of step, bar-g
		26th May 2011		
Initial Injection		-	24.5	132.37
Step 1	06:59 – 08:29	1.30	55	137.1
		05th June 2011		
Initial Injection		-	25	120.5
Step 1	00:06 – 01:20	1.14	55	129.9

Table A.3. 2: Summary of injection tests pressure response for RN-32.

	Time period	Period Length, hr	Injection, L/s	Pressure at the end of step, bar-g
		09th April 2013		
Initial Injection		-	13	23.70
Step 1	21:30 – 22:59	1.29	13	24.4
Step 2	23:00 – 00:29	1.29	35	27.0
Step 3	0:30 – 01:30	1.29	60	23.7
		14th April 2013		
Initial Injection	03:30 – 05:00	-	13	
Step 1	05:00 – 06:06	1.10	13	23.8
Step 2	06:06 – 07:33	1.45	35	24.9
Step 3	07:33 – 08:39	1.10	60	23.6

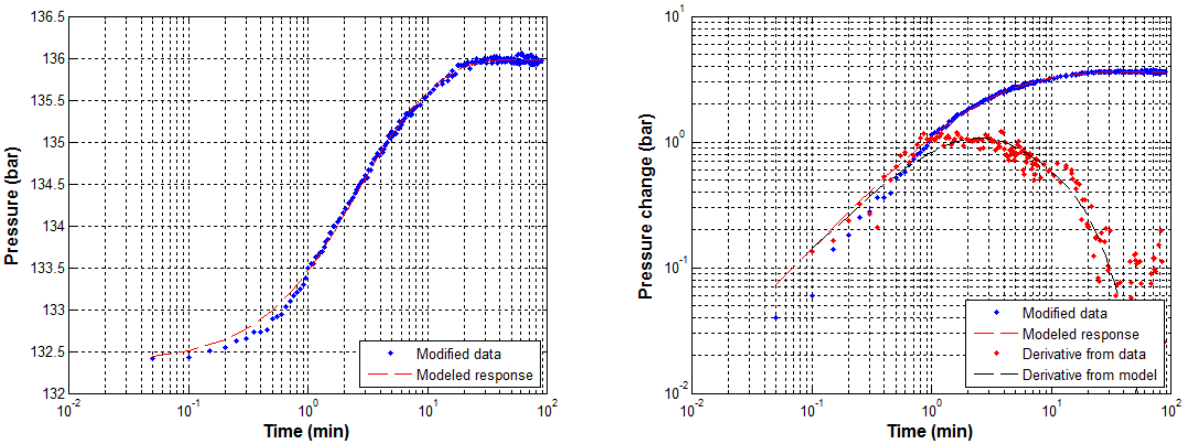

Figure A.3. 1: RN-30 Fit between model and measured data for step 1 using a logarithmic time scale (left) and log-log scale (right) for injection test on 26th May 2011.

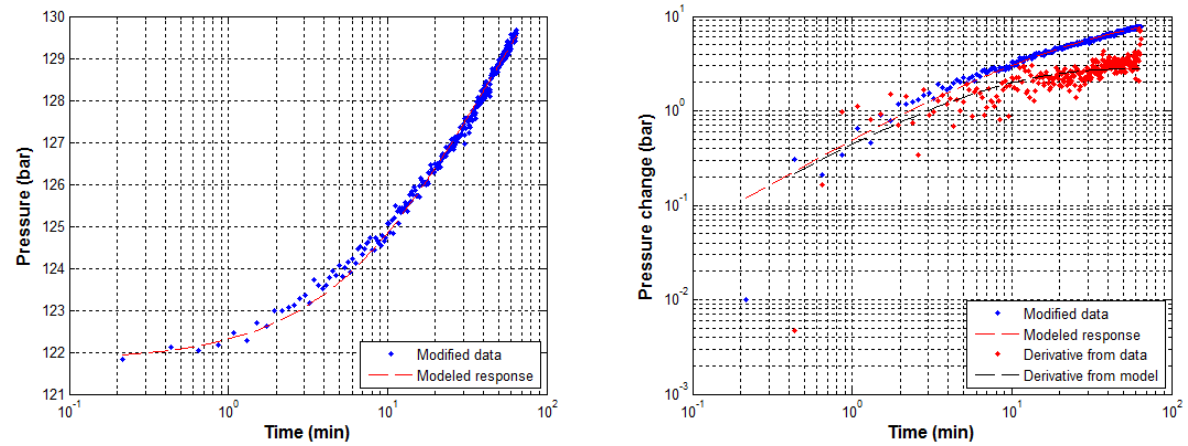

Figure A.3. 2: RN-30 Fit between model and measured data for step 1 using a logarithmic time scale (left) and log-log scale (right) for injection test on 05th June 2011.

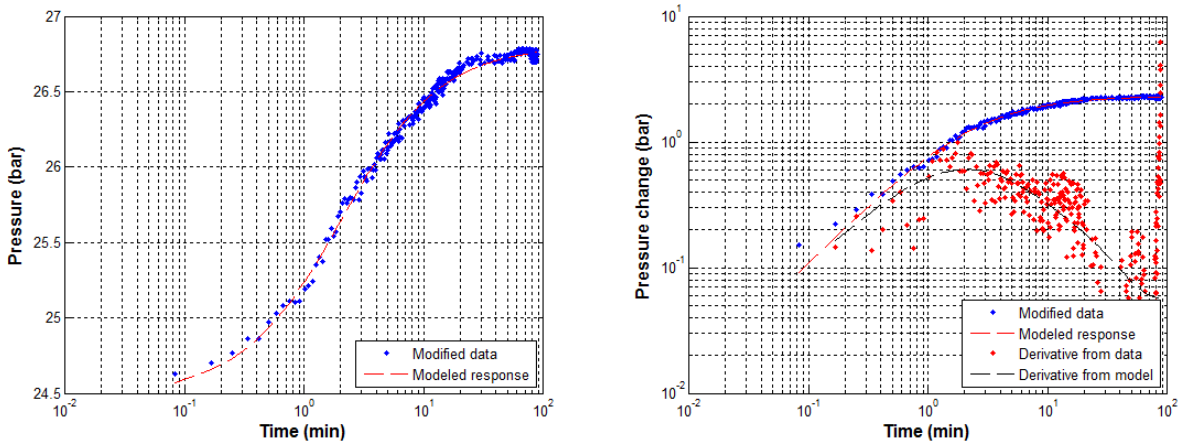

Figure A.3. 3: RN-32 Fit between model and measured data for step 2 using a logarithmic time scale (left) and log-log scale (right) for injection test on 09th April 2013.

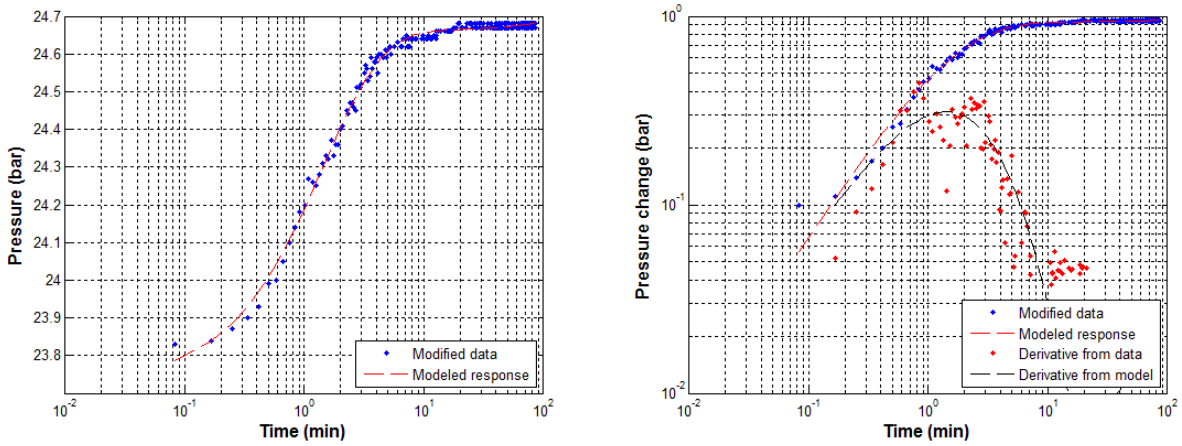

Figure A.3. 4: RN-32 Fit between model and measured data for step 2 using a logarithmic time scale (left) and log-log scale (right) for injection test on 14th April 2013.

A.4: Well design

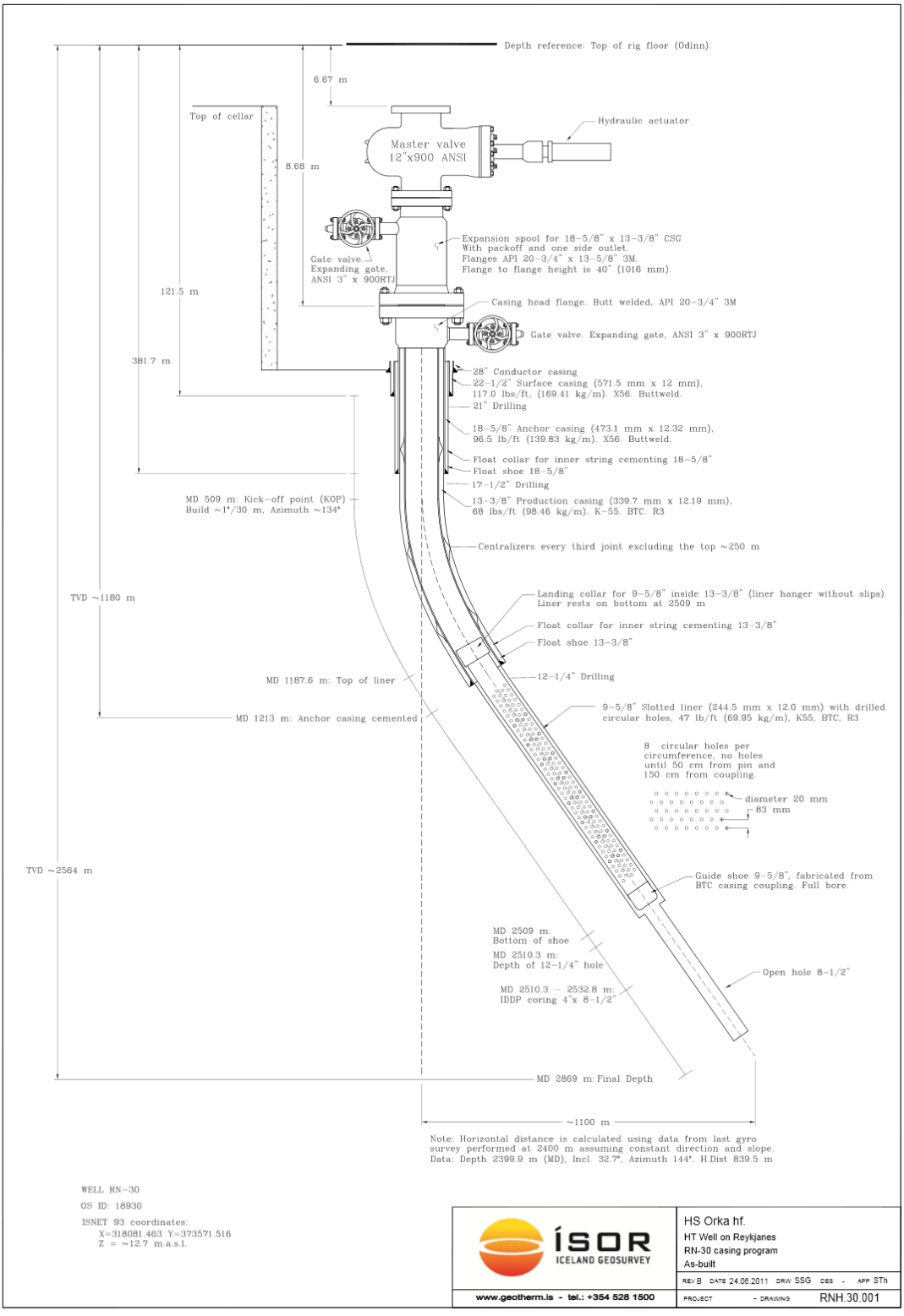

Figure A.4. 1: Casing program for RN-30 (source, ISOR).

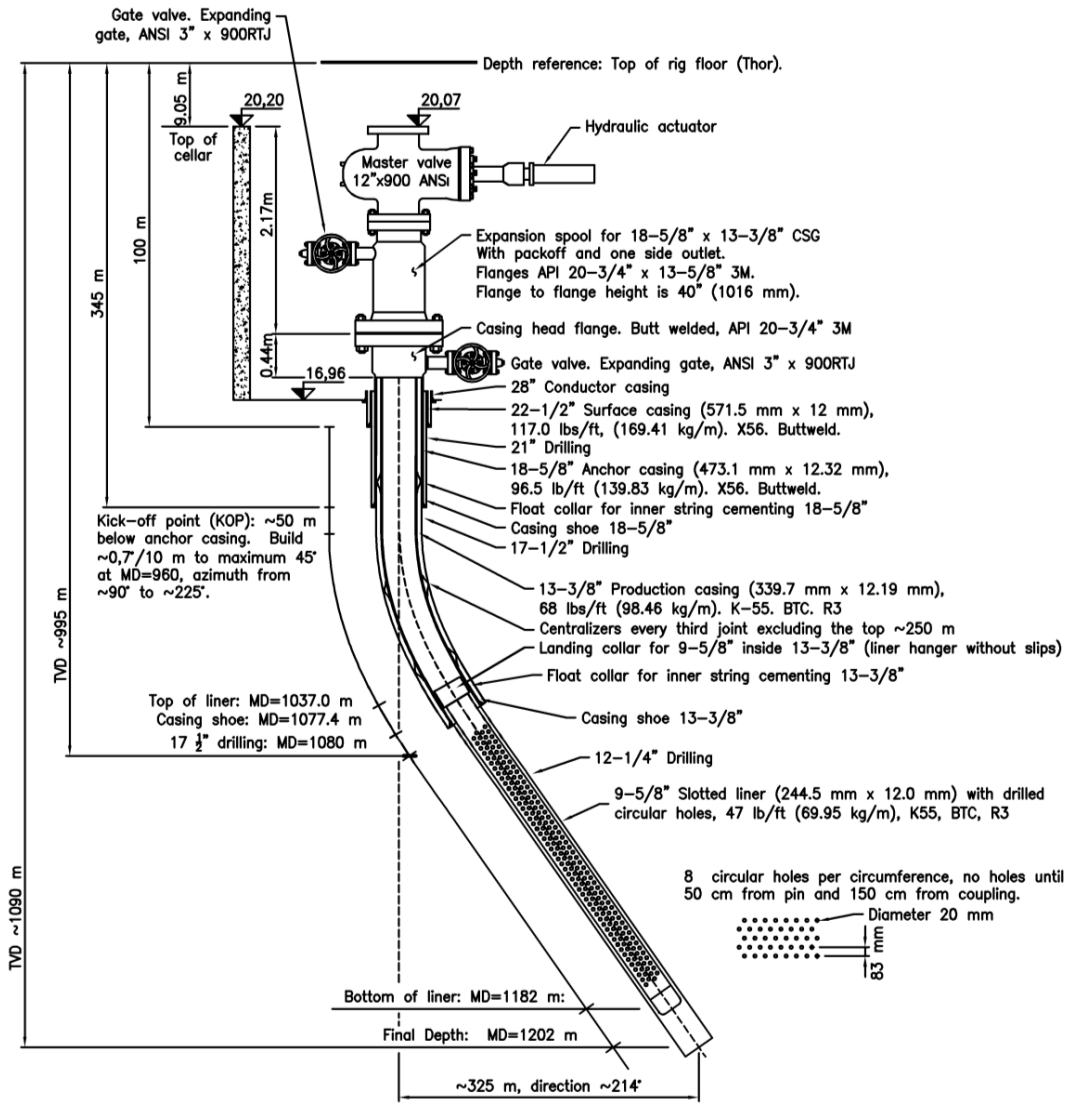

Figure A.4. 2: Casing program for RN-32 (source, ISOR).

A.5: Discharge test

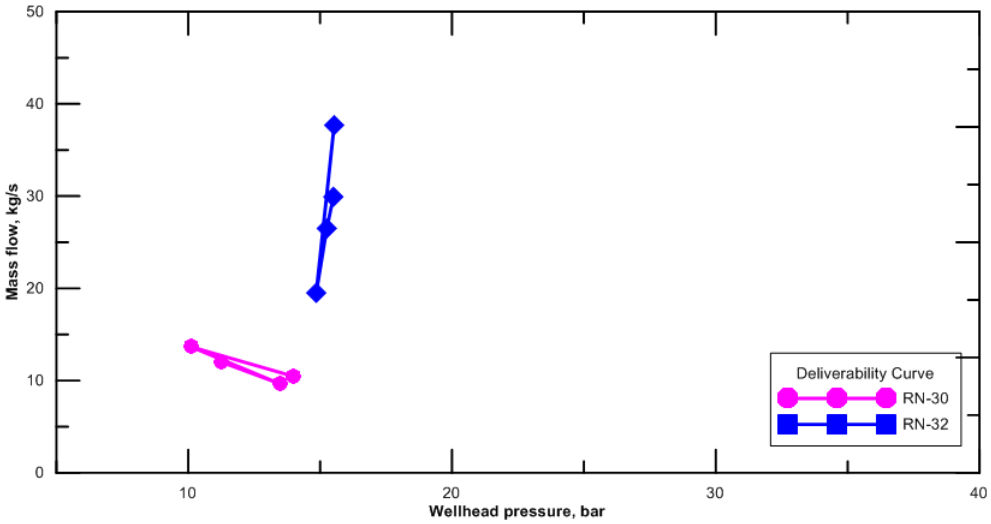

Figure A.5. 1: Deliverability curve of wells RN-30 and RN-32.

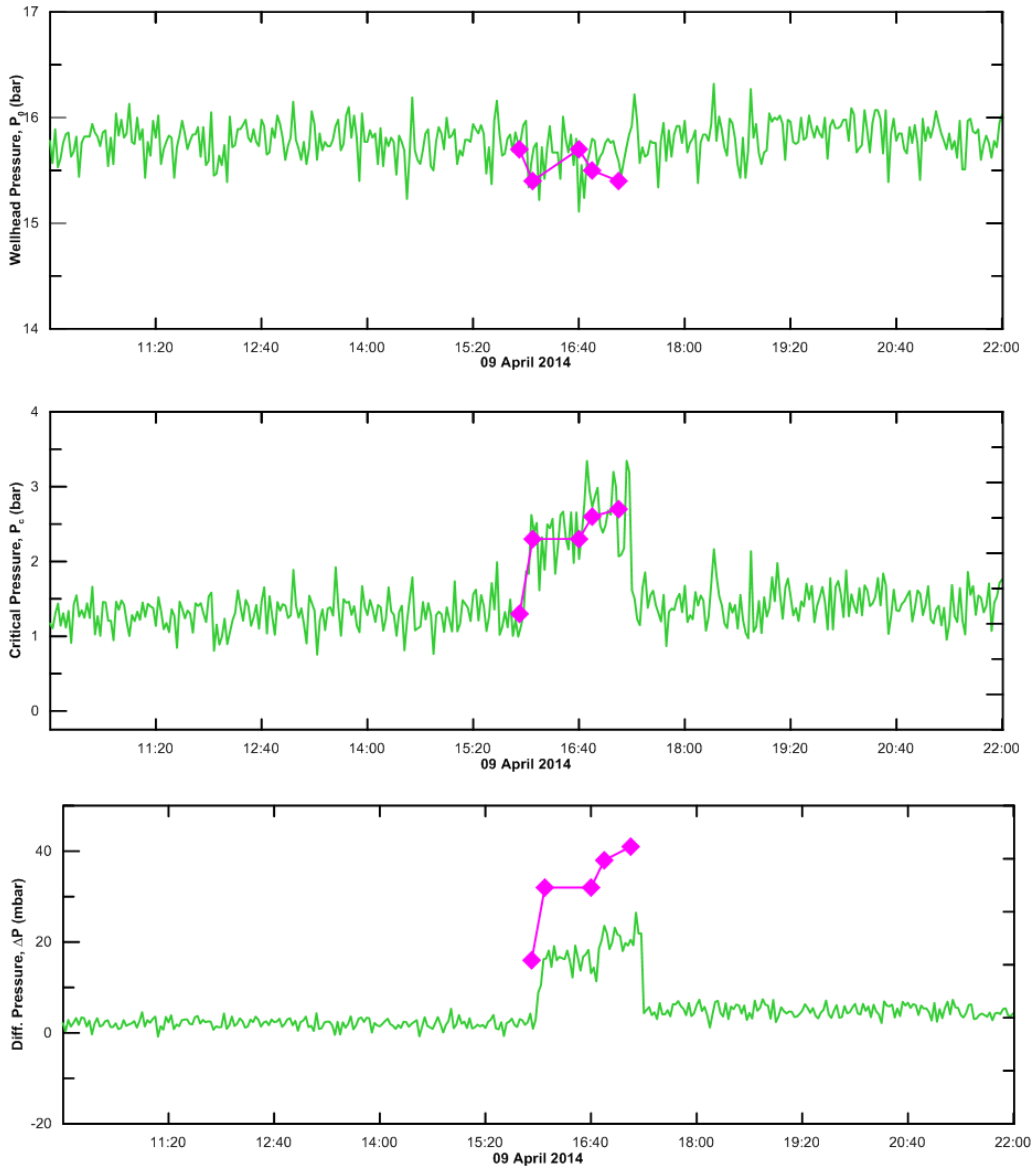

Figure A.5. 2: Plots of automatic and manual reading of the wellhead (a), critical (b) and differential pressures (c) for the discharge test of RN-32.